NATIONAL ADVISORY COMMITTEE FOR AERONAUTICS

TECHNICAL NOTE 3352

EXPERIMENTAL INVESTIGATION OF MISALINING COUPLES AND ECCENTRICITY AT ENDS OF MISALINED PLAIN BEARINGS

By G. B. DuBois, F. W. Ocvirk, and R. L. Wehe

Cornell University

Washington

February 1955

1S

NATIONAL ADVISORY COMMITTEE FOR AERONAUTICS

TECHNICAL NOTE 3352

EXPERIMENTAL INVESTIGATION OF MISALINING COUPLES AND ECCENTRICITY AT ENDS OF MISALINED PLAIN BEARINGS

By G. B. DuBois, F. W. Ocvirk, and R. L. Wehe

SUMMARY

An experimental investigation was conducted at Cornell University as a part of a research program sponsored by the National Advisory Committee for Aeronautics to study the behavior of full journal bearings under steady load when acted upon by a steady misalining couple. Displacements of the ends of the journal axis relative to the bearing axis were measured with either an axial couple applied in the plane of the central load or a twisting couple in the plane normal to the central load. Oil-flow-rate and bearing-temperature measurements were also made to determine the effect of misalining couples on these quantities.

Journals $1\frac{3}{8}$ inches in diameter were used at length-diameter ratios of 2, $1\frac{1}{2}$, 1, and $\frac{3}{4}$ with clearances ranging from 0.0018 to 0.0038 inch. Journal speeds from 1,200 to 5,000 rpm and central loads to 1,290 pounds were used with misalining couples as high as 288 inch-pounds. SAE 10 oil, at an inlet pressure of 80 pounds per square inch, was fed through a single $\frac{1}{8}$-inch-diameter oil hole located opposite the applied central load.

The displacement data obtained are presented as charts relating the misalining couple to the eccentricity at the end of the bearing in relation to the central load and other variables in nondimensional form. Charts are also presented comparing the effect of a misalining couple on maximum eccentricity with an equivalent central load which is a multiple of the applied central load. This multiple is called "load ratio" and shows the relatively large effect of small misalining couples on eccentricity. Data are also presented to show that misalining couples have a negligibly small effect on bearing temperature and on oil flow rate, provided the oil film is not ruptured.

INTRODUCTION

Engineering information for the design of journal bearings with the journal axis misalined relative to the bearing axis is needed since most practical engineering cases involve misalinement due to (1) elastic or thermal deflection, (2) known applied couples on single bearings, or (3) unavoidable difficulties of alinement in manufacture. Examination of failed bearings will often show evidence that the failure originated at one end of the bearing. Fortunately, the ability of soft bearing materials to conform or run-in is of considerable aid in cases where the misalined deflection assumes a stable value. On harder materials less able to run-in to conform in alinement with the deflected shaft, misalinement becomes an important problem.

Some experimental and analytical data on oil film pressure distribution for cases of misalinement have been published. DuBois, Mabie, and Ocvirk in an earlier report on this project (ref. 1) presented photographs of five plaster models of experimentally measured oil-film pressure distributions showing that the oil film pressure distribution is distorted and the peak film pressure is considerably increased when misalining couples are applied either in the plane of the load or in a plane normal to the load.

Walther and Sassenfeld (ref. 2) presented an analytical solution giving the film pressure distribution for a misalined bearing. They have employed a mathematical method of differences in satisfying Reynolds' lubrication equation and present pressure-distribution curves of an example. They report that the computations in their solution are not difficult in principle but are troublesome and tedious.

Studies have been made by this investigation to determine the practicability of obtaining an analytical solution for the misalined bearing. Unless simplifying assumptions are made, any solution of Reynolds' differential equation for the misalined case evidently requires integrations by numerical methods, first for pressure distribution, and subsequently for loads and couples. A function for film thickness is required for journal and bearing axes which are nonparallel and nonintersecting in the general case of misalinement. Three parameters are necessary in the film-thickness function as contrasted with one parameter, the eccentricity ratio, for bearings without misalinement. The three parameters for misalinement may be stated as the eccentricity ratio at the center of the bearing and two orthogonal angular displacements of the journal axis relative to the bearing axis. The three parameters may also be taken as the eccentricity ratios at the two ends of the bearing and an angular displacement between these eccentricity ratios. If numerical methods are used in performing the integrations, the number of individual cases depending upon combinations of the three parameters makes the work voluminous. Even if results were obtained from the integrations, methods of plotting these results would be complex.

In view of the theoretical difficulties, it was felt that a direct experimental approach to obtaining information on misalinement was desirable. Comprehensive experimental data were taken and subsequently reduced to charts having nondimensional coordinates. The charts presented in the following sections of this report are the result of extensive cross plotting. Many intermediate steps were of value chiefly to indicate a better method. Introduction of several variables which may be said to have been experimentally or semiempirically determined rather than theoretically derived became necessary.

This investigation was conducted at Cornell University under the sponsorship and with the financial assistance of the National Advisory Committee for Aeronautics.

SYMBOLS

a lever arm or offset of misalined load, in.

c_d diametral bearing clearance, in.

$\frac{c_d}{d}$ clearance ratio

c_r radial bearing clearance, $c_d/2$, in.

C_m couple variable, $C_m = \frac{M}{Pl}\left(\frac{d}{c_d}\right)^{1/2}\left(\frac{l}{d}\right)^{1/2}$ for $\frac{l}{d} \geqq 1.0$,

$$C_m = \frac{M}{Pl}\left(\frac{d}{c_d}\right)^{1/2}\left(\frac{l}{d}\right)^{1/2}\frac{1}{\left(\frac{l}{d}\right)^2} \quad \text{for} \quad \frac{l}{d} \leqq 1.0$$

C_n capacity number, $\frac{\mu N'}{p}\left(\frac{d}{c_d}\right)^2\left(\frac{l}{d}\right)^2$ for $\frac{l}{d} \leqq 1.0$ (see S)

C_{n_e} equivalent capacity number due to misalinement, $\frac{\mu N'}{L_R p}\left(\frac{d}{c_d}\right)^2\left(\frac{l}{d}\right)^2$

d bearing diameter, in.

e eccentricity for central loading, in.

e_c eccentricity at center of bearing for misalinement, in.

e_e eccentricity at end of bearing for misalinement, in.

l bearing length, in.

$\frac{l}{d}$ length-diameter ratio

L_R load ratio, $\frac{L_R P}{p} = \frac{S}{S_e} = \frac{C_n}{C_{n_e}}$

m_a misalined attitude, $\frac{n_e - n}{1 - n}$

M misalining couple, in-lb

M_a axial misalining couple, in-lb

$\frac{M_a}{Pl}$ axial couple ratio, $\frac{Pa}{Pl} = \frac{a}{l} = \frac{\text{Percent misalinement}}{100}$

M_t twisting misalining couple, in-lb

$\frac{M_t}{Pl}$ twisting couple ratio

n eccentricity ratio or attitude for central loading, e/c_r

n_c eccentricity ratio at bearing center for misalinement, e_c/c_r

n_e eccentricity ratio at bearing end for misalinement, e_e/c_r

N journal speed, rpm

N' journal speed, rps

p applied central unit bearing load on projected area, lb/sq in.

p_c capsule pressure of load, lb/sq in.

p_o inlet oil pressure, lb/sq in.

P applied central bearing load, lb

Q experimental total rate of oil flow for central loading, lb/sec

Q_m experimental total rate of oil flow for misalinement, lb/sec

r bearing radius, in.

S Sommerfeld number, $\frac{\mu N'}{p}\left(\frac{d}{c_d}\right)^2$ for $\frac{l}{d} \geqq 1.0$ (see C_n)

S_e equivalent Sommerfeld number due to misalinement, $\frac{\mu N'}{L_R p}\left(\frac{d}{c_d}\right)^2$

T temperature, $^{\circ}F$

μ oil viscosity, reyns = $\frac{\text{centipoises}}{6.9 \times 10^6}$

ϕ attitude angle, deg

Subscripts:

c at bearing center

e at bearing end; equivalent with values of S and C_n

h horizontal

v vertical

NATURE OF MISALINEMENT

Discussion

An analytical approach to the characteristics of misalinement may well begin with an explanation of the displacement of the journal axis relative to the bearing axis. Figure 1 shows the geometric configuration of these axes for the general case, in which the axes are nonparallel and nonintersecting. It may be seen from figure 1 that the eccentricity e and its direction or attitude angle ϕ are variable along the length of the bearing axis. In general, the midpoint of the journal has some "central" eccentricity e_c and the eccentricity at one end of the bearing is greater than that at the other end of the bearing. The maximum eccentricity at one end of the journal is called the end eccentricity e_e and is of special interest as it is indicative of the minimum oil film thickness.

It was found experimentally that the condition shown in figure 1 could be obtained by eccentric loading, or by applying a load at the

center of the bearing plus a couple acting in the plane containing the load and the bearing axis. This couple is called an axial couple as shown in figure 2.

If the line of action of the load is eccentric, or offset from the bearing center, the effect is analogous to a central load plus an axial couple. In practice an axial couple may occur in three ways: As the load P times an offset a, or as a moment M produced by couple forces shown in figure 2, or as a result of journal misalinement as shown. In these experiments it was convenient to apply the couple M by a system of weights, lever arms, and small cables over pulleys, leaving the machine adjusted so that the load from the loading capsule and the spherical seat passed as nearly as possible through the bearing center.

Figure 2 also shows a twisting misalining couple tending to rotate the bearing shell about the load line. The twisting misalining couple is applied in a plane normal to the central load line. Referring to the plane of the axial couple and the normal plane of the twisting couple, the third principal plane is that of bearing rotation and friction torque in which the bearing is not sensitive to misalining couples.

Central eccentricity ratio.- Since the eccentricity and eccentricity ratio are variable along the bearing axis, the subscript c is used to designate values at the bearing center. Thus n_c is the eccentricity ratio e_c/c_r at the bearing midplane.

End eccentricity ratio.- The subscript e is used to designate the eccentricity ratio at the end of the bearing having the maximum value of n, called n_e. This is the point at which the closest approach to metallic contact occurs.

Method of Approach

As indicated in the following paragraphs, the approach to the misalinement problem taken by this investigation is that journal displacements by misalinement may be related to the displacements by central loads. In this way misalining couples are compared with equivalent central loads which would give eccentricities equivalent to the end eccentricities actually obtained.

The curved line in figure 3(a) represents the experimental data from figure 4 showing the displacement of a journal in a bearing when acted upon by a central load without misalinement. The eccentricity ratio n is plotted as a function of either the Sommerfeld number S for values of $l/d \geqq 1$ or the capacity number C_n for values of $l/d \leqq 1$:

$$S = \frac{\mu N'}{p}\left(\frac{d}{c_d}\right)^2 \quad \text{for} \quad l/d \geq 1.0 \tag{1}$$

$$C_n = \frac{\mu N'}{p}\left(\frac{d}{c_d}\right)^2\left(\frac{l}{d}\right)^2 \quad \text{for} \quad l/d \leq 1.0 \tag{2}$$

Referring to figure 3(a), a typical case of central load without misalinement might be represented as point a with an eccentricity n and a capacity number C_n.

When a misalining couple is applied and misalinement occurs the eccentricity ratio at one end of the bearing n_e would become larger than n, as represented by point b directly over a. The capacity number C_n is unchanged since it is computed on unit (central) bearing load which is unchanged, assuming the temperature, viscosity, speed, and so forth are held constant.

The method of attack used in this investigation is to modify the load term in the Sommerfeld number or the capacity number by a factor L_R so that the point b would fall on the established curve at point c. Thus the "equivalent" Sommerfeld or capacity number for eccentric or misalined loading is

$$S_e = \frac{\mu N'}{L_R p}\left(\frac{d}{c_d}\right)^2 \tag{3}$$

$$C_{n_e} = \frac{\mu N'}{L_R p}\left(\frac{d}{c_d}\right)^2\left(\frac{l}{d}\right)^2 \tag{4}$$

Load ratio.- The factor L_R is called the load ratio:

$$L_R = \frac{L_R p}{p} = \frac{S}{S_e} = \frac{C_n}{C_{n_e}} \tag{5}$$

The load ratio is represented in figure 3(a) as the abscissa of the point b, or C_n, divided by the abscissa of point c on the curve, or C_{n_e}. The load ratio is always greater than one. In equation (4) note that since the unit load p is in the denominator, the C_n term is inverted; that is, C_n is greater than C_{n_e}.

Meaning of load ratio.- The relatively large numerical magnitude of the load ratio results from consideration of the meaning of the points a, b, and c in figure 3(a). Point a represents a light load without misalinement. Point b shows the effect on eccentricity at one end of the bearing of applying a misalining couple. Point c on the other hand represents an "equivalent" central load without misalinement, where the eccentricity of c occurs all the way across the bearing rather than at one end only. The load for point c is naturally several times the central load at a. A light central load plus a misalining couple results in a reduction in oil film thickness at one end of the bearing, and the load ratio L_R represents the increase in the central load that would be required to produce the same reduction on oil film thickness all the way across the bearing. Point c has been termed the "equivalent" central load since it gives the same maximum eccentricity as point b does by misalinement.

A simpler visual meaning of load ratio is obtained by simply regarding it as the ratio of the two values of C_n in figure 3(a) as shown in equation (5).

Misalined attitude.- While misalined displacement is of an angular nature, the value of the minimum oil film thickness at the end of the bearing, or end eccentricity ratio n_e, is of greater interest. An angular value would depend on the l/d ratio since the angle is affected by the bearing length. A fundamental measure is desired which will be zero when no angular misalinement exists and which will approach 1.0 when the journal approaches metallic contact at one end of the bearing. The measure chosen should bear the same relation to the misalined case that the eccentricity ratio n does to the central load case. This result is given by the following ratio:

$$m_a = \frac{n_e - n}{1 - n} \tag{6}$$

Graphical representation of misalined attitude.- The misalined attitude m_a is also represented in figure 3. The vertical distance for point a is n, and that for b is n_e. The distance from a to b is labeled $(n_e - n)$. The distance from a to the top line is labeled $(1 - n)$. Thus, the misalined attitude m_a is the ratio of the distance ab to the distance from a to the top line. Misalined attitude m_a as a ratio represents how far the point b has progressed toward the top line where n equals 1.0.

The relative geometrical position of the bearing and the journal will depend not only on the magnitude of the central load and the misalining couples but will also depend on the usual hydrodynamic variables.

In an experimental program covering a number of length-diameter ratios and clearances, the number of possible cases to be investigated is large. To limit the number of experiments in this investigation, data were obtained giving displacements due to misalining couples applied either in the plane of the central load as axial couples, or in the plane normal to the load line as twisting couples. Combinations of the two appear to be of less practical importance and so far have not been included in this investigation.

From the curve of n against S or n against C_n for central loading as in figure 3, a family of curves may be constructed showing the relationship of m_a, L_R, and S or C_n. For a given value of S or C_n, the corresponding value of n is known from the curve. Then for arbitrary values of n_e and corresponding values of S_e or C_{n_e} both m_a and L_R may be calculated from equations (6) and (5).

The curved line in figure 3 is obtained from reference 3 and figure 4 which presents experimental data for centrally loaded bearings of length-diameter ratios 2, $1\frac{1}{2}$, 1, and 3/4. As shown in figure 4(a) the experimental values of eccentricity ratio fall closely on a single line for all length-diameter ratios if the abscissa is S for the long bearings ($l/d \geq 1.0$) and C_n for the short bearings ($l/d \leq 1.0$). Figures 4(b) and 4(c) show the same data but show the long- and short-bearing data separately. Experimental curves are shown drawn through the experimental data, and the analytical short-bearing curve of reference 3 is also shown for comparison.

On the basis of the experimental curves in figures 4(b) and 4(c) misalinement curves of m_a against S and m_a against C_n were constructed with load ratio L_R as a parameter in figures 5(a) and 5(b). Calculations were made using equations (5) and (6). The shape of the misalinement curves depends entirely upon the shape of the curve for central loading. On the basis of the analytical short-bearing curve figures 5(a) and 5(b) would be the same. However, it is conservative to use the experimental curves of figures 4(b) and 4(c) especially in the region of high central loads where S and C_n are low.

The curves of figures 5(a) and 5(b) indicate that for a given central load, as given by S or C_n, the misalined attitude m_a increases with load ratio L_R. For the limiting condition of metallic contact ($m_a = 1.0$), the load ratio becomes greater as the central load becomes smaller. These curves show the relation between the misalined attitude m_a and the load ratio L_R, but lack information in regard to the misalining couples required.

An extensive test program was required to relate the applied couples to load ratio and misalined attitude. Since the size of the couple seems to be most closely related to the bearing load and the bearing length, these terms were combined in a nondimensional form as given below.

Couple ratio.- In these experiments the misalining couples were applied as a pure moment on the bearing in inch-pounds, designated as M. In order to obtain a nondimensional quantity, the bearing load P and bearing length l are introduced:

$$\text{Couple ratio} = \frac{M}{Pl} \tag{7}$$

As already mentioned, an axial couple M_a is analogous to offsetting the bearing load from the center of the bearing by a distance a:

$$\begin{aligned} M_a &= Pa \\ a &= \frac{M_a}{P} \end{aligned} \tag{8}$$

An axial couple ratio has a visual meaning as follows:

$$\text{Couple ratio} = \frac{M_a}{Pl} = \frac{Pa}{Pl} = \frac{a}{l} = \frac{\text{Percent misalinement}}{100} \tag{9}$$

Thus an axial couple ratio of 0.5 or 50-percent misalinement indicates a is one-half of l and is analogous to having the line of action of the load pass through one end of the bearing. Beyond this point the bearing oil film pressure apparently becomes negative at the opposite end of the bearing and the journal tends to tilt across the clearance. A similar situation occurs when the central load is zero, and a misalining couple is applied. To expedite this program, these conditions have been considered as a separate case not included in this program.

The photographs of plaster models showing distortion of the oil film pressure distribution for a case of misalinement, given in reference 1, were obtained using "16-percent misalinement." Thus, 16 percent is a couple ratio of 0.16 or $a/l = 1/6$. One-sixth of the distance from the bearing center is $(0.50 - 0.16)l$ or $0.34l$, and for the plaster models the load may be considered as applied at a one-third point on l.

Couple variable.- In an attempt to make the couple independent of l/d and d/c_d, additional couple variables C_m are introduced:

$$C_m = \frac{M}{Pl}\left(\frac{d}{c_d}\right)^{1/2}\left(\frac{l}{d}\right)^{1/2} \quad \text{for} \quad l/d \geqq 1 \tag{10}$$

$$C_m = \frac{M}{Pl}\left(\frac{d}{c_d}\right)^{1/2}\left(\frac{l}{d}\right)^{1/2}\frac{1}{\left(\frac{l}{d}\right)^2} \quad \text{for} \quad l/d \leqq 1 \tag{11}$$

The couple variables in the nondimensional forms shown in equations (10) and (11) were determined by trial-and-error methods in the search for a variable which would collect experimental data as a function of load ratio as shown in figures 6(a) to 6(d). Four experimental curves of C_m versus L_R are shown separately for long and short bearings and for axial and twisting misalinement.

By combining the experimental data of figures 6(a) to 6(d) with the misalinement curves of figures 5(a) and 5(b), load ratio may be eliminated, giving the four misalinement curves of figures 7(a) to 7(d).

The curves of figures 7(a) to 7(d) show the relationship of misalining couples, central load, and misalined attitude in nondimensional form. It may be seen that load ratio has been employed as a parametric device in order to formulate a method of approach to the misalinement problem. The discussion and interpretation of the experimental data are given in the following sections of this report.

APPARATUS

The bearing-testing machine used in the misalinement experiments is the same as that described in reference 3. A photograph of the machine appears in figure 8. The manner in which the test elements were supported and loaded is shown in figures 9, 10, and 11. Figure 12 shows the mechanical system for measuring journal displacements, and figure 13 gives the locations of the thermocouples used to determine bearing temperatures.

Test Bearing and Journals

A single bronze bearing and five steel shafts of $1\frac{3}{8}$- inch nominal diameter were used in the configuration shown in figure 9. Each of the shafts represented a given length-diameter ratio and a given clearance as listed on the following page:

Shaft	l/d	Average diametral clearance, c_d, in.	Clearance ratio, $\frac{c_d}{d}$, in./in.
6A	2	0.00252	0.00183
6B	2	.00376	.00273
6C	$1\frac{1}{2}$	.00196	.00142
6D	1	.00183	.00133
6E	$\frac{3}{4}$	.00258	.00187

These test elements were also used in the experiments with central loading as shown in figure 4. SAE 10 oil was used as the test lubricant and was fed to the test bearing at a pressure of 80 pounds per square inch through a 1/8-inch-diameter oil hole located opposite the central load. The oil was preheated to 140° F near the pump although the measured temperature of the oil entering the bearing was less because of heat losses in the oil lines.

The test shafts were driven by a high-speed, direct-current, variable-speed aircraft motor, having a speed range of 1,000 to 10,000 rpm.

Loading Apparatus

As shown in figure 10, the central load was applied hydraulically by a pressure capsule and was transmitted to the bearing through a piston and an oil-pressurized spherical seat. The oil flow through the spherical seat floats the bearing giving it freedom to displace on the application of central load and misalining couples. Figure 10 also shows the method of applying axial and twisting misalining couples. Combinations of 1/2-, 1-, and 2-pound weights were used to transmit force through light steel cables to tubular members projecting from the bearing as shown. The pulleys shown were ball bearing mounted to minimize frictional resistance in the system. To restrain the axial movement of the test bearing on the shaft without restraining angular movements, self-alining ball-bearing links and a gimbal ring were used as shown in figure 11. The links and gimbal ring provide the necessary axial resisting force on application of the misalining weights such that a pure misalining couple acts on the bearing as shown.

The coordinate displacements of the journal ends relative to the bearing were measured by the mechanical arrangement in figure 12 in which horizontal and vertical motions were transmitted by bronze riders on levers through vertical rods to four 0.0001-inch dial indicators. This is the same system reported in reference 3 except that the levers were modified to give a 2-to-1 magnification of the actual displacements to improve the accuracy in reading the dials. A duplicate set of rods is used for temperature compensation.

Iron-constantan thermocouples were used to measure bearing temperatures at 14 locations in the bearing hub within 1/16 inch of the bearing surface as shown in figure 13. Thermocouple 9 gave the bearing-hub temperature at a point 2 inches from the oil film, and thermocouple 16 was used to determine the temperature of the incoming oil at the oil inlet to the test bearing.

As shown in figure 10, a drain hole in the bottom of the machine housing allowed the oil flowing from the test bearing to be collected in a pan which could be removed for weighing. Also shown are the slinger rings and baffles which prevented the mixing of the test-bearing oil with the oil from the support bearings and the spherical seat.

TEST PROCEDURE

For each of the five test shafts a series of displacement experiments were conducted at a number of speeds and with combinations of central load and either axial misalining couples or twisting misalining couples. Only a few experiments were made to determine oil flow characteristics because it was early discovered that misalinement had a negligibly small effect on oil flow rate.

Omission of Friction Tests

Although friction-measuring apparatus is incorporated in the test machine (ref. 3), no friction data were taken in this series of misalined tests because no acceptable method was devised for applying misalining couples without small components of the couple affecting the friction torque measurements. From many attempted friction tests made early in the program, it was found that the pull on the misalining wires resulted in a small torque component in the plane of the friction torque which was of the order of magnitude of the friction torque. Thus, the friction data under misalinement were erratic and failed to repeat satisfactorily. By shifting the journal axially with respect to the bearing, it is possible to obtain a combination of central load and axial misalinement which would not have an extraneous effect on the friction measurement; however,

for the long bearings, the bearing machine permits a shaft movement of only 1/16 inch either side of bearing center which is insufficient for an acceptable magnitude of misalining couple.

Misalinement Displacement Experiments

Variations in displacement were obtained by varying the misalining couple and holding the central load constant at constant speed and constant inlet oil pressure. It was found that by operating under these conditions the variations in bearing temperature were small. A nearly constant temperature of the apparatus at thermal equilibrium assured a minimum thermal effect in the measurements. Prior to taking data the test elements and the measuring apparatus were brought to equilibrium temperature by running at constant speed and central load for a period of 20 to 30 minutes.

At the end of the warm-up period, the central load and the inlet oil pressure were reduced to zero so that the indicator dials could be set to a datum position representing zero displacement of the journal relative to the bearing. The central load and inlet oil pressure were then applied and held constant. Displacement data as read from the four dials were then recorded for various increments of axial misalinement couples. The misalining load was increased in 4 to 8 increments and then decreased in the same increments to permit averaging of data. To allow further averaging of data, the same increments of axial misalining weights were then applied on the "left" end of the bearing if the first set of weights had been on the "right." As shown in the sample log sheet of table I, the following data were recorded: Journal displacements, capsule pressure of central load, misalining weights, bearing temperatures at critical locations, inlet oil pressure, speed, direction of rotation, time, inlet oil temperature, room temperature, and oil temperature after the heater. The same procedure was followed for the opposite direction of rotation so that the data could be averaged for the two rotations.

Axial misalinement experiments were then repeated at the same speed and oil pressure at increased central loads. Further experiments were made at the same speed and oil pressure to obtain data for twisting misalinements at the same conditions of central load as in the axial misalinement runs. Constant-speed runs at approximately 1,200, 2,500, and 5,000 rpm were conducted for each of the five test shafts to determine the effects of l/d and clearance on bearing misalinement characteristics.

For all tests a constant inlet oil pressure of 80 pounds per square inch at 140° F (at the heater) was used. The maximum applied central load in the tests was 1,290 pounds for shaft 6A, and the maximum unit central load on projected area was 600 pounds per square inch on shaft 6D. The maximum value of misalining couple applied was 287.5 inch-pounds (on

shaft 6A) obtained by applying the maximum misalining weight of 20 pounds. In the axial misalining experiments the moment arm of the couple was $18\frac{3}{4}$ inches, and in the twisting misalining experiments, $14\frac{3}{8}$ inches. Maximum bearing temperature recorded was 179° F at 5,000 rpm.

Oil Flow Measurements

A few oil-flow-rate experiments were conducted under conditions of axial and twisting misalinement using shafts 6A and 6C, at values of l/d of 2 and 1.5. At each misalining load, after the oil flow reached the steady state, the flow rate was measured by collecting the oil in a pan for periods of 1 to 2 minutes and recording the net weight of oil. Several central loads were applied. The chief variable affecting the oil flow rate was the central load, and the effect of applying misalining couples was negligibly small by comparison.

RESULTS

The major results of this investigation are summarized in the curves shown in figures 7(a) to 7(d) in which the couple variable is plotted versus the Sommerfeld or capacity number for central load with misalined attitude as a parameter. These charts are in the form of design charts to determine the relation between the couple and the misalined attitude of a bearing having a central load. Figures 6(a) to 6(d) show the experimental data giving the couple variable as a function of load ratio; these data, when combined with the curves of figures 5(a) and 5(b), eliminate load ratio and permit the plotting of the design charts of figures 7(a) to 7(d).

Figures 14(a) to 14(d) present experimental data of couple variable versus load ratio for the individual bearings of shafts 6A, 6B, 6C, and 6D, each representing a given l/d and d/c_d. These four figures have been combined in figure 6(a) to give the axial misalining characteristics of long bearings ($l/d \geq 1.0$) as a function of load ratio. Similar individual experimental charts were used to obtain the summary curves of figures 6(b), 6(c), and 6(d) but only the summary curves are presented.

To show graphically the range of the experimental program in regard to magnitudes of misalined attitude m_a, load ratio L_R, and Sommerfeld number S or capacity number C_n, the 12 sets of curves in figures 15(a) to 15(l) are presented. The first six figures, figures 15(a) to 15(f), show the range of m_a, L_R, and S or C_n for each of the five shafts in the axial-misalinement experiments; similar curves are shown for the

twisting-misalinement experiments in the second set of six figures, figures 15(g) to 15(l). As may be seen, maximum values of m_a of 1.0 were reached. The maximum load ratio attained was in the neighborhood of 10, and the range of Sommerfeld or capacity numbers was from a minimum of 0.045 to a maximum of 0.45. Misalinement data with zero central load cannot be plotted in these charts because the load ratio is infinite for all values of m_a. As already mentioned, zero central load has been considered a separate case in order to expedite the test program.

Polar diagrams are presented in figures 16(a) to 16(d) to show pictorially the eccentricity ratios at the two ends of the bearing as misalining couples are applied. They show also the effect of the central load on the end eccentricity ratios. Curves for shafts 6A ($l/d = 2$) and 6D ($l/d = 1.0$) only are shown, two sets of curves for axial misalinement and two sets for twisting misalinement.

Curves of oil flow rate as a function of misalinement are given in figures 17(a) and 17(b). The curves show the ratio of Q_m/Q which is the oil flow rate with a misalinement couple and central load divided by that for central load alone. Axial misalinement tends to decrease oil flow slightly, whereas twisting misalinement slightly increases it.

Calculations of the several nondimensional quantities are shown in the sample calculation sheet, table II. The necessary data for the calculations are given in the sample log sheet of table I.

Phenomena at Zero Central Load

A number of misalined experiments were conducted at zero central load obtained by counteracting the effect of gravity on the parts. These experiments, and others at very light central loads, were unsatisfactory because of what appeared to be two possible values of displacement for a given couple. On application of the couple, an apparently stable displacement was noted; however, with the elapse of several minutes of time, the displacement suddenly changed to a higher value. In central-load experiments without misalinement (ref. 3), similar instabilities were encountered with very light loads. With misalinement, it was again noticeable that inlet oil pressure influenced displacements at lightly loaded conditions. By using inlet oil pressures of 20, 40, and 80 pounds per square inch in the misalinement experiments at zero central load, it was found that the bearing was "stiffer" against misalinement as the oil pressure was increased; that is, the misalining displacements were smaller. However, higher oil pressures did not eliminate the double displacements although the difference between the high and low values was reduced somewhat.

Misalined Attitude

In order to determine the misalined attitude m_a from equation (6), it was necessary to calculate n_e and n from the measured displacements. Coordinate vertical and horizontal displacements of the shaft were measured at the riders which are located beyond the ends of the bearing $1\frac{11}{16}$ inch to the left and to the right of the center line of the bearing as shown in figure 9.

A typical set of displacement data for a misalinement run is shown in table I. Eight observations of a coordinate displacement were averaged to determine the mean value of the displacement for a given couple. For example, for a given misalining weight placed at the "right" as shown in figure 10, the maximum vertical displacement is at the left end of the bearing. For the left end, two vertical displacement values were taken as the misalinement load was increased and then decreased. For the same misalining weight placed at the "left," the two up and down observations were read at the right end. Four more similar observations were made for the opposite direction of rotation of the journal. All eight observations were then averaged directly to yield a mean value of vertical displacement. A similar value was obtained for the horizontal displacement, thus arriving at the coordinates of the displacement at the riders at one end of the bearing for a given misalining couple. For the same couple, the coordinates of the displacement at the other end of the bearing were also determined in a similar manner.

Corrections, datum point.- The slight displacements at zero load and zero inlet oil pressure, at which it was assumed that the journal and bearing axes were coincident, were averaged and subtracted from the averaged values of displacement under misalinement. All displacement values were then halved because of the 2-to-1 multiplication of the measuring system.

Corrections for slope.- The displacements discussed above are at the riders rather than at the ends of the bearing as shown in figure 18. Because of the inclined attitude of the journal relative to the bearing axis, it was necessary to make a correction for slope to determine the eccentricities at the end boundaries of the bearing. Similar triangles are used in making the correction, and, to simplify calculations, these corrections for slope were made graphically. Both horizontal and vertical end eccentricities were corrected in this manner.

Deflection corrections.- Another correction was made to account for the deflection of the shaft by the central load. As shown in figure 18, the shaft axis was assumed to be bent by the central load in a symmetrical parabolic shape lying in the vertical plane. Bending by the misalining couple was assumed negligibly small compared with the central-load

deflection curve. Calculations of shaft bending deflection were based on a uniformly distributed central load over the length of the bearing and varying moments of inertia for the slightly stepped shaft. Since the experimental shaft was bent, corrections for deflection were made to give the vertical end eccentricities e_{e_V} of a straight journal as shown in figure 18. By simulating the displacement of a straight journal in this manner, the data presented are intended to represent characteristics of an ideal straight journal and bearing to facilitate application of the user's actual deflection. By comparison to the centroid of a fourth-degree parabola, the axis of the straight journal is located below the apex of the parabolic curve by one-fifth of the height of the deflection curve within the bearing length as shown in figure 18. No deflection corrections were made in determining horizontal end eccentricities because the central load acts in the vertical plane, other deflections being negligible.

In determining the eccentricity e for the condition of zero misalinement with central load, corrections were made for deflection but those for slope were accomplished by averaging. The measured displacements at the two ends invariably showed a slight slope indicating the existence of a small misalining couple due to an unavoidable remaining eccentricity of the central load. By averaging the displacements of both ends, an average eccentricity of the journal under central load was determined. Any tare misalinement present in the misalinement data is greatly minimized, if not eliminated, by averaging right and left misalinement displacements as discussed in an earlier paragraph.

Bearing clearance at running temperature.- The bearing clearance for running conditions was determined by subtracting the change in clearance given in figure 19 from the clearance at room temperature. The curve of figure 19 represents the calculated change in clearance caused by differential thermal expansion of bearing and journal as a function of the temperature gradient in the bearing housing. Thermocouple 4 and thermocouple 9 were 1/16 inch and 2 inches, respectively, from the bearing surface giving temperatures T_4 and T_9 which are indicative of the temperature gradient in the bearing wall. The slope of the curve indicates a change in diametral clearance of 0.00001 inch per $^{\circ}F$ of the temperature difference $(T_4 - T_9)$.

This slope is approximately one-third of the slope of the curve used in an earlier report of this investigation (ref. 3). Additional study indicates that the earlier slope should theoretically be smaller and would slightly reduce the spread of the earlier data. The differential expansion problem has been re-evaluated analytically after Timoshenko (ref. 4). The larger slope obtained by the earlier experimental "seizure" method may be explained by the possibility that the experiment curve does not allow for the thermal and elastic stresses set up in the instant before seizure.

Coordinates of displacement.- For the condition of zero misalinement with central load, the eccentricity ratio n was determined from

$$\left.\begin{aligned} n_v &= \frac{e_v}{c_r} \\ n_h &= \frac{e_h}{c_r} \\ n &= \sqrt{n_v^2 + n_n^2} = \frac{e}{c_r} \end{aligned}\right\} \tag{12}$$

where the subscripts v and h indicate the vertical and horizontal components of the eccentricity e and the eccentricity ratio n. The radical clearance at running conditions is c_r.

For misalinement conditions, the eccentricity ratios n_e at the ends of the bearing were determined from

$$\left.\begin{aligned} n_{e_v} &= \frac{e_{e_v}}{c_r} \\ n_{e_h} &= \frac{e_{e_h}}{c_r} \\ n_e &= \sqrt{n_{e_v}^2 + n_{e_h}^2} = \frac{e_e}{c_r} \end{aligned}\right\} \tag{13}$$

Although the end eccentricity ratios were calculated for both ends of the bearing, the important value of the two in determining misalined attitude m_a was the maximum value of eccentricity at one end of the bearing.

Misalined attitude m_a was determined from equation (6). Experimental values of m_a as determined above are shown in figures 15(a) to 15(l). As a function of load ratio and S or C_n, experimental data of n and n_e (for both ends) are shown as a function of attitude angle ϕ in figures 16(a) to 16(d).

Sommerfeld Number and Capacity Number

Determinations of Sommerfeld number S and capacity number C_n are based on the unit value p of the applied central load and are not dependent upon misalinement. For any given experimental run, the bearing variables grouped in S or C_n as given in equation (1) were constant as different misalining couples were applied. Oil film viscosity μ and the diametral clearance c_d are taken as constant in a given run because of the relatively small temperature variation. As shown in the sample log sheet of table I, misalining couples caused only a small change in temperature so that average values of T_4 and T_9 for the run were used in determining μ and c_d. Viscosity values for the SAE 10 oil were taken from the curve of figure 20. The unit central load p on projected area was determined from $p = P/ld$, and the total central load P applied by the piston was calculated from $P = 5.0(p_c - 12.5)$ where p_c is the capsule pressure acting on the piston area of 5.0 square inches, and 12.5 pounds per square inch represents the tare weight of the bearing and the apparatus attached to the bearing housing. The load piston was arranged to provide either of two areas of 15 or 5 square inches.

Load Ratio

Load ratio L_R was calculated from equation (5) as the ratio S/S_e or C_n/C_{n_e} in which S_e and C_{n_e} are the equivalent Sommerfeld and capacity numbers related to point c in figure 3(a). Values of S_e were taken from the experimental curve of central-load eccentricity ratio of figure 4(b) for long bearings of $l/d \geq 1.0$. For a given misalining couple, the larger value of n_e of the two ends of the bearing was used to determine S_e. In this way, n_e is regarded as the eccentricity ratio n of a bearing with an increased equivalent central load at a correspondingly decreased Sommerfeld number. The load ratio then is the ratio of the two Sommerfeld numbers or the two central loads. At zero misalinement the load ratio is 1.0 and for increasing misalinement the load ratio increases and is always greater than 1.0. For short bearings of $l/d \leq 1.0$, the experimental curve of 4(c) was used to determine load ratio.

Couple Variable

The nondimensional grouping of numbers including the misalining couple M appears in two forms, one of which applies to long bearings ($l/d \geq 1.0$) and the other, to short bearings ($l/d \leq 1.0$):

$$C_m = \frac{M}{Pl}\left(\frac{d}{c_d}\right)^{1/2}\left(\frac{l}{d}\right)^{1/2} \quad \text{for long bearings} \tag{10}$$

$$C_m = \frac{M}{Pl}\left(\frac{d}{c_d}\right)^{1/2}\left(\frac{l}{d}\right)^{1/2}\left[\frac{1}{\left(\frac{l}{d}\right)^2}\right] \quad \text{for short bearings} \tag{11}$$

Here C_m is the couple variable and M is the misalining couple called M_a for axial misalinement and M_t for twisting misalinement. The experimental values of M_a were determined by multiplying the misalinement weight in pounds by the moment arm of $18\frac{3}{4}$ inches; for M_t the moment arm was $14\frac{3}{8}$ inches.

Couple variable appears as a function of load ratio in the four summary curves of figure 6 and in the curves of figure 14 for the individual shafts. Couple variable appears also in the design charts of figure 7 in which load ratio is eliminated.

ANALYSIS AND DISCUSSION

Method of Attack

Referring to figure 3(a), it can be seen that for a given curve for the central-load case (fig. 4) a cross plot can be set up showing the relation between arbitrary values of misalined attitude m_a and the corresponding values of load ratio L_R as shown in figure 5. It remained to find a curve showing the relation between the load ratio L_R and the couple variable by experimental tests. After this curve became available a chart was set up showing the relation between misalined attitude and the couple variable directly, thus eliminating the load ratio.

This method of attack has the advantage of making available the information most needed, that is, the effect on oil film thickness or maximum eccentricity at the end of the bearing, cutting through the intricacies of coordinate location shown in figure 3(b) and figure 16. Curves are presented which show these relations for several cases of l/d ratio for both axial and twisting misalining couples.

Nearly Motionless Pivot Point

The polar diagrams of figure 16 indicate that the central eccentricity n_c of the bearing with misalinement remains very nearly at the value of n for central loading. At light central loads, the central eccentricity tends to show the greatest change in position. Figure 21 shows the change in position of the central eccentricity for a typical lightly loaded case. It is interesting to note that the change in position is a change in attitude angle with almost no change in eccentricity. For practical purposes, it may be concluded that $n_c = n$ represents a point in the central plane of the bearing about which the journal axis pivots. This phenomenon is useful in determining the angular limits for misalinement.

Effect of Angular Misalinement on Bearing Eccentricity

The concept of the motionless pivot point facilitates calculating the effect of the angular misalinement and shaft deflection on a bearing. If the slope of the deflection curve is calculated, it may be assumed that the location of the center of the misalined journal is given by the eccentricity ratio n for central loading. The shaft deflection in the half bearing length in the form of e/c_r can be added vectorially to the central eccentricity ratio to obtain the eccentricity ratio at the bearing end n_e. At high values of n_c, where n_c is nearly parallel to the load, little error results if e/c_r is added directly to n_c.

Effect of a Couple on Misalined Attitude

Another useful form of the experimental data of this investigation appears in the four curves of figure 7 in which the misalined attitude m_a may be used as a limiting criterion to determine the couple capacity of a misalined bearing acted upon by a central load. A misalined attitude $m_a = 1.0$ is the limit at which contact of the bearing surfaces occurs at the bearing end. A factor of safety is needed to limit the allowable value of m_a at a reasonable value less than 1.0.

For a given misalinement attitude, the couple variable C_m permits the determination of the couple in terms of the central load.

For the extreme condition where the central load is great enough for n to approach one, the allowable couple is zero.

The curves of figure 7 do not by test data embrace the opposite extreme of zero central load where S, C_n, and C_m are infinite.

However, as will be shown later, the curves show that the couple passes through a maximum value and is falling as the load reduces further.

Effect of a Couple on Load Ratio

The meaning of figures 6(a) and 6(c) can be illustrated best by an example. Assuming a bearing with a length-diameter ratio of 1 and a clearance-diameter ratio of 0.0025, the value of the couple variable then becomes

$$C_m = \frac{M_a}{Pl}\left(\frac{1}{0.0025}\right)^{1/2} (1)^{1/2} \frac{1}{(1)^2}$$

$$= \frac{M_a}{Pl}(400)^{1/2}$$

$$= \frac{M_a}{Pl}(20)$$

If a value of $M_a/Pl = a/l = 10$ percent is assumed, the couple variable has a value of $0.10(20) = 2$, giving a value of load ratio of 2.2 on both 6(a) and 6(c). This means that for this example 10-percent misalinement reduces the oil film thickness locally at one end to a value given on figure 4(a) by multiplying the central load by 2.2.

If a value of 25-percent misalinement is used, the couple variable is 25 percent of 20 or 5, giving a load ratio on 6(a) of 5.8 for long bearings and on 6(c) of 8.5 for short bearings. Apparently 25 percent is approaching a practical limit of a/l.

The load ratio L_R is the variable which appears to be basically a function of the couple variable C_m as shown in the four curves of figure 6. The form of the couple variable as shown was determined empirically by trial-and-error processes. Dividing the misalining couple M by the load P and the bearing length l was the first step used to determine a nondimensional form: M/Pl. In the case of axial misalinement, M may be regarded as the couple Pa produced by axially offsetting the central load a distance such that $M/Pl = a/l$. In the case of twisting misalinement, the offset ratio does not have the same physical meaning as for axial misalinement. However, M/Pl may be accepted as a nondimensional form for both cases of misalinement.

Couple variable.- By trial-and-error methods the terms $(d/c_d)^{1/2}$ were found to draw curves of M/Pl against L_R together. This was

especially apparent for the long-bearing experimental data of shafts 6A and 6B having the same l/d but significantly different clearances. Also, it was found that the term $(l/d)^{1/2}$ is influential in drawing together data for shafts having different values of l/d as in shafts 6A, 6B, 6C, and 6D. Studies were made to determine the effects of viscosity and speed on the couple variable, but no basic effects seemed apparent.

As shown in figures 6(a) and 6(b) for long bearings, the curves of couple variable C_m against load ratio L_R show that a bearing with central load has a greater couple capacity for twisting misalinement than for axial misalinement. A comparison of the numerical values of C_m as given in table III shows that the twisting-couple capacity is greater than the axial-couple capacity by a factor of approximately 1.4, but no reason has been found that would explain a need for a factor so near $\sqrt{2}$.

In the case of short bearings as in figures 6(c) and 6(d) the couple variable C_m is expressed in a somewhat different form because the central-load capacity of short bearings is sensitive to l/d ratio. It was found that by introducing $(l/d)^2$ in the denominator of the couple variable, the experimental data for shafts 6D ($l/d = 1.0$) and 6E ($l/d = 3/4$) were drawn together. This may be logical since the couple capacity of the short bearing depends upon the central-load-carrying capacity which includes a similar term. As shown in figure 4, central-load capacity of long bearings is almost independent of l/d whereas short-bearing central loading depends upon $(l/d)^2$. Axial and twisting values of C_m for short bearings in figures 6(c) and 6(d) are not as greatly different as in the case of long bearings. A comparison of numerical values as given in table III shows that the twisting misalining capacity is greater by a factor of about 1.2, approximately $\sqrt[4]{2}$.

That the twisting-couple variable should be greater than the axial-couple variable may be logical in that the extent of the load-carrying oil film may be greater. As shown in the plaster models of reference 1, the load-carrying film for central loading is small in angular extent. The inclination of the journal axis by axial misalinement causes the pressure distribution to shift without an appreciable increase in the extent of the working oil film. In the case of twisting misalinement the journal inclination causes a pressurization of the film in areas which represent an increase in working oil film extent and lever arm.

Couples in other planes.- The misalining characteristics of bearings determined by this investigation are limited to the two cases in which the couples are in either the plane of the central load or in a normal plane. For all other planes of the couple, the characteristics are still to be determined. However, since the numerical order of magnitude of the axial and twisting misalinement characteristics are not greatly different,

it may follow that for all other planes the characteristics may not be greatly different. A couple in an intermediate plane would involve a combination of coordinate couples in the axial and twisting planes at the same time, a condition which has not been investigated.

Double values at $l/d = 1$.- As may be seen in figures 6 and 7, for bearings of $l/d = 1.0$, two values of couple variable may be obtained, since $l/d = 1.0$ appears in both the long-bearing chart and the short-bearing chart. This is a direct consequence of using different experimental curves for central-loading characteristics as given by the curves of figure 4.

The experimental data for central loading in figure 4(a) are grouped well enough together to suggest the drawing of a single experimental curve through the data so that the number of curves in figures 5, 6, and 7 would be halved. In this way the long- and short-bearing axial misalinement characteristics of figure 7 would appear on one chart in which the classes of bearings would be distinguished only by the $(l/d)^2$ term in both the ordinate and abscissa following the device used in figure 4(a). However, this possibility deserves further study.

In figure 7 the zero value of the couple variable C_m corresponds with a small but finite value of S or C_n. In figure 7(a), for $C_m = 0$, $S = 0.02$. If the experimental curves of figure 4 were to pass through $S = 0$ at $n = 1.0$, as indicated by theory, then C_m would be zero at zero values of S or C_n.

Maximum couple.- It is not directly apparent from figure 7 under what condition a bearing carries the maximum couple. For a given value of m_a, the couple depends upon both the central load P and the couple variable C_m. However, C_m depends upon the central load as given in S or C_n. Therefore, as the central load is increased, the couple will increase with P but at the same time will decrease with C_m. Figure 22 has been prepared to illustrate numerically the magnitudes of the couple M as a function of the central load P for $m_a = 1.0$; numerical values of μ, N, l, d, and c_d are given, and M and P are calculated in inch-pounds and pounds, respectively. It may be seen that the ability of a bearing to resist misalinement increases as the central load increases up to a given point and that at very high central loads the couple capacity then decreases rapidly to zero as the central load becomes great enough to give $n = 1.0$. The two sets of maximum curves reflect the double values obtainable at $l/d = 1$, as discussed above.

Point contact at end of a bearing.- Figure 15 shows that many experimental data points were in the vicinity of $m_a = 1.0$, and in some cases

this value was exceeded. The actual end eccentricities as tested were slightly greater than those shown because the plotted data give values of n_e and m_a for an ideal straight shaft. During the experiments there was no visible indication that a value of $m_a = 1.0$ was a sign of impending bearing failure as in the case of central loading where n approaches 1.0. A possible explanation is that the area of metallic surface contact is smaller for misalinement than for central loading; also for soft bearing metals such as bronze or babbitt, the point contact by misalinement is more easily accommodated than is the line contact by central loading. Because of the small magnitude of the loads involved in incipient point contact under misalined loading, the heat generated is small and causes less temperature rise. The increase in load that can be carried by boundary lubrication appears to be appreciable.

The approach to the misalinement problem taken by this investigation has been a simplified one in which quantitative relationships including attitude angle are absent. The attitude angles of the end and central eccentricities apparently are also a function of the applied misalining couples. An analytical solution of misalinement behavior is needed to reveal practical methods of plotting attitude-angle data.

CONCLUSIONS

The following conclusions may be drawn from the results of this experimental investigation of misalining couples and eccentricity at the ends of misalined plain bearings:

1. The experimentally determined characteristics of misalined journal bearings are summarized in the form of design charts which show the relation between the misalining couple and the misalined attitude of a bearing having a central load.

2. For practical purposes the center of the bearing may be assumed to remain at approximately the eccentricity for parallel central loading with the axes tilting about this point as a pivot as misalinement occurs. The displacement of the center of the journal caused by misalinement is practically negligible at heavy central loads. At light central loads the motion of the bearing center becomes measurable, tending to move along an arc at approximately the same eccentricity ratio.

3. Where two or more bearings are used on a shaft, the effect of angular misalinement and shaft bending deflection on oil film thickness can be estimated by calculating the slope of the deflection curve at the bearing and applying the slope correction in the bearing half length about a pivot point at the center located by the eccentricity ratio n

for central loading. Correction for the parabolic deflection curvature of the shaft within the bearing length may also be applied.

4. Single bearings have relatively little resistance to axial misalining couples, which are analogous to offsetting the line of action of the load away from the bearing center. Offsetting the load 10 percent of the bearing length away from the center reduces the oil film thickness locally at one end of the bearing to a film thickness corresponding to doubling the load at the bearing center. An offset of 25 percent in which the load line is half way between the bearing center and one end is comparable in local oil film thickness to increasing the central load over five times. These ratios apply to bearings having a length-diameter ratio of 1 or more, and a clearance-diameter ratio of 0.0025 or less. Twisting misalining couples have a similar but slightly smaller effect.

5. Misalinement has little effect on oil flow rate and bearing temperature if the amount of misalinement is small enough to prevent metallic contact.

6. The misalined attitude and the couple ratio appear to be fundamental variables and their use simplifies the treatment of misalinement. The exponents of the clearance ratio and the length-diameter ratio in the couple variable are empirically chosen and are a tentative approximation based on the data available.

The method of plotting misalined loading used in this report is limited to the case where a steady central load is not zero and the line of action of the load passes within the confines of the bearing length.

Cornell University,
Ithaca, N. Y., December 31, 1953.

REFERENCES

1. DuBois, G. B., Mabie, H. H., and Ocvirk, F. W.: Experimental Investigation of Oil Film Pressure Distribution for Misalined Plain Bearings. NACA TN 2507, 1951.

2. Walther, A., and Sassenfeld, H.: Pressure Distribution and Load in a 360° Bearing with an Inclined Shaft. Outline of Procedure with an Explanatory Example. Rep. No. 13. Sponsored Res. (Germany), British Dept. Sci. and Ind. Res.

3. DuBois, George B., and Ocvirk, Fred W.: Analytical Derivation and Experimental Evaluation of Short-Bearing Approximation for Full Journal Bearings. NACA Rep. 1157, 1953. (Supersedes TN 2808 and TN 2809.)

4. Timoshenko, S.: Strength of Materials. Part II – Advanced Theory and Problems. Second Ed., D. Van Nostrand Co., Inc., 1941, pp. 258-264.

TABLE I.- SAMPLE LOG SHEET FOR DISPLACEMENT AND OIL FLOW MEASUREMENTS FOR SHAFT 6A

(a) Displacement measurements; axial-misalinement run; $18\frac{3}{4}$-in. couple arm.

[$l/d = 2$; 1,200 rpm; $p_o = 80$ lb/sq in.; SAE 10 oil; $d = 1\frac{3}{8}$ in.; $l = 2\frac{3}{4}$ in.; $c_d = 0.00252$ in. (room temperature); bronze bearing; steel shaft; 1/8-in.-diameter oil hole opposite central load]

Time	Shaft rotation (a)	Speed, rpm	Capsule pressure, lb/sq in.	Displacements by dials, in.				Temperature, °F, in thermocouple at –							°F	Test oil			Misaligning couple		
								Test bearing													
								Loaded side			Unloaded side	Block	Oil inlet	Air							
				Left vertical	Right vertical	Left horizontal	Right horizontal	1	4	7	14	9	16	24	Room temperature by thermometer,	Type	Temperature after heater,	Inlet pressure, lb/sq in.	Type	Direction	Weight, lb
2:03	CW	1,200	12.5	0	0	0	0	---	---	---	---	---	---	--	--	---	---	0	-----	-----	0
			12.5	0	-2 x 10^{-5}	0	0	128	128	128	126	122	114	82	82		140	80	-----	-----	0
			270	232 x 10^{-5}	237	-68 x 10^{-5}	-81 x 10^{-5}	131	131	131	128	124	132						-----	-----	0
				259	212	-63	-85	132	132	132	129	124	132						Axial	Right	3
				288	187	-60	-92	132	132	132	130	126	134								7
				308	171	-57	-92	133	133	133	130	126	133								10
				332	140	-50	-97	133	133	133	130	126	134								14
				308	172	-51	-94	134	134	134	131	127	134								10
				290	191	-57	-87	134	134	134	130	127	134								7
				265	218	-62	-85	134	134	134	130	127	134								5
				240	238	-69	-81	134	134	134	131	128	134						-----	-----	0
			12.5	3	-1	-8	-3	134	134	134	131	128	130						-----	-----	0
			12.5	-5	0	-9	-3	---	---	---	---	---	---					0	-----	-----	0
			12.5	1	-3	-8	-3	133	133	133	132	128	121			SAE 10		80	-----	-----	0
			270	237	239	-78	-81	134	134	134	131	128	134						-----	-----	0
				220	259	-79	-82	134	134	134	132	128	134						Axial	Left	3
				188	282	-87	-79	135	135	135	132	128	134								7
				163	302	-87	-79	135	135	135	132	128	134								10
				134	325	-89	-78	135	135	135	132	128	134								14
				163	304	-88	-79	135	135	135	132	129	134								10
				187	283	-87	-79	135	135	135	133	129	134								7
				217	262	-87	-81	135	135	135	132	129	135								5
				232	241	-85	-87	135	135	135	133	129	135						-----	-----	0
			12.5	-6	-2	-9	-11	135	135	135	133	129	126						-----	-----	0
2:50			12.5	-10	-1	-9	-11	---	---	---	---	---	---					0	-----	-----	0
2:51	CCW		12.5	-10	2	4	17	---	---	---	---	---	---	--	--		140	0	-----	-----	0
			12.5	-7	2	5	18	132	132	132	131	129	120	82	82			80	-----	-----	0
			270	212	235	102	141	135	135	135	132	129	135						-----	-----	0
				192	253	98	142	135	135	135	132	129	135						Axial	Left	5
				169	272	97	139	135	135	135	132	129	134								7
				148	292	96	135	136	136	136	132	129	134								10
				128	317	100	132	136	136	136	132	130	135								14
				150	295	100	133	136	136	136	132	130	135								10
				163	269	98	138	136	136	136	132	129	133								7
				190	251	95	140	136	136	136	132	130	134								3
				209	237	92	141	135	135	135	133	130	135						-----	-----	0
			12.5	-9	7	7	29	135	135	135	132	130	128						-----	-----	0
			12.5	-9	3	7	24	---	---	---	---	---	---					0	-----	-----	0
			12.5	-10	3	3	22	134	134	134	132	130	122					80	-----	-----	0
			270	202	237	78	142	136	136	136	133	130	135						-----	-----	0
				218	218	77	142	136	136	136	133	130	134						Axial	Right	3
				233	192	77	142	136	136	136	133	130	134								7
				258	181	76	143	136	136	136	133	130	135								10
				279	153	70	144	136	136	136	133	130	136								14
				258	180	69	142	136	136	136	133	130	134								10
				233	195	70	144	136	136	136	133	130	134								7
				217	218	72	140	137	137	137	134	130	134								5
				198	200	74	141	137	137	137	134	130	136						-----	-----	0
			12.5	-13	0	0	22	135	135	135	134	130	124						-----	-----	0
3:30			12.5	-15	-1	0	21	---	---	---	---	---	---					0	-----	-----	0

[a] CW, clockwise; CCW, counterclockwise.

TABLE I.- SAMPLE LOG SHEET FOR DISPLACEMENT AND OIL FLOW MEASUREMENTS FOR SHAFT 6A - Concluded

(b) Oil flow measurements; twisting-misalinement run; $1\frac{3}{8}$-in. couple arm.

[l/d = 2; 1,200 rpm; p_o = 80 lb/sq in.; SAE 10 oil; d = $1\frac{3}{8}$ in.; l = $2\frac{3}{4}$ in.; c_d = 0.00252 in. (room temperature); bronze bearing; steel shaft; 1/8-in.-diameter oil hole opposite central load; $T_{h(av)}$ = 135° F; $T_{g(av)}$ = 127° F; μ = 2.06×10^{-6} reyn; c_d = 0.00246 in. (running temperature); $(d/c_d)^2 = 0.313 \times 10^6$; $(d/c_d)^{1/2} = 25.7$; P = 5(180 - 12.5) = 838 lb; p = 221 lb/sq in.; F' = 20 rpm; S = 0.059; $C_m = 0.0145\ M_t$]

Time	Shaft rotation (a)	Speed, rpm	Capsule pressure lb/sq in.	Temperature, °F, at thermocouple in — Test bearing: Loaded side: 1	4	7	Unloaded side: 14	Block: 9	Oil inlet: 15	Air: 24	Air temperature by thermometer, °F	Test oil: Type	Temperature after heater, °F	Inlet pressure, lb/sq in.	Misaligning couple: Type	Direction	Misaligning weight, W, lb	Oil flow: Flow, lb	Time, min	Flow rate, lb/min	Average flow rate, Q_{av}, lb/min	Q_{av}/Q (b)	Misaligning couple, M_t, in-lb (c)	Couple variable, C_m (d)	Misaligned attitude, ϵ_h (e)
2:50	CW	1,200	180	129	129	129	127	123	128	81	80		139	80	-------	-----	0	0.189	2	0.095	0.100	1.00	0	0	0
				130	130	130	128	124	129						Twisting	Right	5	.193		.097	.101	1.01	72	1.04	.25
				130	130	130	129	125	130								10	.195		.098	.102	1.02	144	2.08	.50
				132	132	132	130	126	130								15	.197		.099	.102	1.02	216	3.12	.88
				132	132	132	130	126	130						-------	-----	0	.199		.100					
				132	132	132	130	126	130						Twisting	Left	5	.200		.100					
				132	132	132	130	127	131								10	.203		.102					
				133	133	133	131	127	131								15	.205		.102					
3:40	CCW	1,200	180	—	—	—	—	—	—						-------	-----	0	.204		.102					
				133	133	133	131	128	132	81	80	SAE 10	139	80	Twisting	Left	5	.204		.102					
				134	134	134	131	128	132								10	.205		.103					
				134	134	134	132	129	132								15	.206		.103					
				134	134	134	131	128	131						-------	-----	0	.208		.104					
				134	134	134	132	128	132						Twisting	Right	5	.208		.104					
				134	134	134	132	128	132								10	.207		.104					
4:25				134	134	134	132	128	132								15	.206		.103					

[a] CW, clockwise; CCW, counterclockwise.

[b] Q = 0.100 lb/min.

[c] $M_t = 1\frac{3}{8}\ W$.

[d] $C_m = \frac{M_t}{Pl}\left(\frac{l}{c_d}\right)^{1/2}\left(\frac{l}{d}\right)^{1/2}$

[e] From fig. 7(b).

TABLE II.- SAMPLE CALCULATION SHEET FOR AXIAL MISALIGNMENT OF SHAFT 6A GIVING END ECCENTRICITY RATIOS, MISALIGNED ATTITUDE, LOAD RATIO, COUPLE RATIO, AND COUPLE VARIABLE

[$l/d = 2$; 1,200 rpm; $p_o = 80$ lb/sq in.; SAE 10 oil; $d = 1\frac{3}{8}$ in.; $l = 2\frac{3}{4}$ in.; $c_d = 0.00252$ in. (room temperature); $c_d = 0.00246$ in. (running temperature); $T_{h(av)} = 135^\circ$ F; $T_{g(av)} = 129^\circ$ F; $d/c_d = 0.558 \times 10^3$; $(d/c_d)^2 = 0.312 \times 10^6$; $(d/c_d)^{1/2} = 23.6$; N' = 20 rps; $\mu = 2.18 \times 10^{-6}$ reyn]

Misaligning weight, w, lb	Capsule pressure, p_o, lb/sq in.	Coordinate and displacements, in.				Misaligning couple, M_m, in-lb (a)	Central load, P, lb (b)	Coordinate end eccentricity ratios				Maximum end eccentricity ratio, n_e	$n_e - n$ (c)	Misaligned attitude, θ_m (d)	Equivalent Sommerfeld number, S_e (e)	Load ratio, L_R (f)	Couple ratio, M_m/Pl	Couple variable, C_m (g)
		Left vertical	Right vertical	Left horizontal	Right horizontal			Vertical, n_{e_v}		Horizontal, n_{e_h}								
								Left	Right	Left	Right							
Average displacements at riders (h).																		
0	0	-5×10^{-5}	-5×10^{-5}	----------	----------	0	0	0	0	0	0	0	-----	-----	-----	----	------	----
0	270	226	226	-96×10^{-5}	-96×10^{-5}	0	1288	+.658	+.658	-.391	-.391	.775	0	0	0.045	1.00	0	0
3	↓	248	211	-90	-101	56.3	1288	+.732	+.617	-.374	-.407	.821	.046	.204	.039	1.15	.0159	.53
7		269	184	-87	-104	131.3	1288	+.797	+.520	-.358	-.415	.874	.099	.440	.033	1.36	.0372	1.84
10		290	166	-85	-105	187.5	1288	+.862	+.472	-.350	-.423	.930	.155	.690	.026	1.61	.0530	1.77
14		313	139	-82	-108	262.5	1288	+.935	+.302	-.332	-.431	.992	.217	.965	.022	2.04	.0742	2.48
Correction for slope																		
0	0	-5×10^{-5}	-5×10^{-5}	----------	----------													
0	270	226	226	-96×10^{-5}	-96×10^{-5}													
3	↓	244	215	-91	-100													
7		260	192	-89	-102													
10		276	180	-86	-103													
14		294	158	-84	-105													
Division by 2																		
0	0	-3×10^{-5}	-3×10^{-5}	----------	----------													
0	270	113	113	-48×10^{-5}	-48×10^{-5}													
3	↓	122	108	-46	-50													
7		130	96	-44	-51													
10		138	90	-43	-52													
14		147	79	-42	-53													
-32×10^{-5} correction for: Zero 3×10^{-5}, Deflection -35																		
0	0	0	0	----------	----------													
0	270	81×10^{-5}	81×10^{-5}	-48×10^{-5}	-48×10^{-5}													
3	↓	90	76	-46	-50													
7		98	64	-44	-51													
10		106	58	-43	-52													
14		115	47	-42	-53													

[a] Couple arm = 18.75 in.; M_m = 18.75 W.

[b] Area of loading piston = 5.0 sq in.; $P = 5(p_o - 12.5)$.

[c] $n = 0.775$.

[d] $\theta_m = \frac{n_e - n}{1 - n}$.

[e] From experimental curve of fig. 4(b).

[f] $S = 0.045$; $L_R = \frac{\theta_m}{S}$.

[g] $C_m = \frac{M_m}{Pl}\left(\frac{d}{c_d}\right)^{1/2}\left(\frac{l}{d}\right)^{1/2}$.

[h] Averages of data in table I(a).

TABLE III.- COMPARISON OF AXIAL AND TWISTING MISALINING COUPLE CAPACITIES OF LONG AND SHORT BEARINGS

L_R	C_m(axial)	C_m(twisting)	$\frac{C_m(\text{twisting})}{C_m(\text{axial})}$
Long bearings			
	Fig. 6(a)	Fig. 6(b)	
1.0	0	0	----
1.5	1.05	1.70	1.62
2.0	1.75	2.45	1.40
3.0	2.70	3.70	1.37
4.0	3.55	4.90	1.38
5.0	4.40	6.05	1.38
6.0	5.10	7.10	1.39
7.0	5.85	8.15	1.39
8.0	6.60	9.20	1.39
9.0	7.35	10.25	1.40
Short bearings			
	Fig. 6(c)	Fig. 6(d)	
1.0	0	0	----
1.5	1.0	1.45	1.45
2.0	1.80	1.95	1.08
3.0	2.70	2.75	1.02
4.0	3.35	3.40	1.02
5.0	3.80	4.05	1.07
6.0	4.20	4.60	1.10
7.0	4.55	5.10	1.12
8.0	4.90	5.60	1.14
9.0	5.10	6.10	1.20
10.0	5.30	6.65	1.25

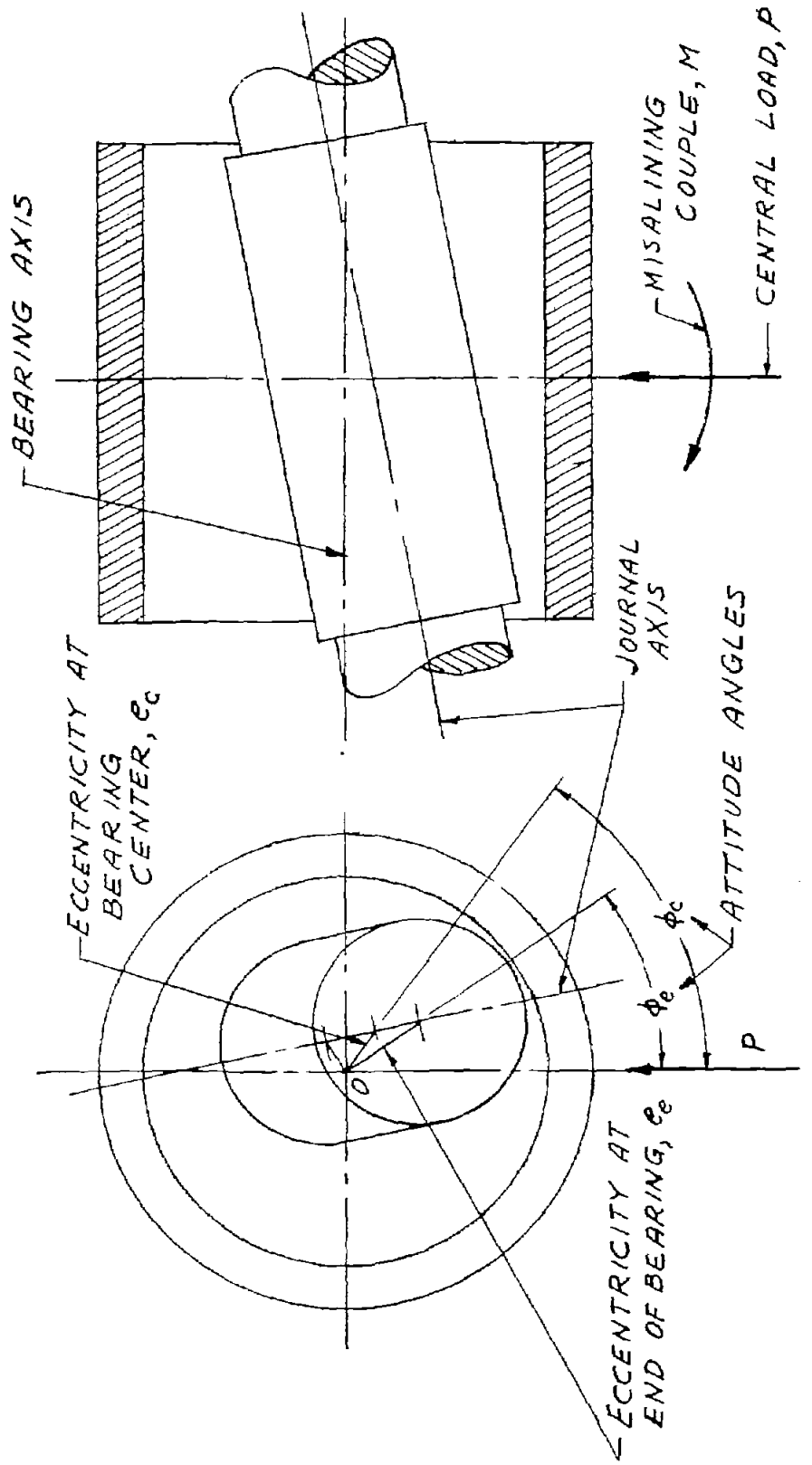

Figure 1.- Relative geometric configuration of journal and bearing axes for a bearing acted upon by a combination of central load and misaligning couple.

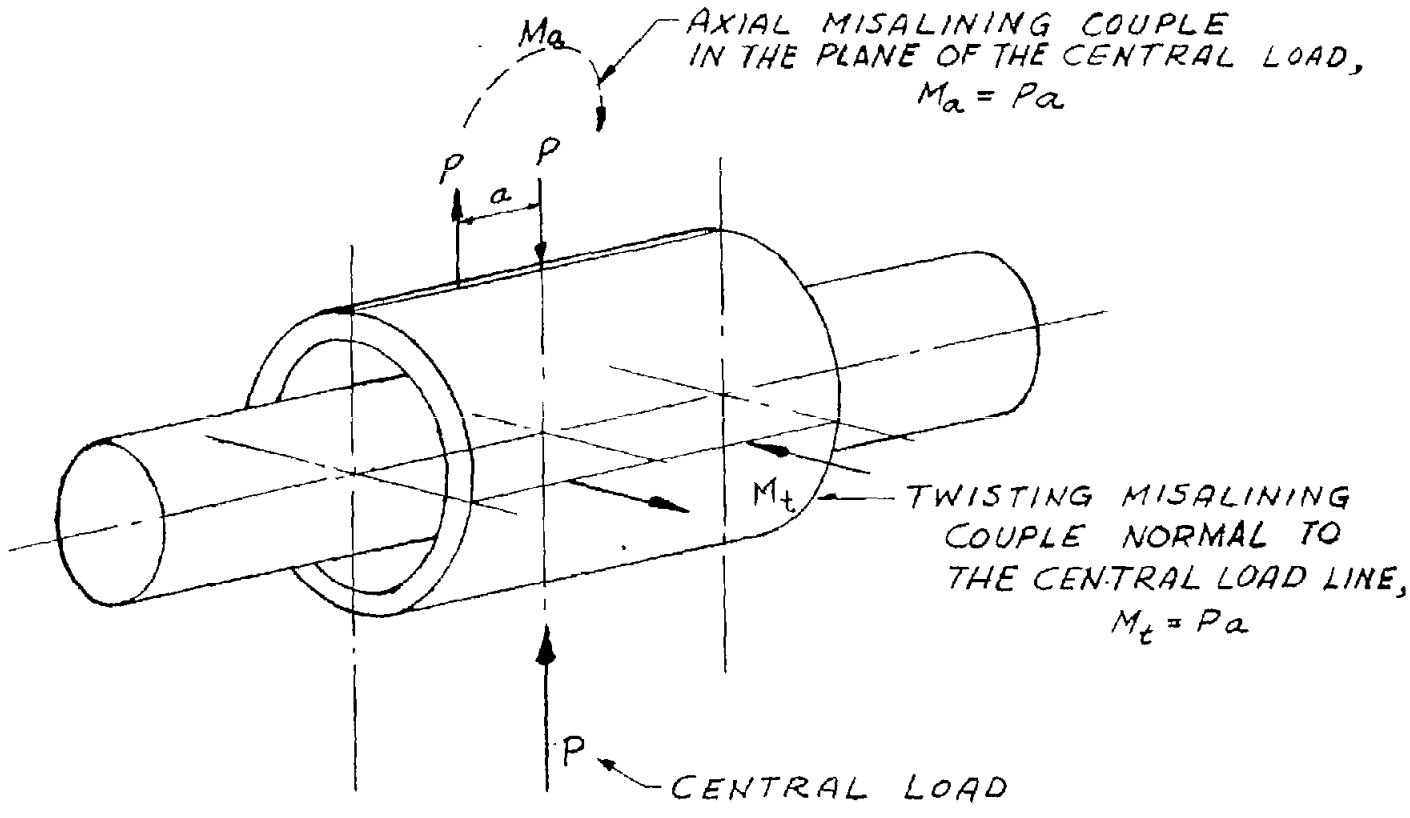

Figure 2.- Diagram showing planes of action of misalining couples relative to line of action of central load, as in experiments.

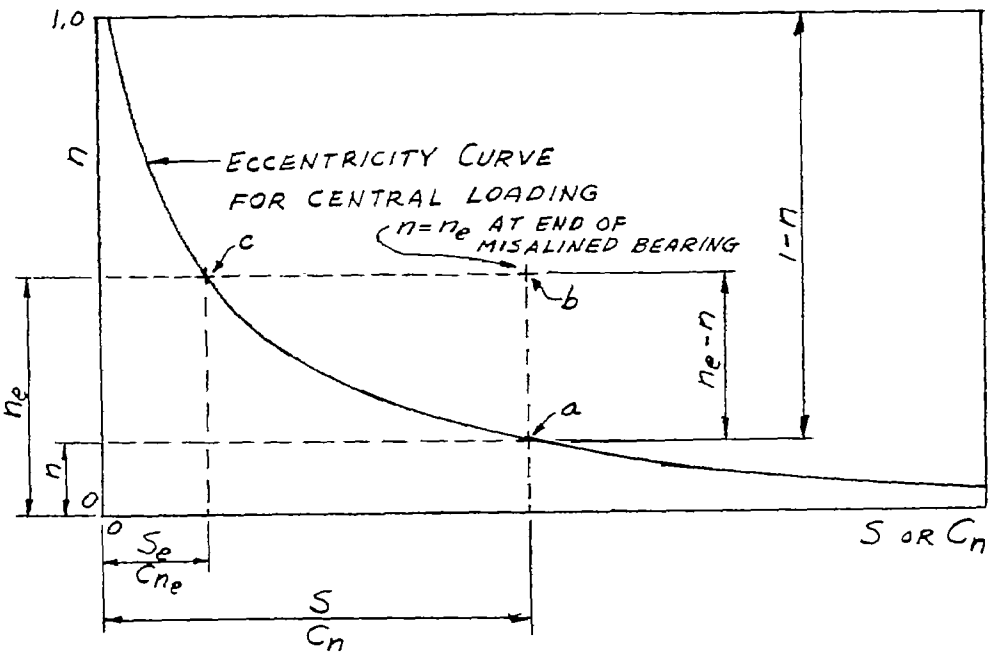

(a)

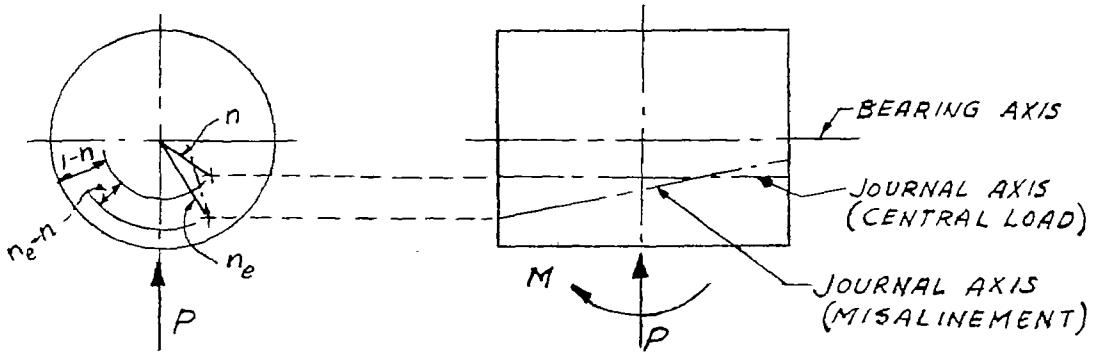

(b)

Figure 3.- Diagram showing method of approach to misalinement using concept of equivalent central load.

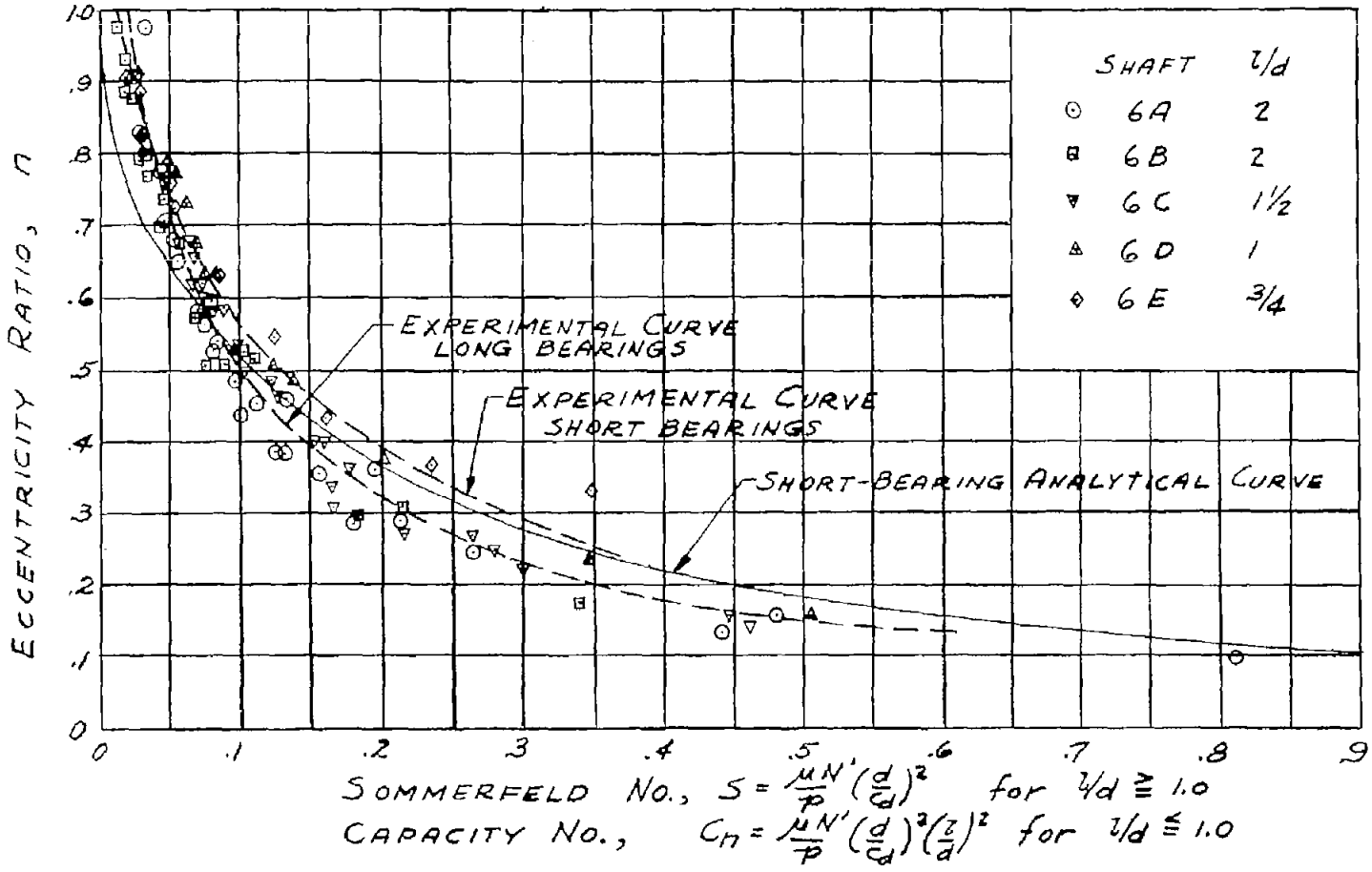

(a) Long and short bearings.

Figure 4.- Eccentricity ratio for central loading.

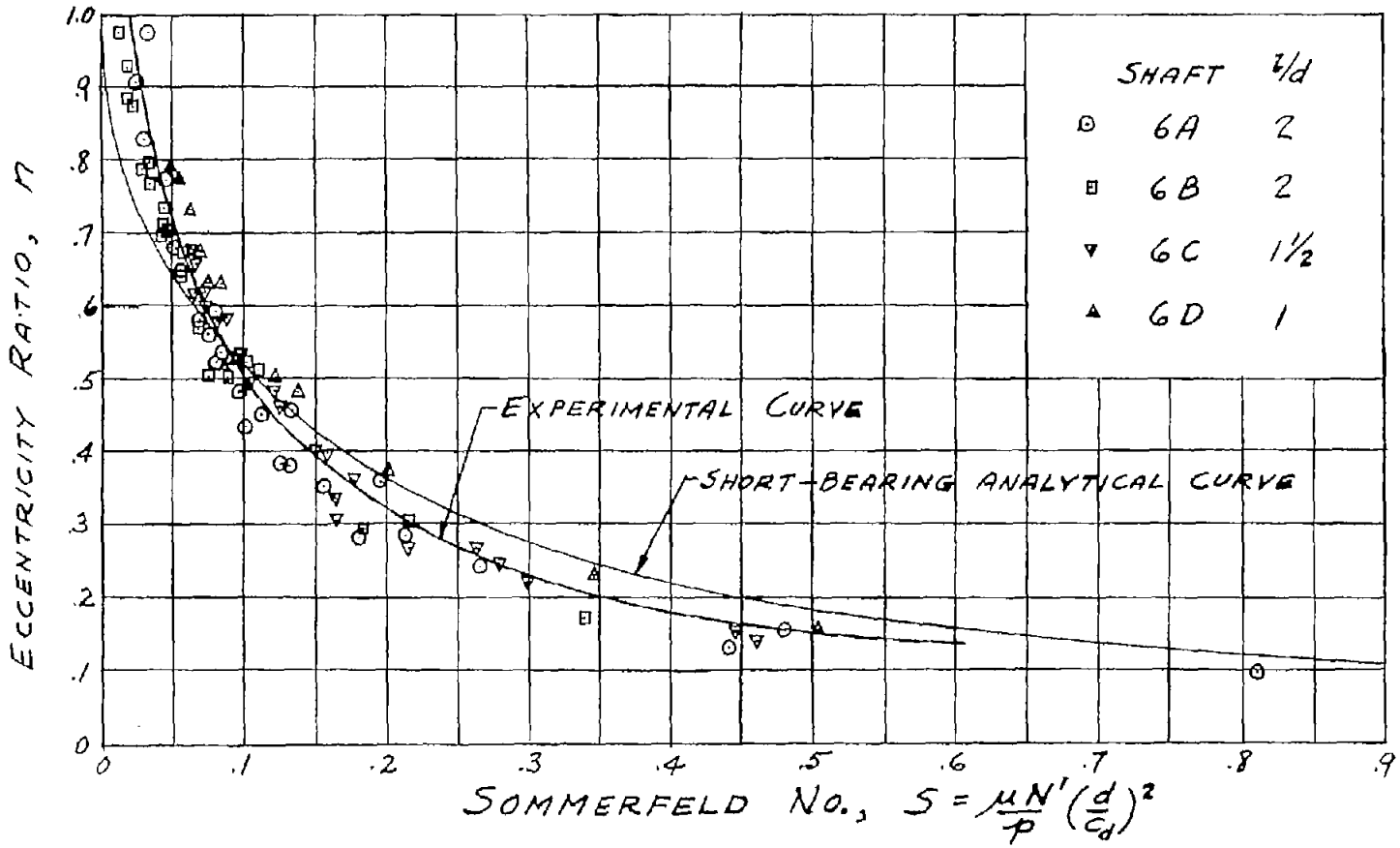

(b) Long bearings only, $l/d \geq 1.0$.

Figure 4.- Continued.

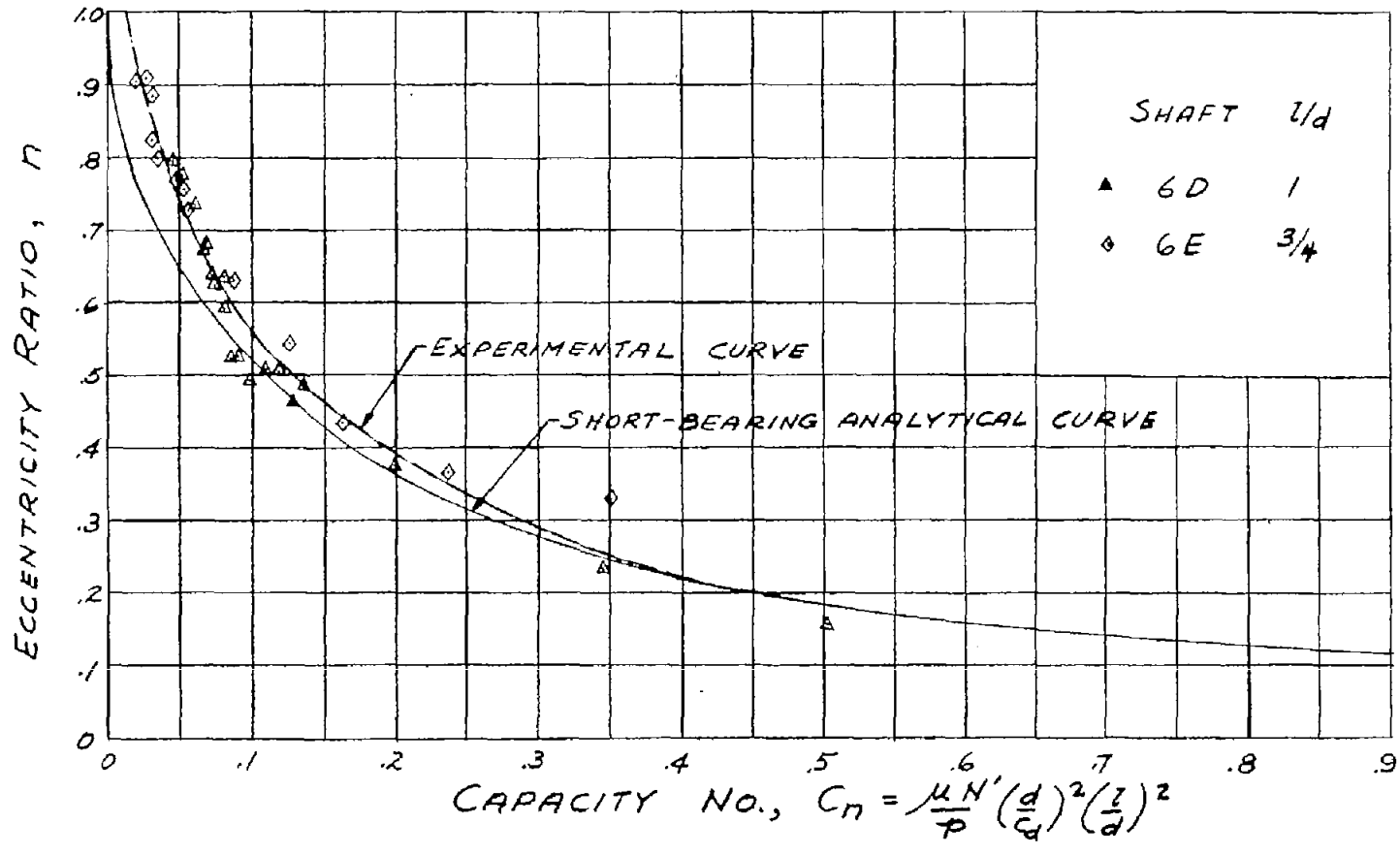

(c) Short bearings only, $l/d \leq 1.0$.

Figure 4.- Concluded.

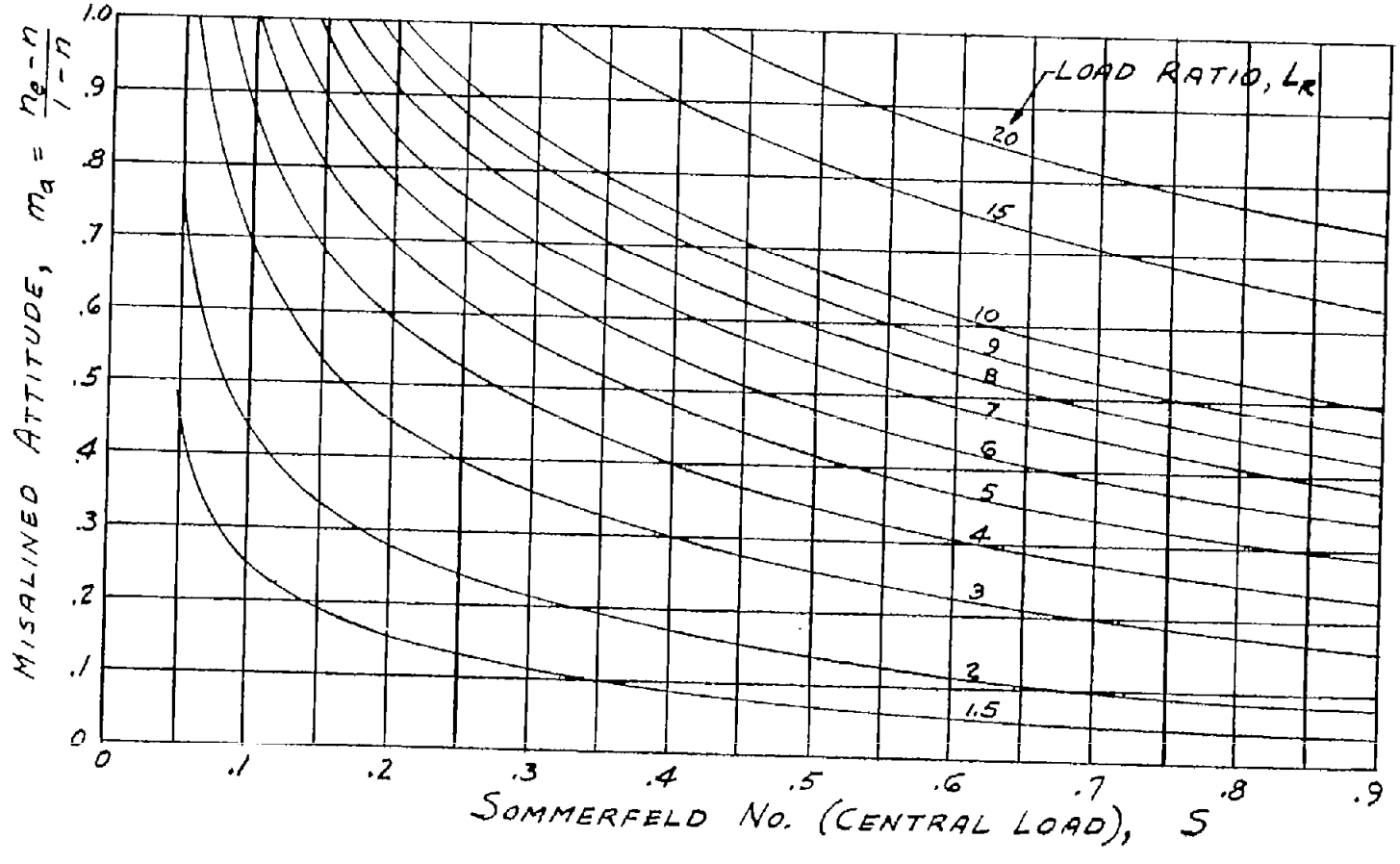

(a) Long bearings, $l/d \leq 1.0$. Curves determined from experimental curve of figure 4(b) and equations (5) and (6).

Figure 5.- Misalined attitude as a function of load ratio and Sommerfeld or capacity number.

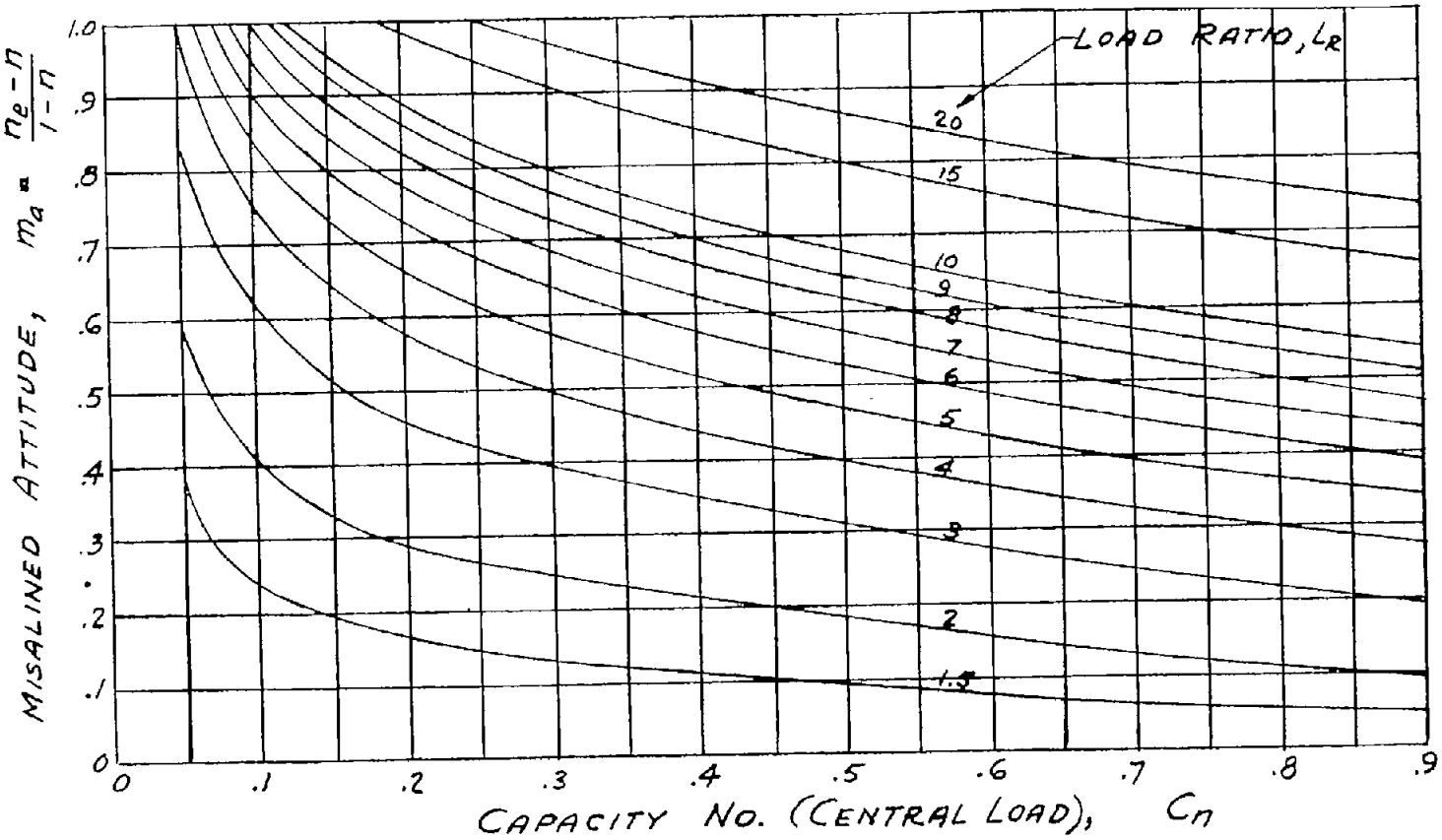

(b) Short bearings, $l/d \leq 1.0$. Curves determined from experimental curve of figure 4(c) and equations (5) and (6).

Figure 5.- Concluded.

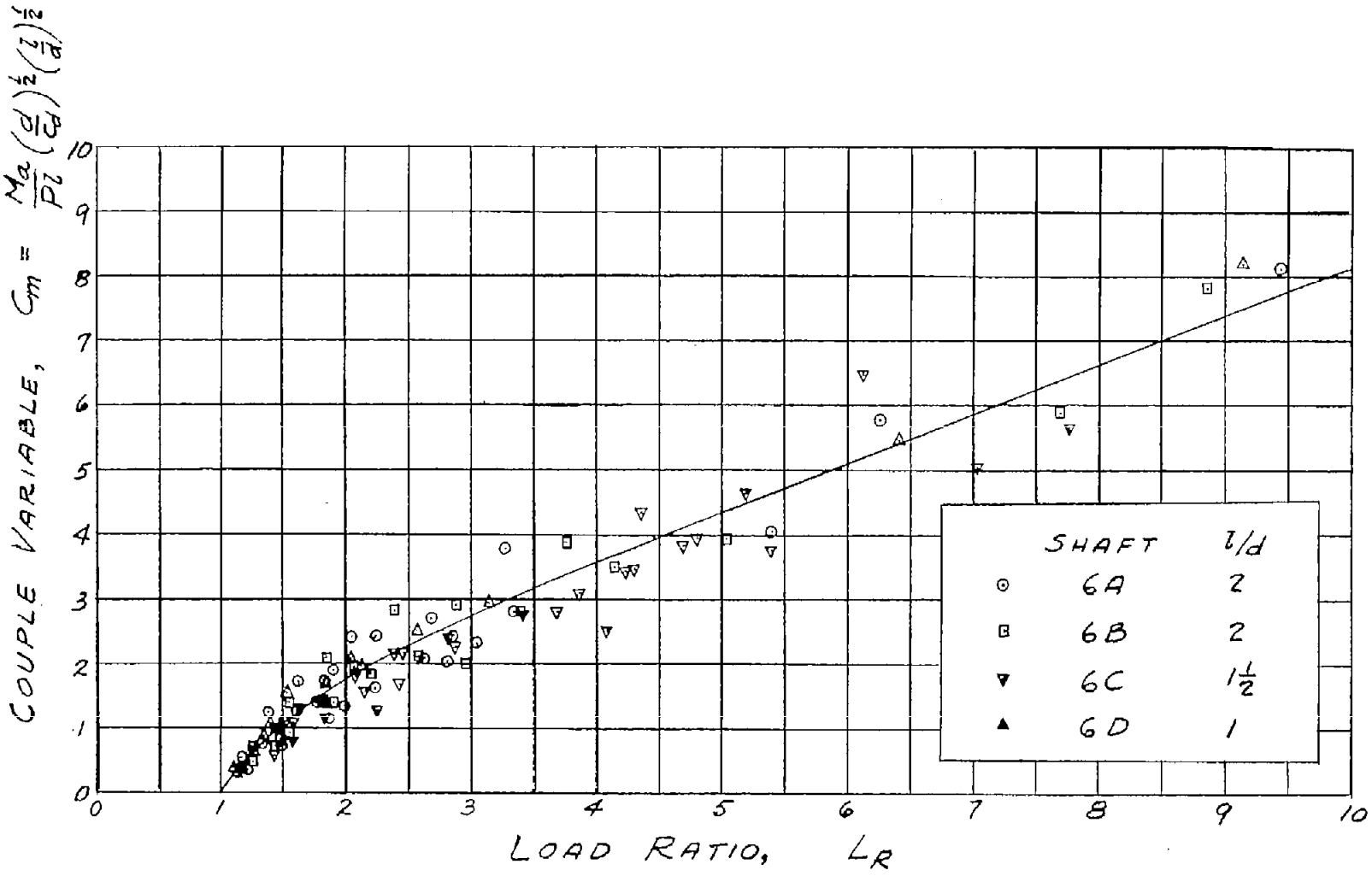

(a) Long bearings, $l/d \geq 1.0$ for axial misalinement.

Figure 6.- Couple variable as a function of load ratio; experimental data.

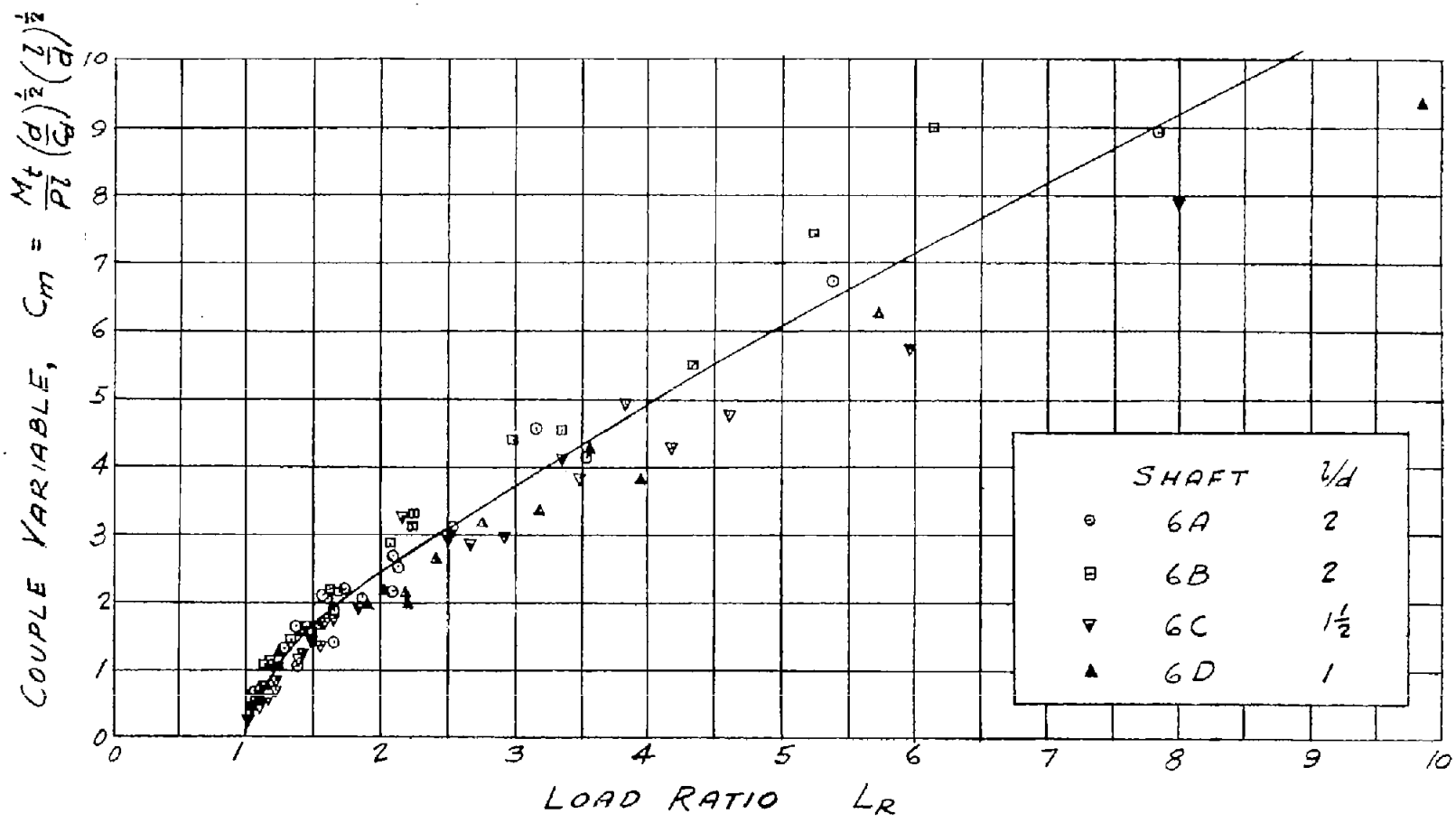

(b) Long bearings; $l/d \geq 1.0$ for twisting misalinement.

Figure 6.- Continued.

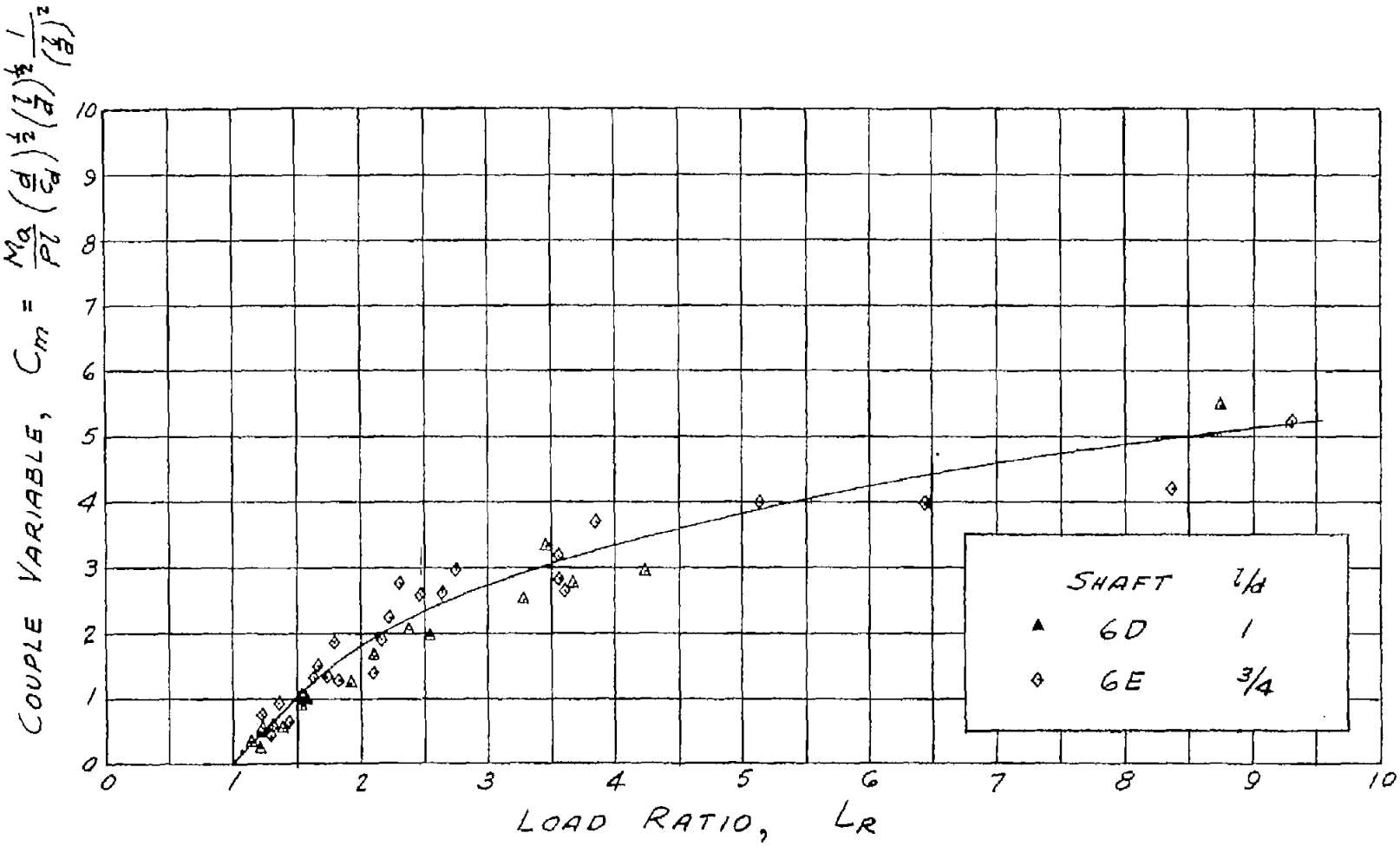

(c) Short bearings; $l/d \leq 1.0$ for axial misalinement.

Figure 6.- Continued.

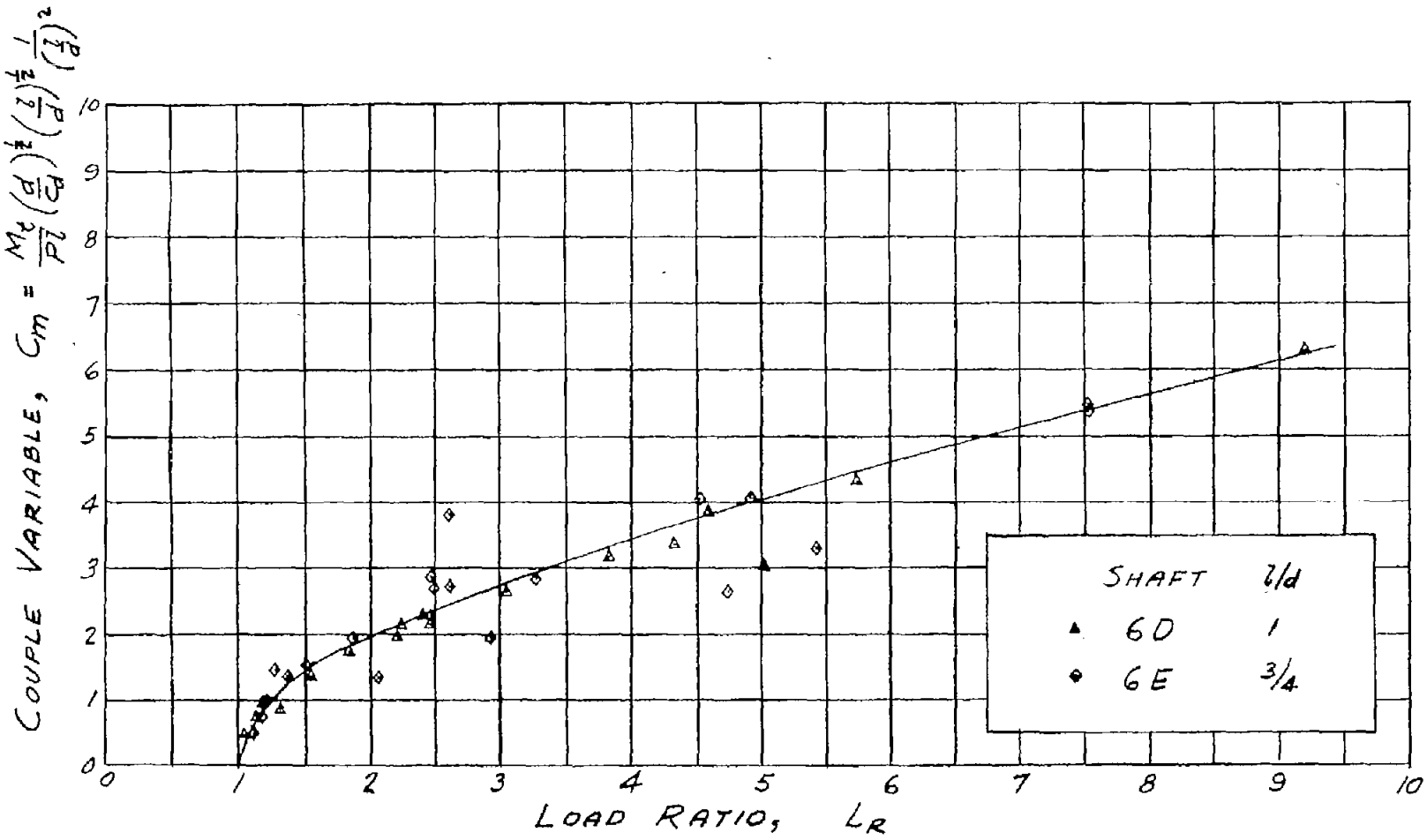

(d) Short bearings; $l/d \leqq 1.0$ for twisting misalinement.

Figure 6.- Concluded.

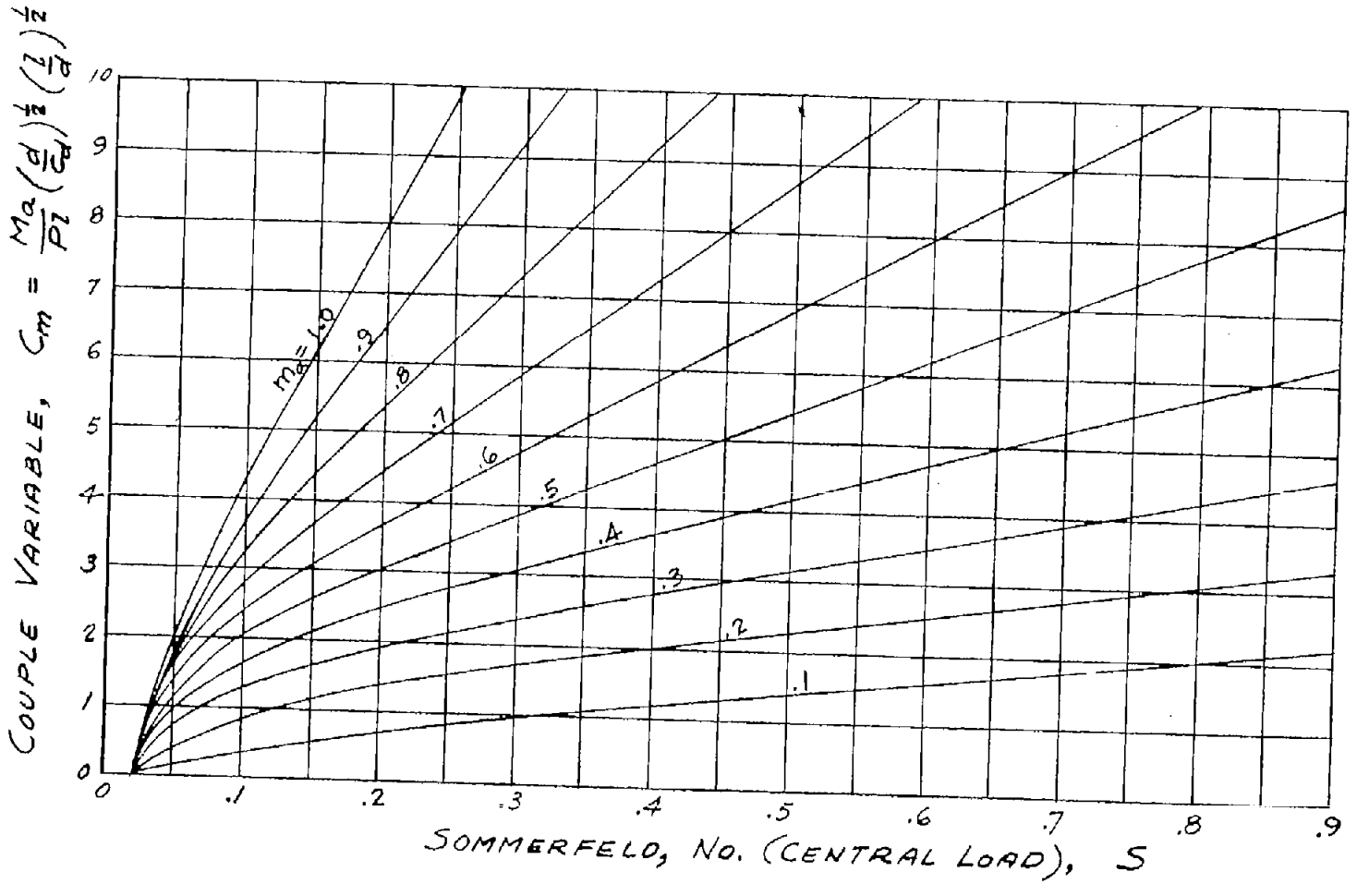

(a) Long bearings; $l/d \geqq 1.0$ for axial misalinement. Curves determined from data of figures 5(a) and 6(a).

Figure 7.- Misalined attitude as a function of couple variable and Sommerfeld or capacity number.

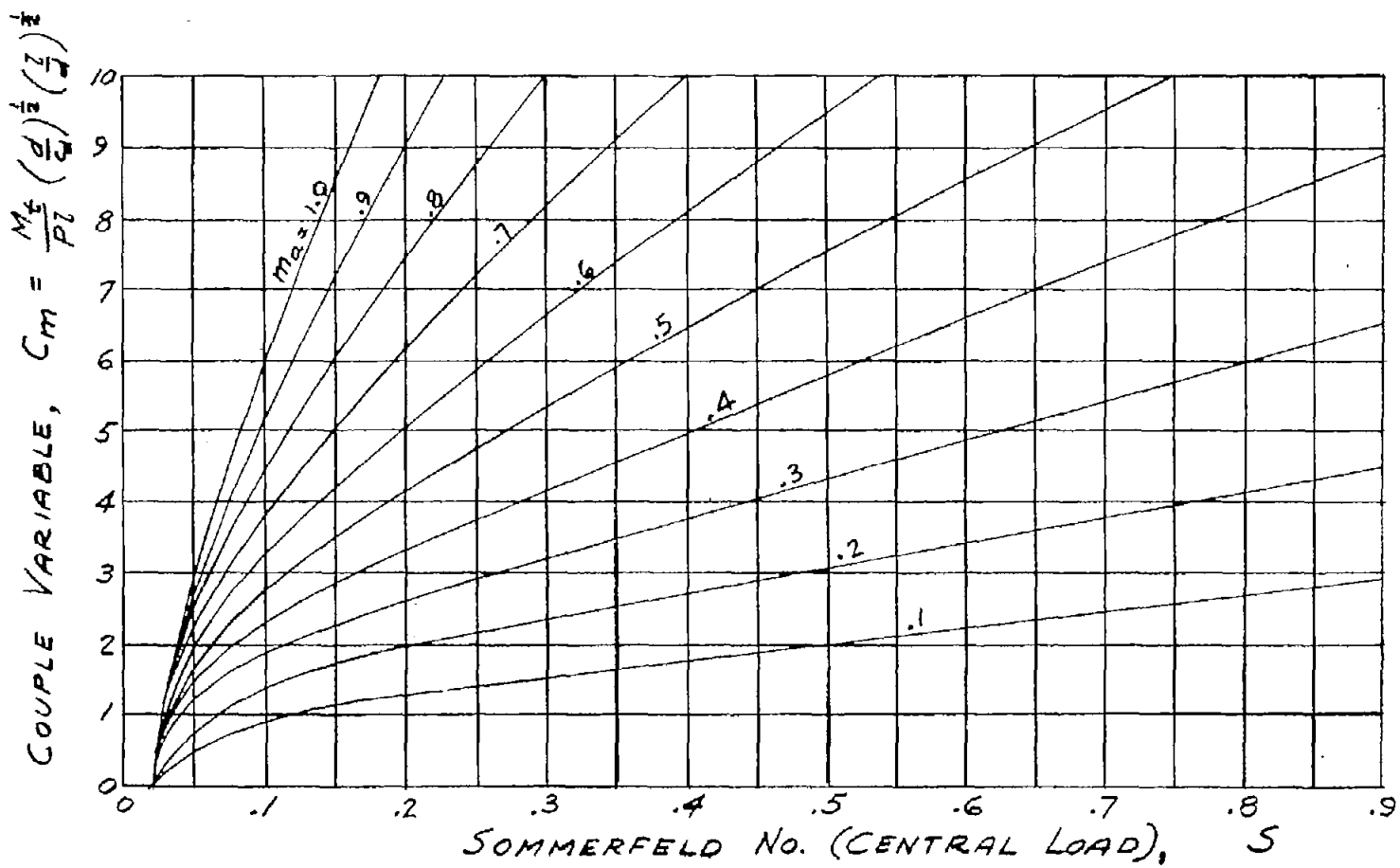

(b) Long bearings; $l/d \geq 1.0$ for twisting misalinement. Curves determined from data of figures 5(a) and 6(b).

Figure 7.- Continued.

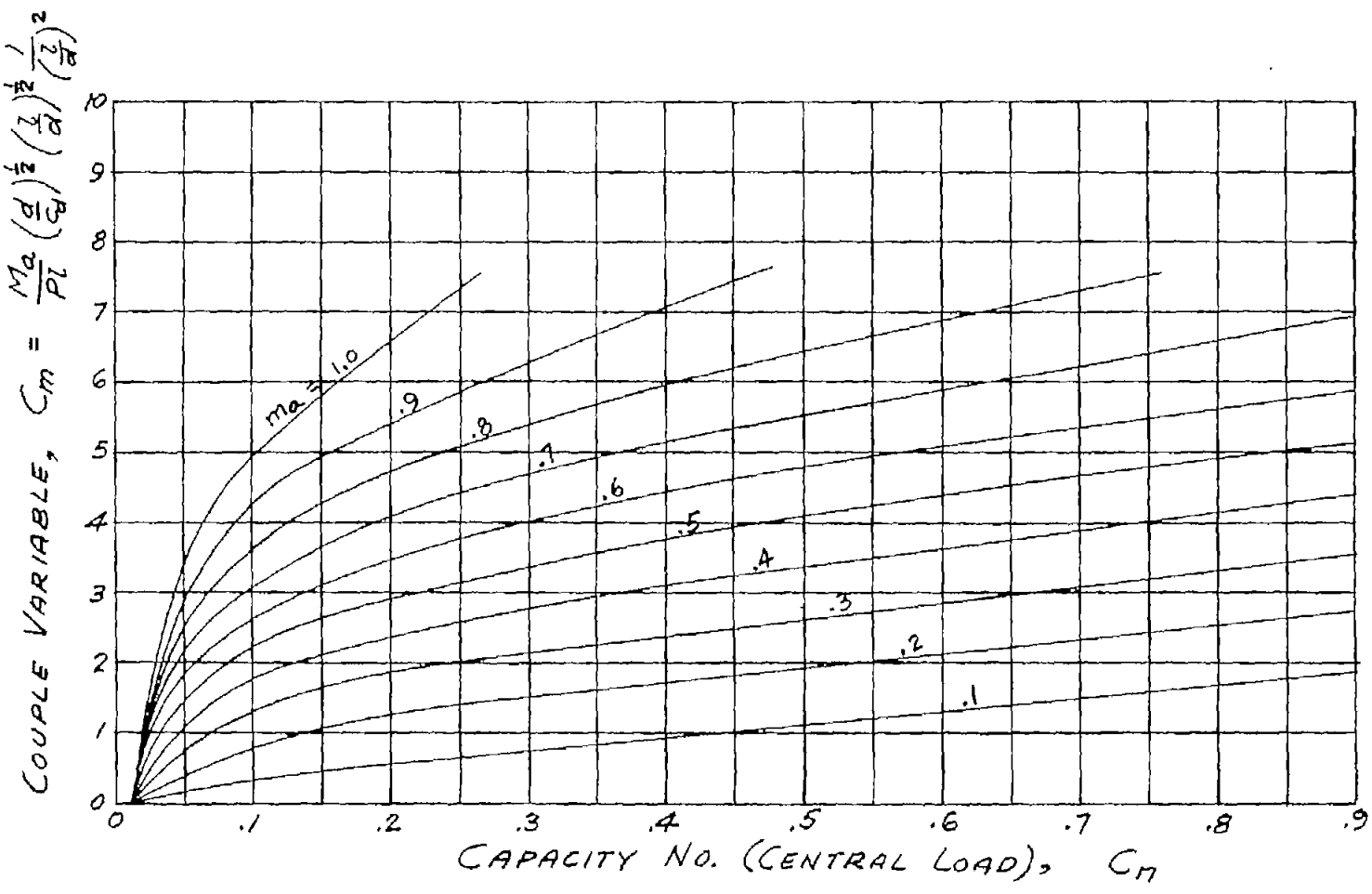

(c) Short bearings; $l/d \leq 1.0$ for axial misalinement. Curves determined from data of figures 5(b) and 6(c).

Figure 7.- Continued.

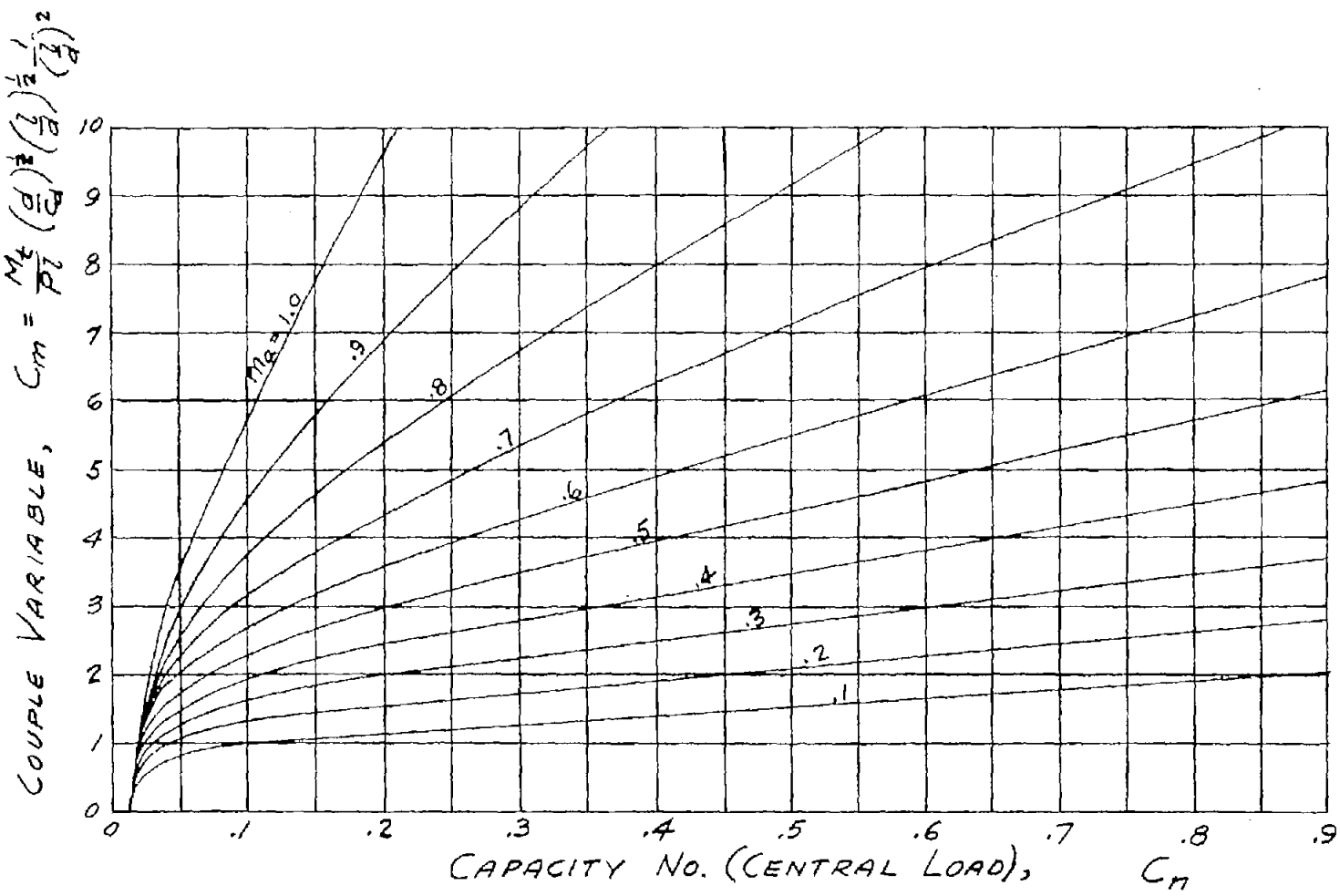

(d) Short bearings; $l/d \leq 1.0$ for twisting misalinement. Curves determined from data of figures 5(b) and 6(d).

Figure 7.- Concluded.

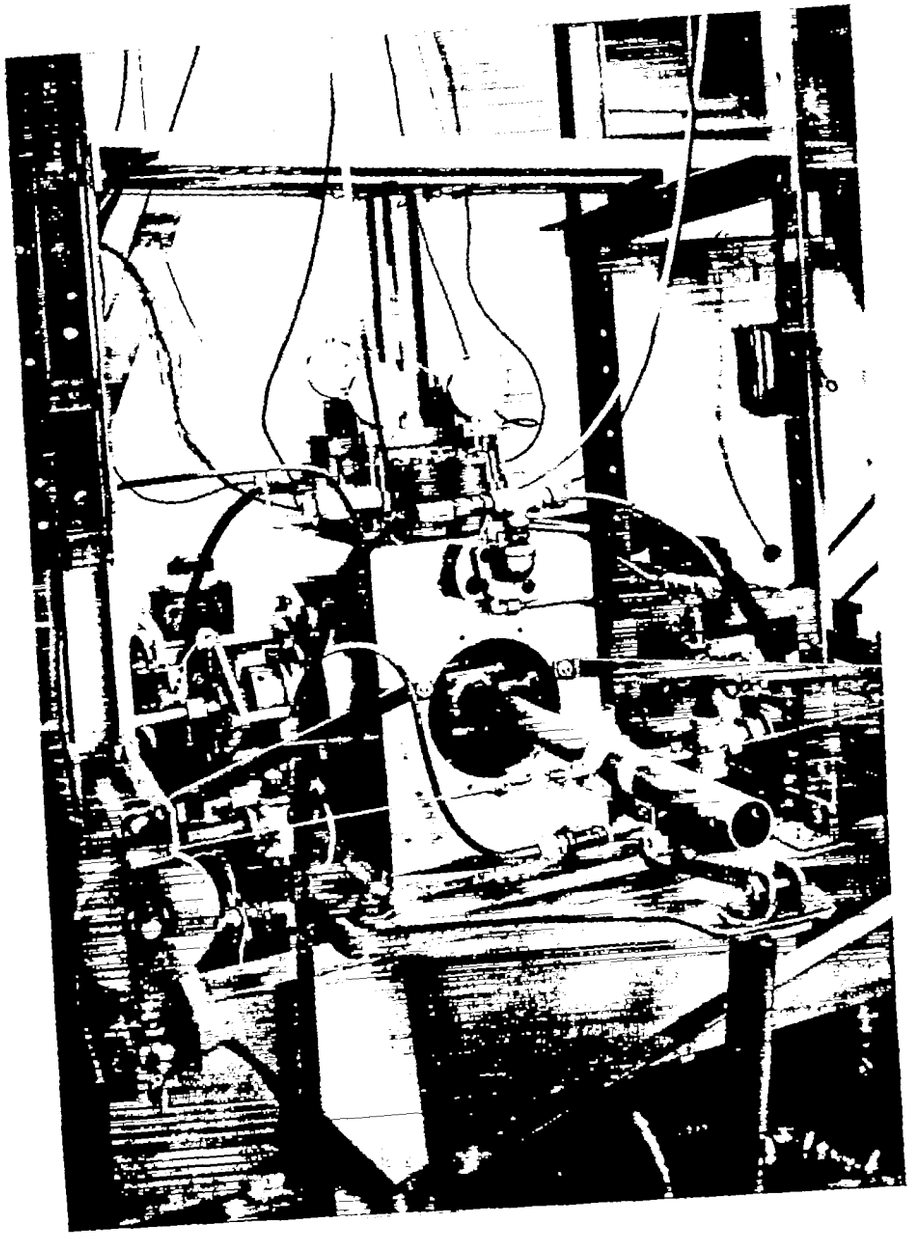

L-85679

Figure 8.- Photograph of bearing test machine showing cable and pulley system for applying misalining couples to tubular extensions from test bearing. System for measuring displacement using 0.0001-inch dial indicators is also shown. The photo-electric oscillographic indicating system was used only in trouble shooting.

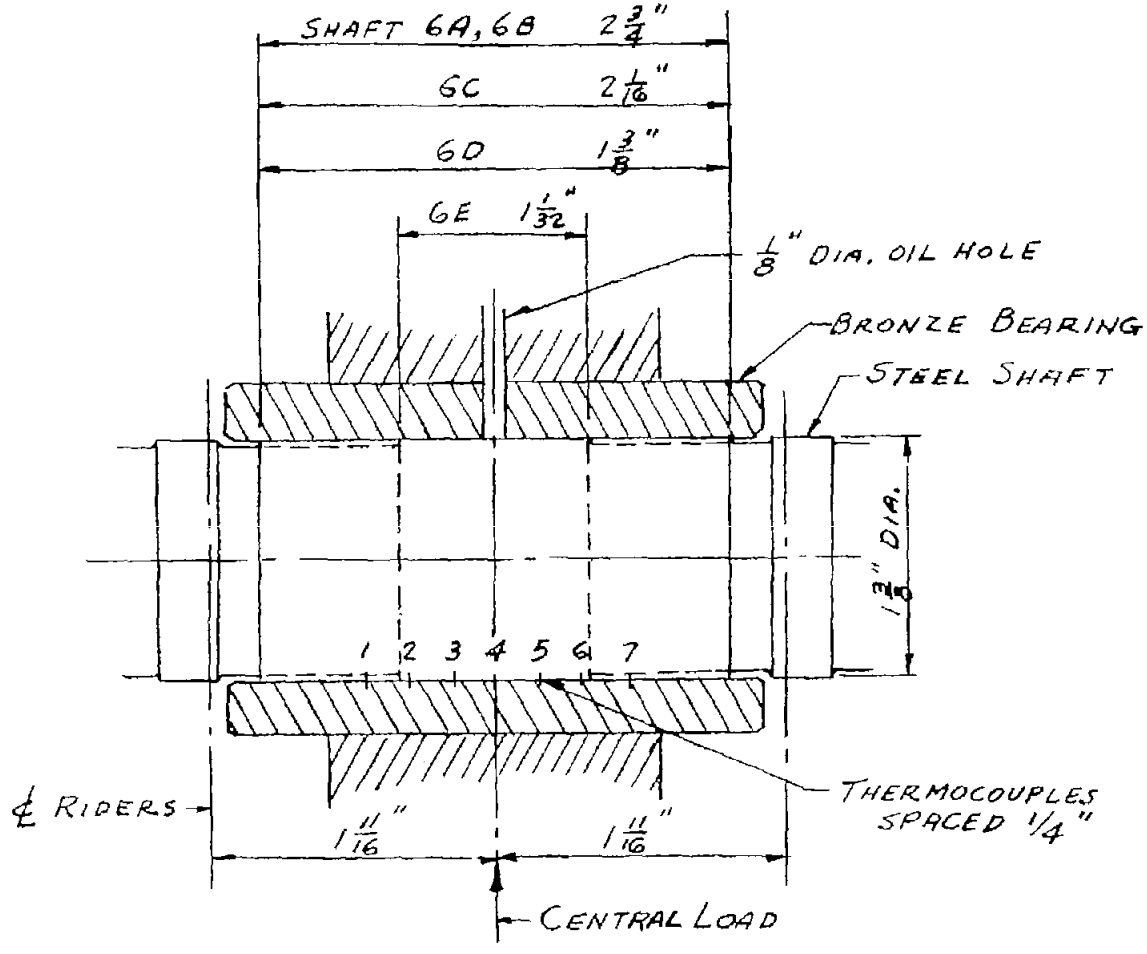

Figure 9.- Configuration of test bearing and test shaft showing location of oil hole and displacement-measuring riders.

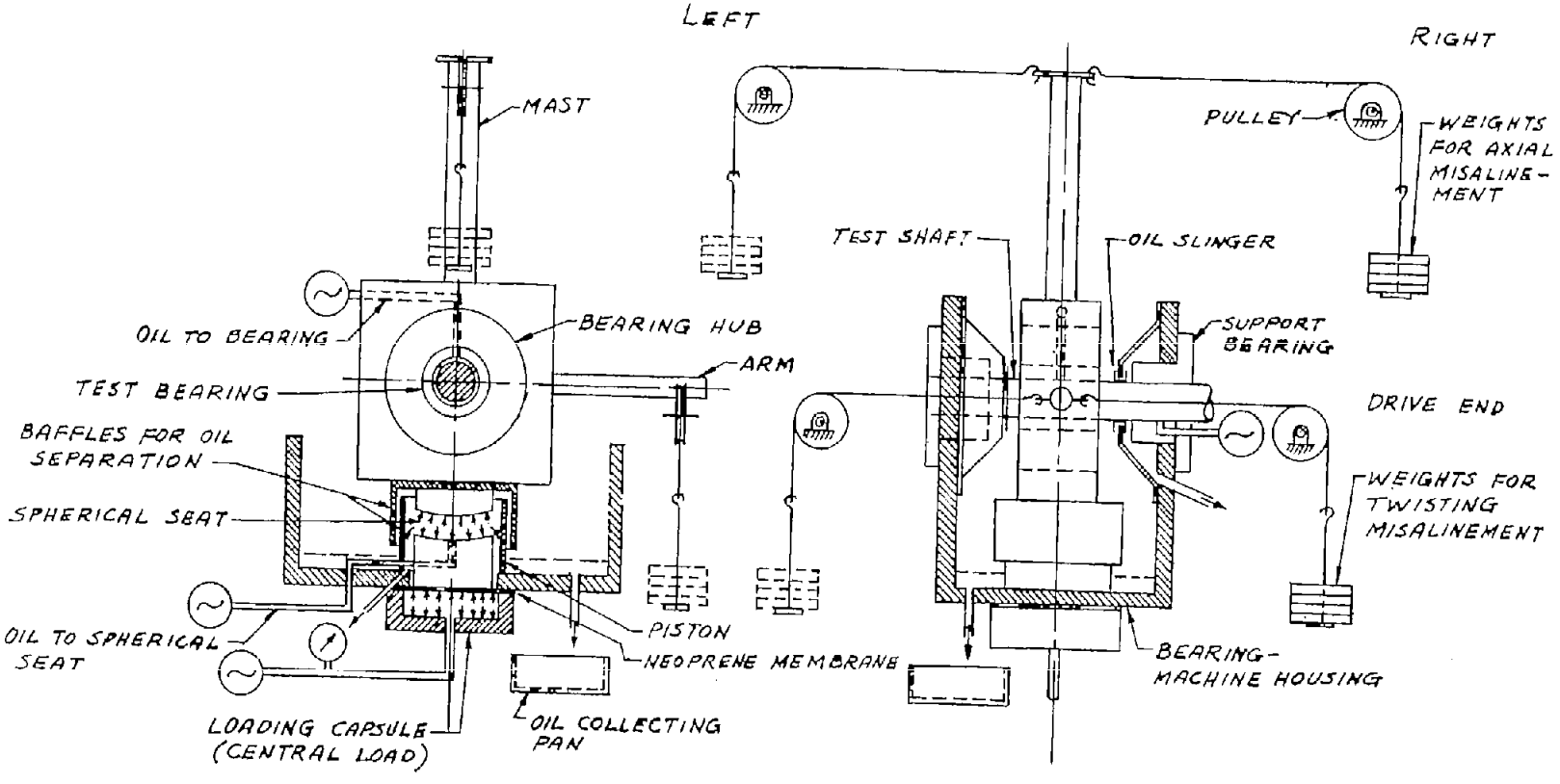

Figure 10.- Schematic diagram showing apparatus for applying central load and misalining couples. Method of measuring oil flow is also shown.

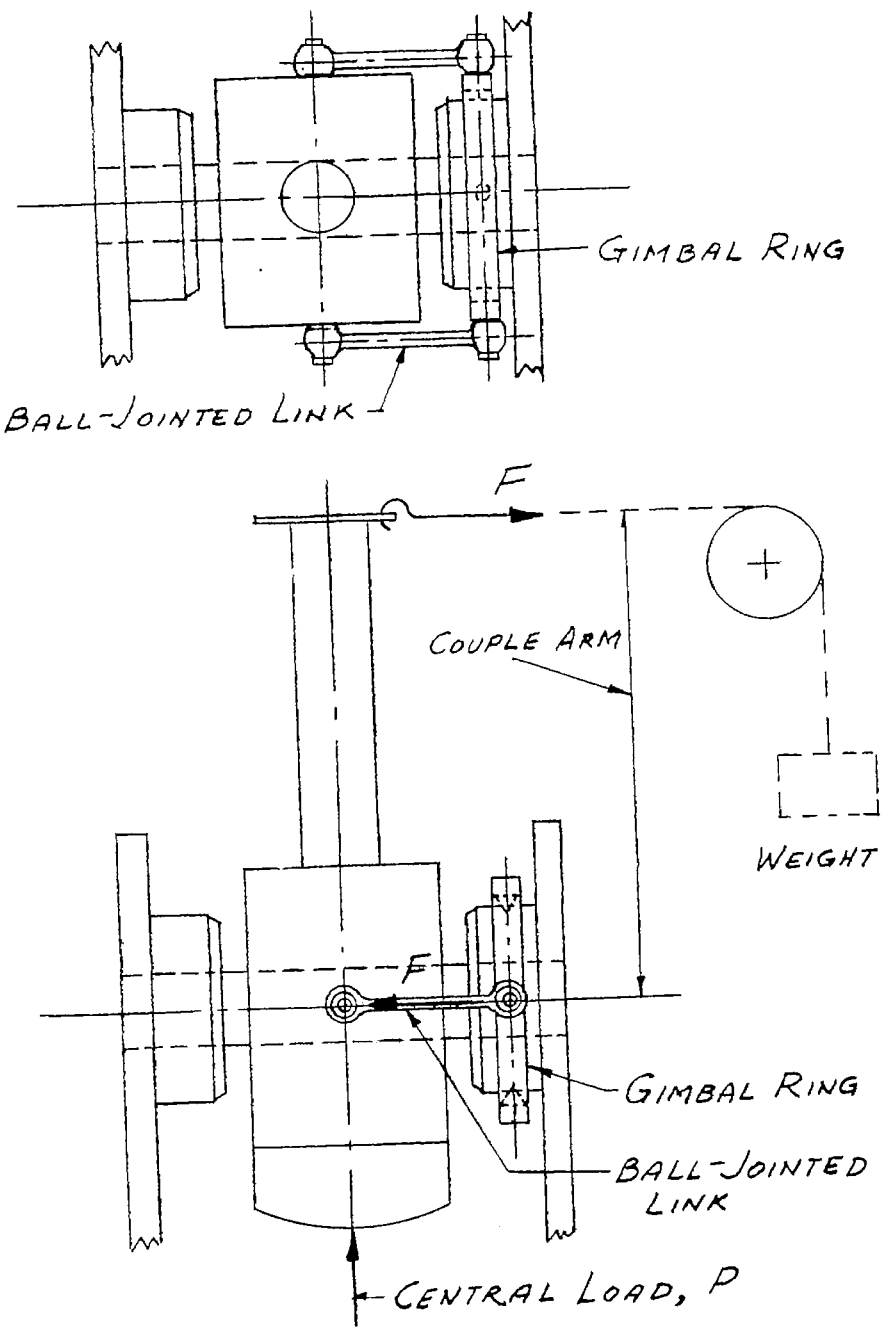

Figure 11.- Gimbal ring and ball-jointed links for restraining axial motion of bearing relative to journal without restraining angular motion.

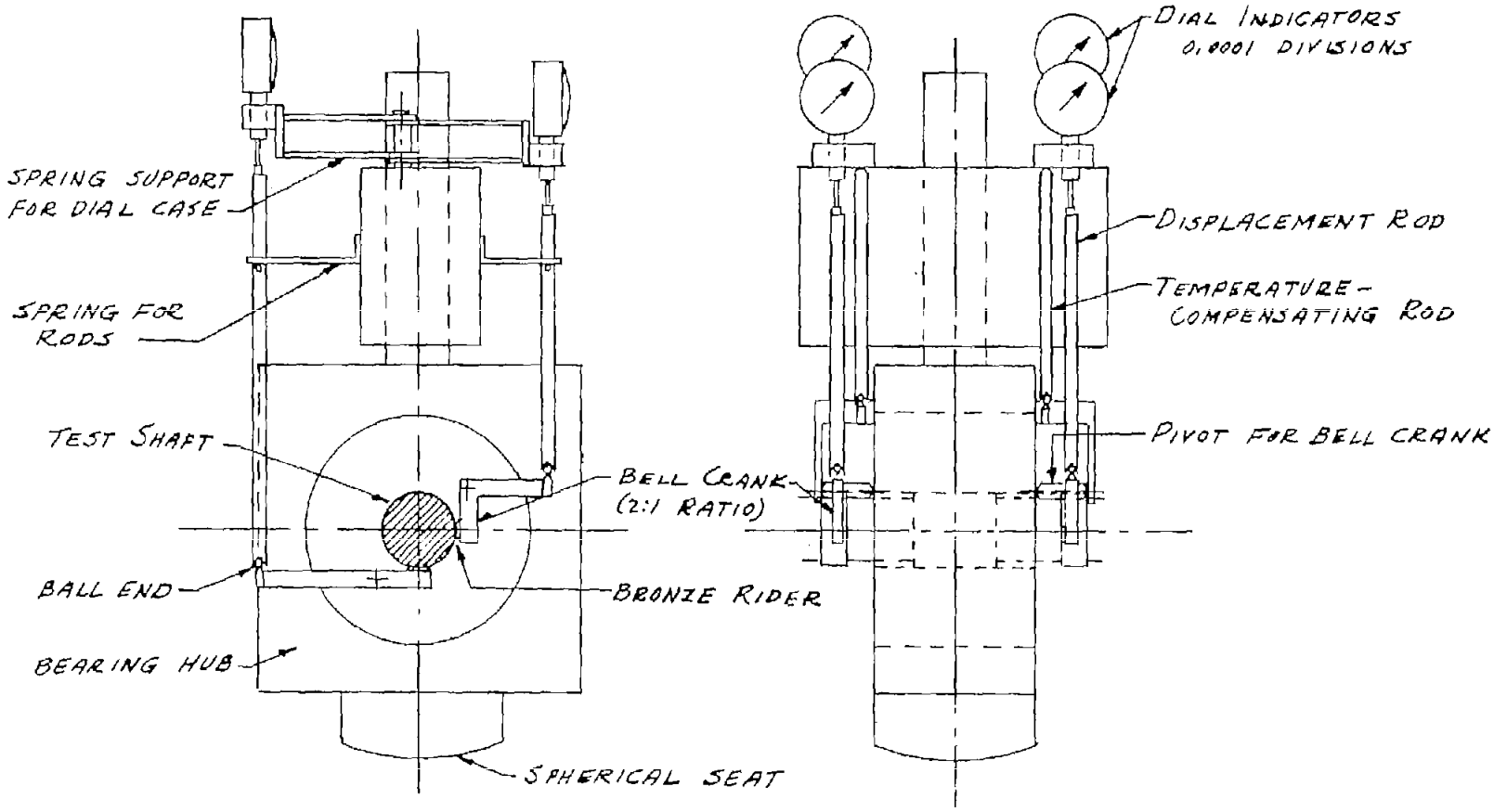

Figure 12.- Mechanical system for measuring displacement of journal relative to bearing.

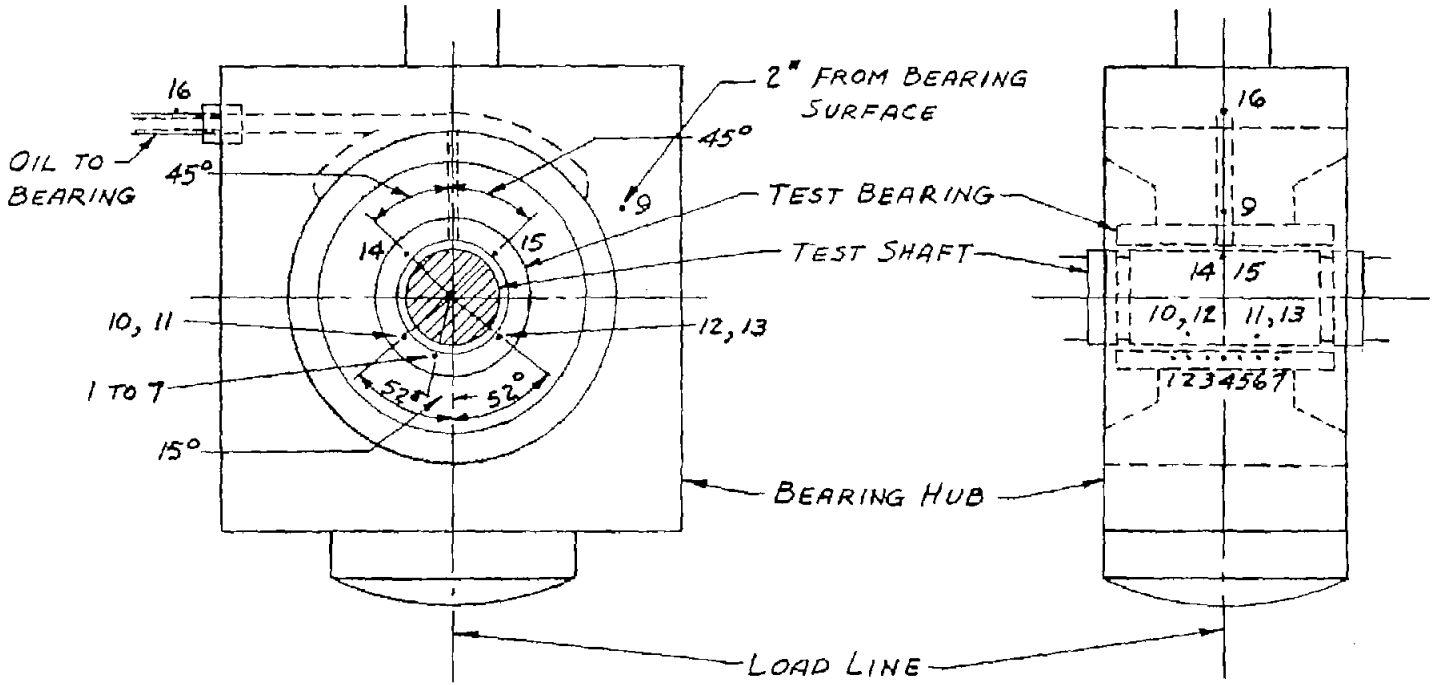

Figure 13.- Diagram of thermocouple locations. Bearing thermocouples are located 1/16 inch from bearing surface.

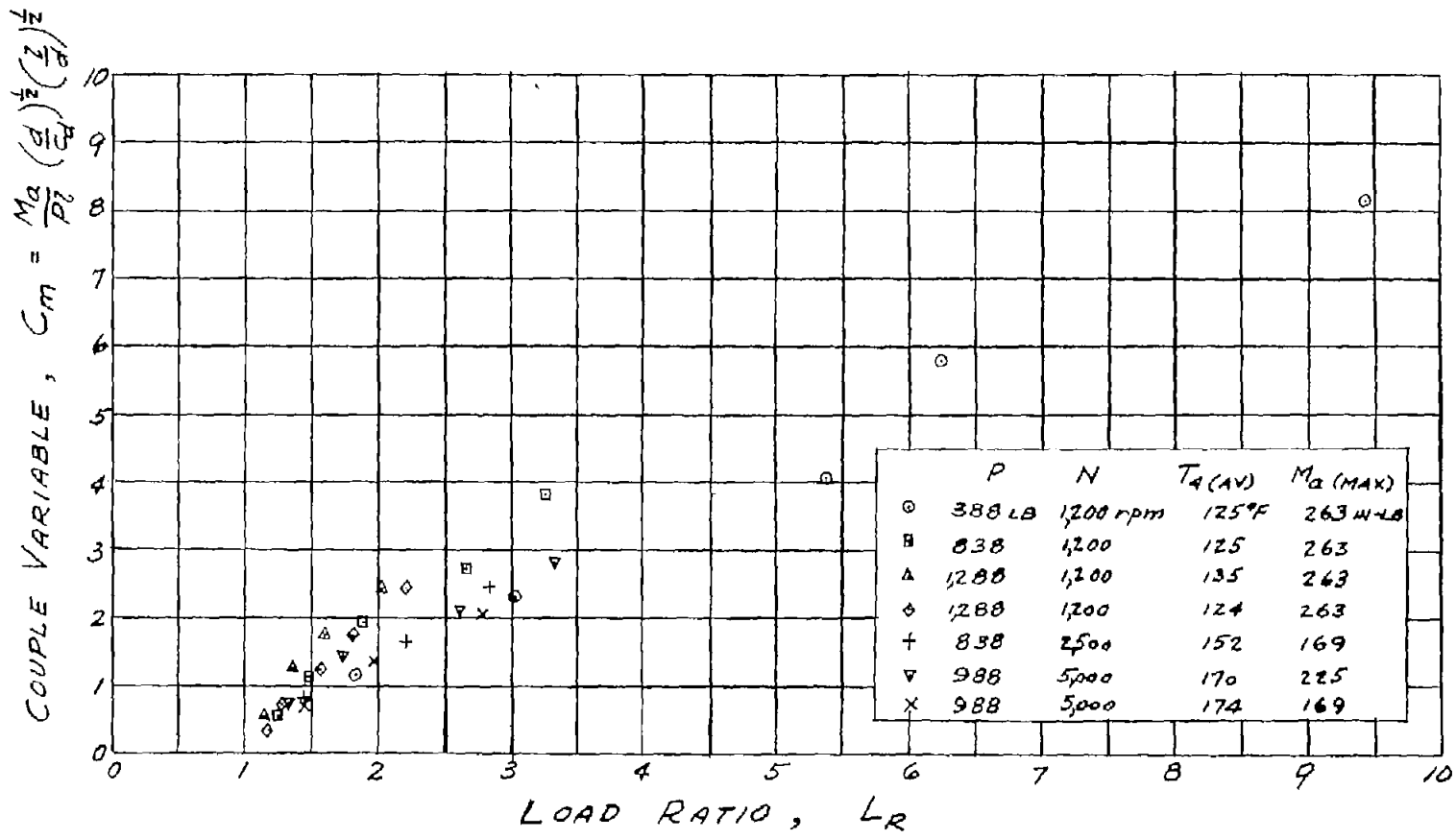

(a) Shaft 6A; $l/d = 2$; $d = 1\frac{3}{8}$ inches; $l = 2\frac{3}{4}$ inches; $c_d = 0.00252$ inch at room temperature.

Figure 14.- Couple variable against load ratio for axial misalinement. SAE 10 oil; 140° F at heater; $p_o = 80$ pounds per square inch; 1/8-inch-diameter oil hole opposite central load; load ratio calculated from equation (5) and based on experimental curve of figure 4(b).

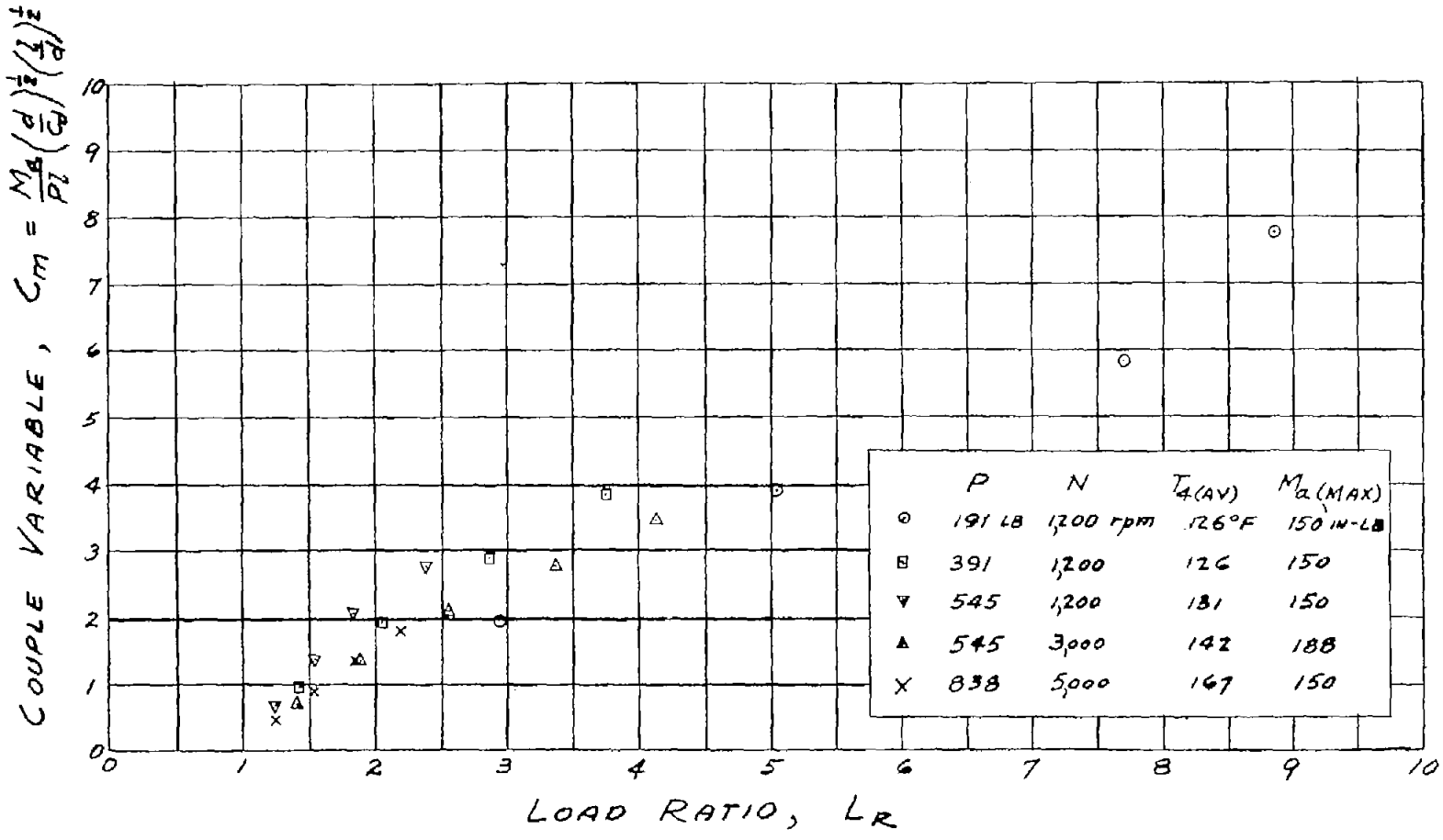

(b) Shaft 6B; $l/d = 2$; $d = 1\frac{3}{8}$ inches; $l = 2\frac{3}{4}$ inches; $c_d = 0.00376$ inch at room temperature.

Figure 14.- Continued.

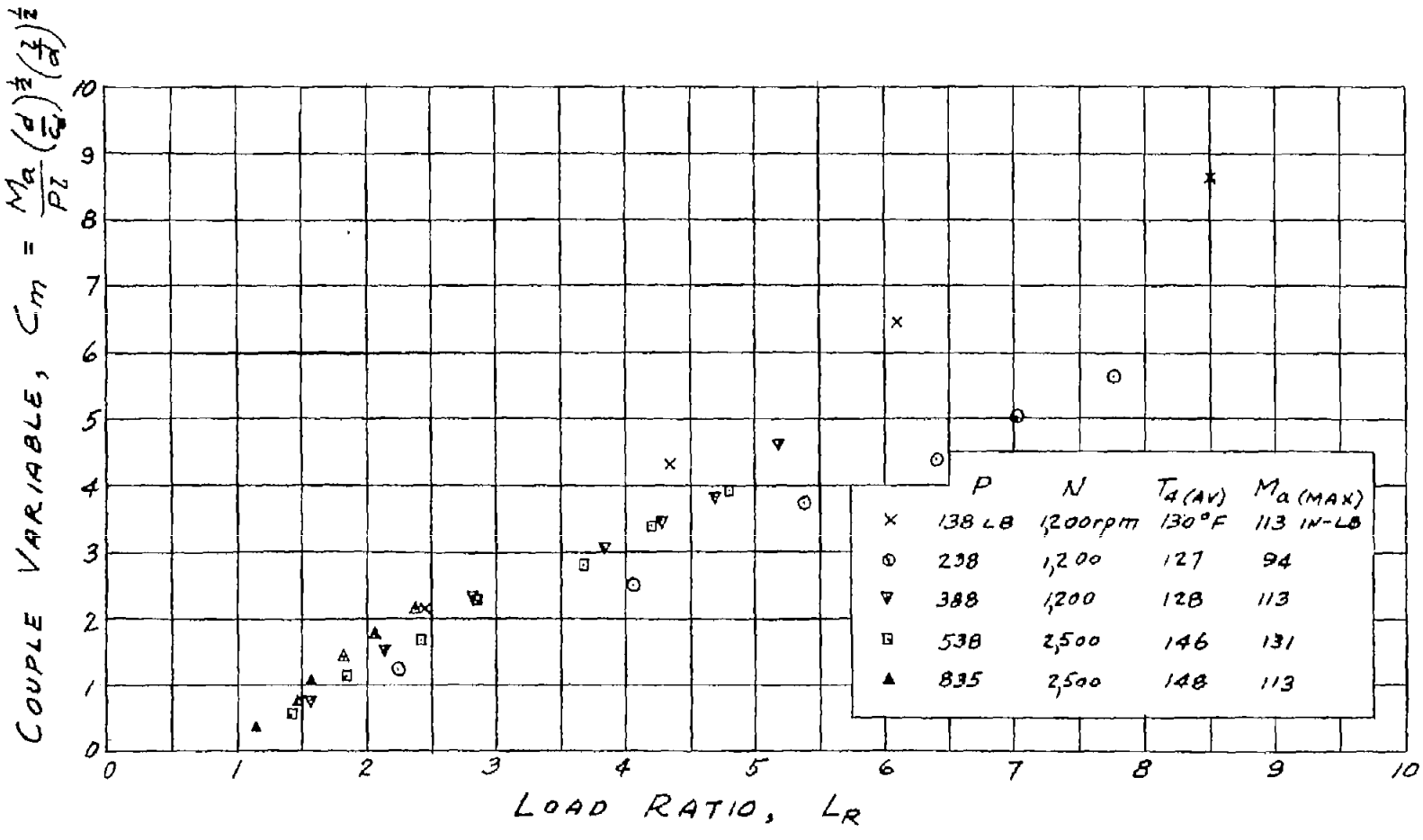

(c) Shaft 6C; $l/d = 1.5$; $d = 1\frac{3}{8}$ inches; $l = 2\frac{1}{16}$ inches; $c_d = 0.00196$ inch at room temperature.

Figure 14.- Continued.

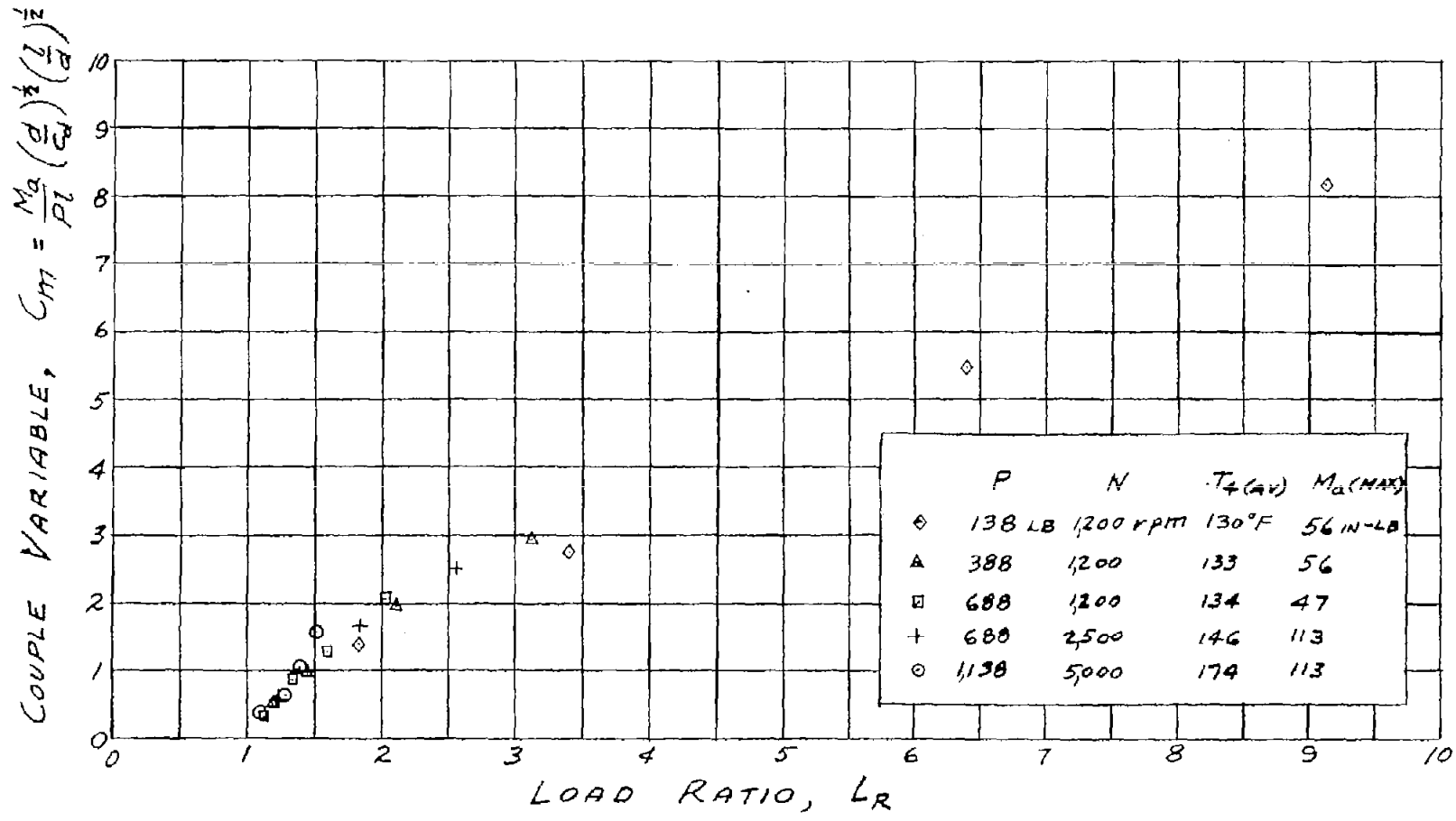

(d) Shaft 6D; $l/d = 1$; $d = 1\frac{3}{8}$ inches; $l = 1\frac{3}{8}$ inches; $c_d = 0.00183$ inch at room temperature.

Figure 14.- Concluded.

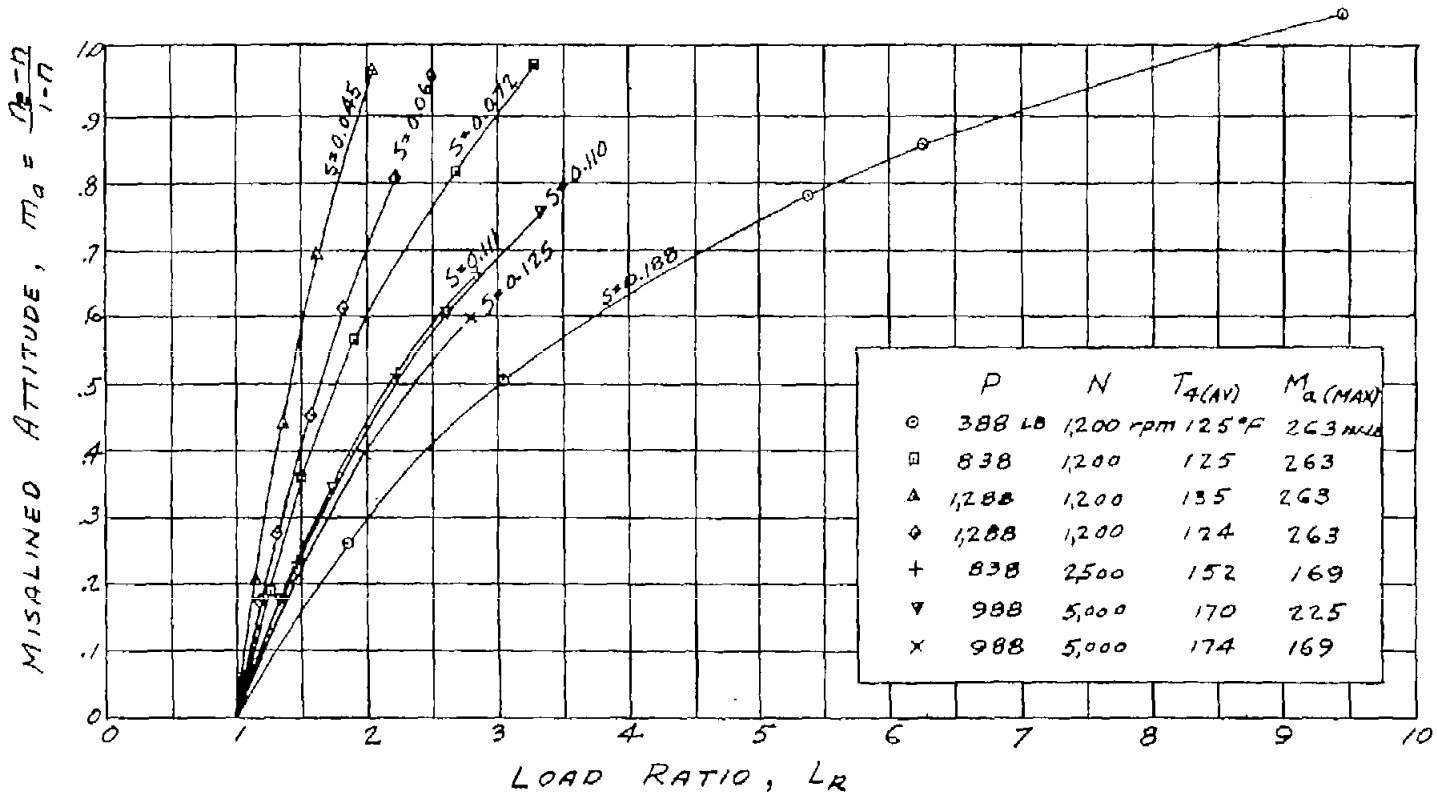

(a) Curves for Sommerfeld number; axial misalinement; shaft 6A; $l/d = 2$; $d = 1\frac{3}{8}$ inches; $l = 2\frac{3}{4}$ inches; $c_d = 0.00252$ inch at room temperature. Load ratio calculated from equation (5) and based on experimental curve of figure 4(b).

Figure 15.- Experimental range of misalined attitude against load ratio. SAE 10 oil; 140° F at heater; $p_o = 80$ pounds per square inch; 1/8-inch-diameter oil hole opposite central load.

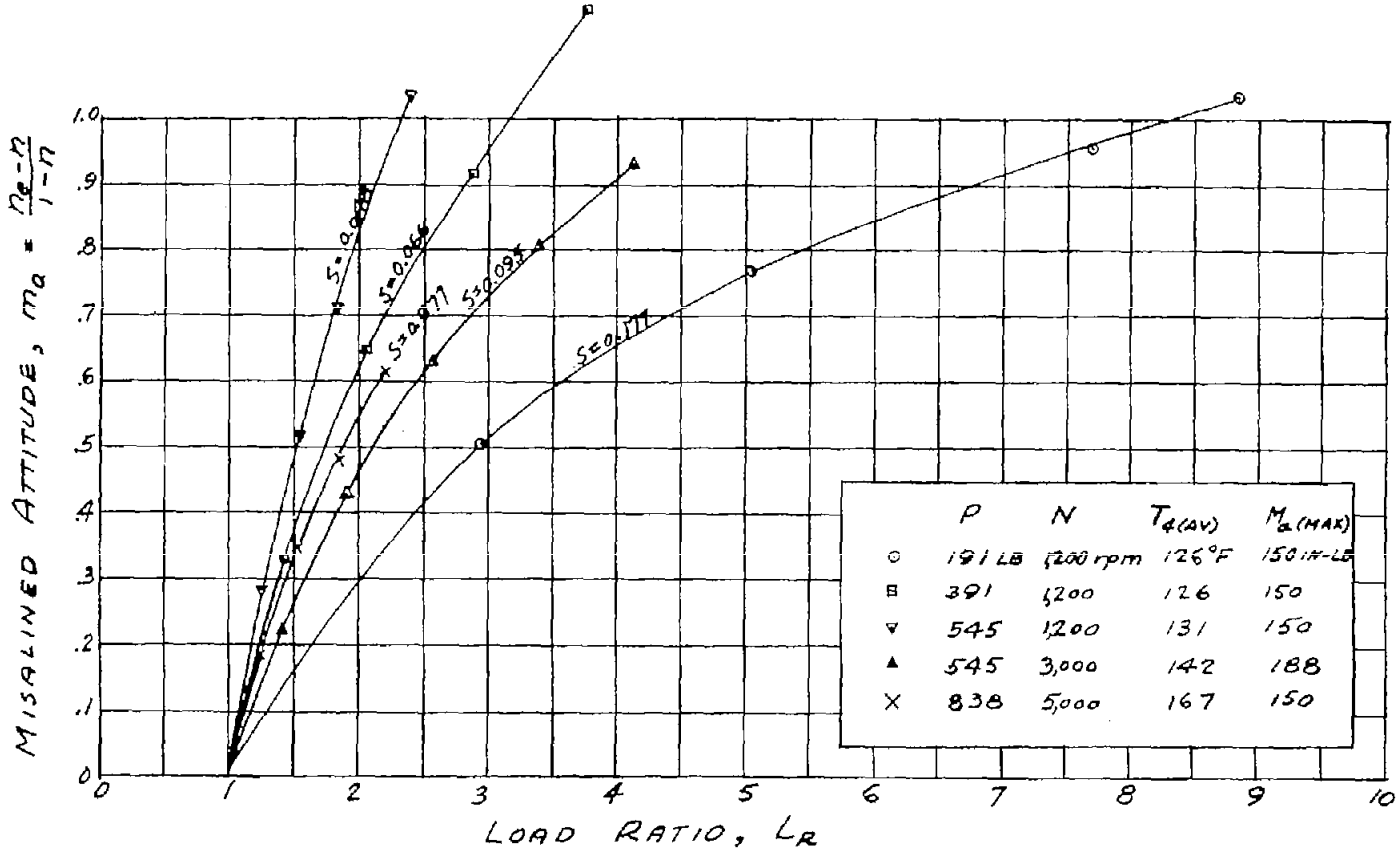

(b) Curves for Sommerfeld number; axial misalinement; shaft 6B; $l/d = 2$; $d = 1\frac{3}{8}$ inches; $l = 2\frac{3}{4}$ inches; $c_d = 0.00376$ inch at room temperature. Load ratio calculated from equation (5) and based on experimental curve of figure 4(b).

Figure 15.- Continued.

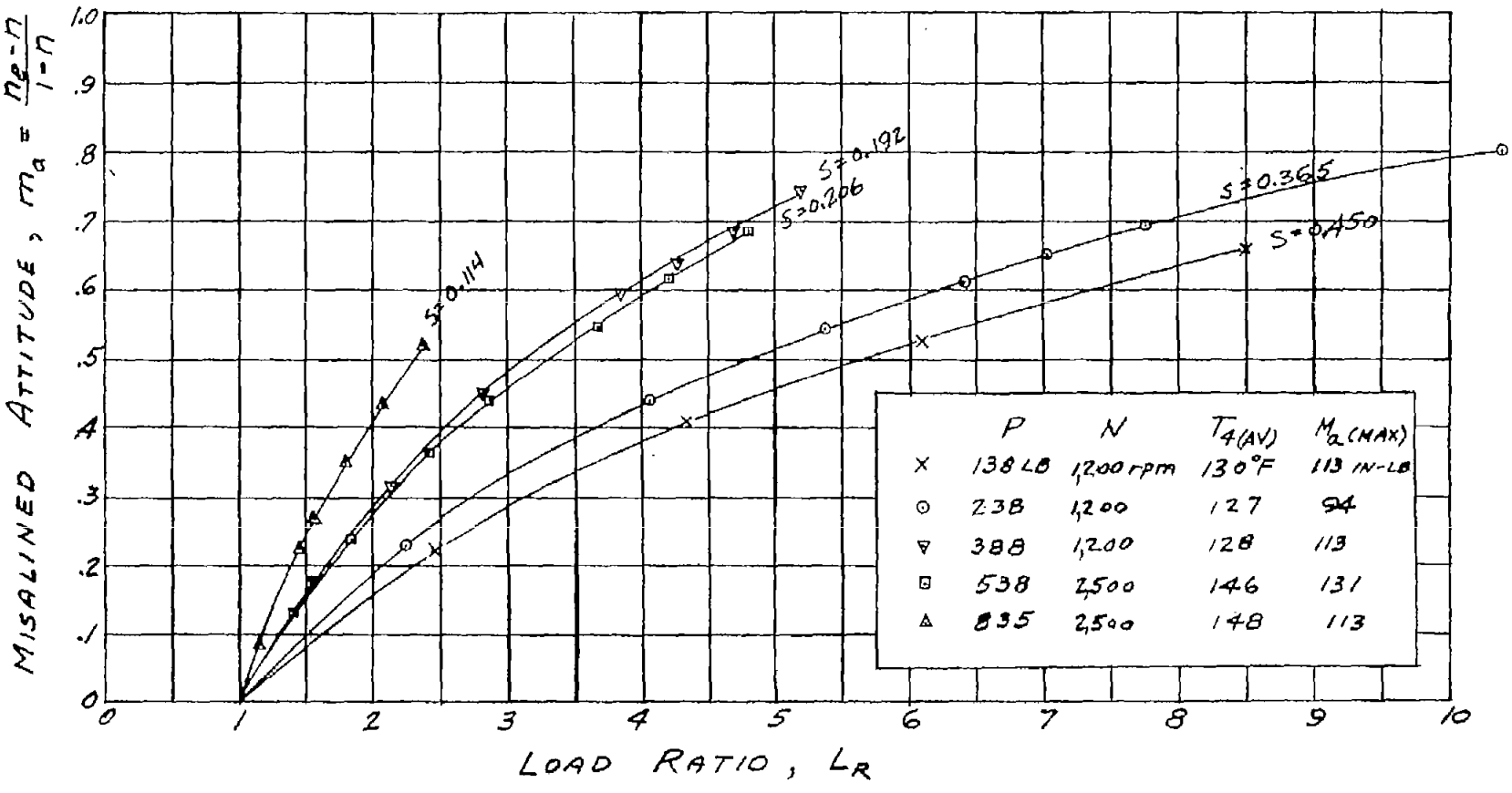

(c) Curves for Sommerfeld number; axial misalinement; shaft 6C; $l/d = 1.5$; $d = 1\frac{3}{8}$ inches; $l = 2\frac{1}{16}$ inches; $c_d = 0.00196$ inch at room temperature. Load ratio calculated from equation (5) and based on experimental curve of figure 4(b).

Figure 15.- Continued.

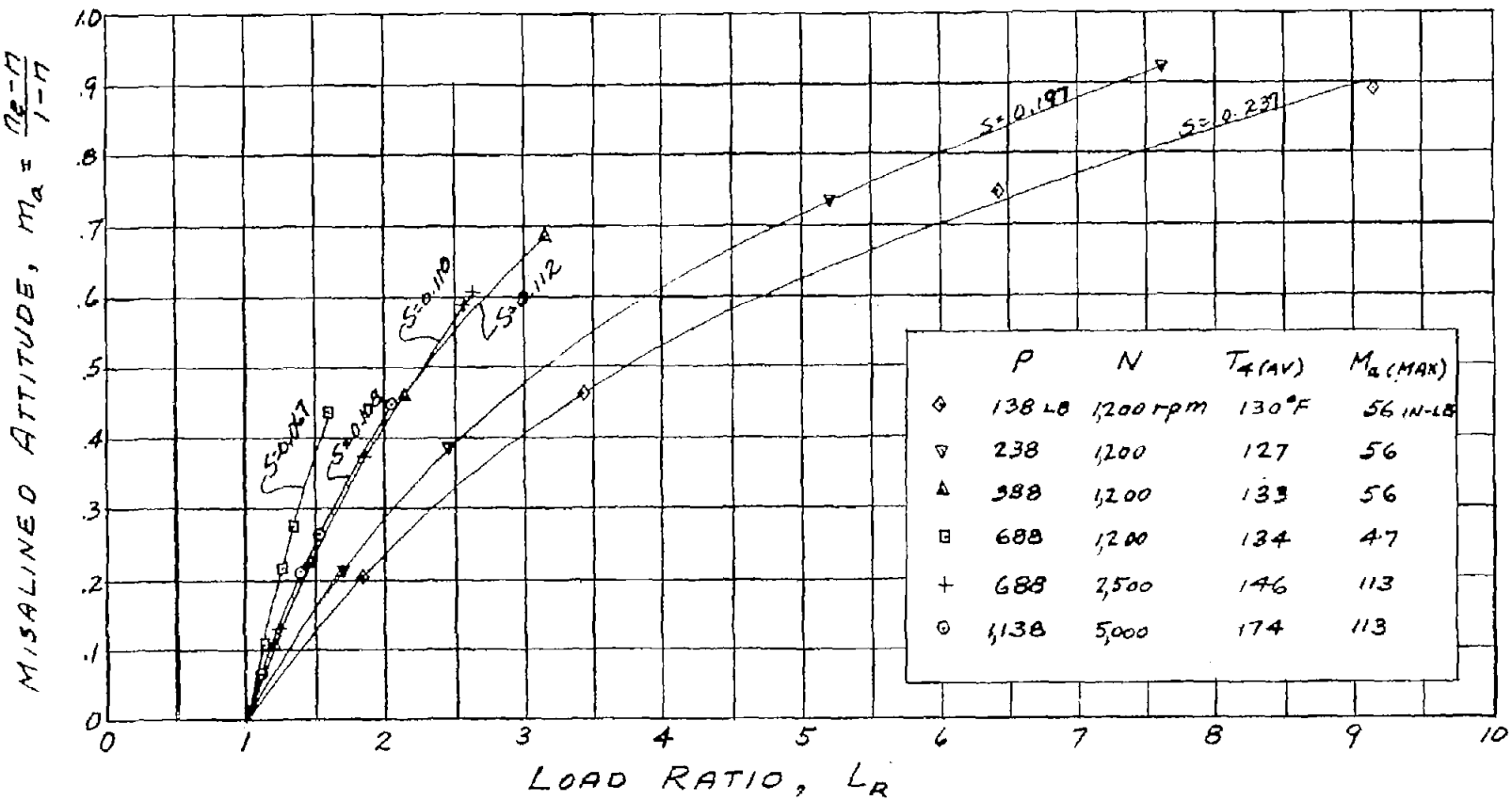

(d) Curves for Sommerfeld number; axial misalinement; shaft 6D; $l/d = 1$; $d = 1\frac{3}{8}$ inches; $l = 1\frac{3}{8}$ inches; $c_d = 0.00183$ inch at room temperature. Load ratio calculated from equation (5) and based on experimental curve of figure 4(b).

Figure 15.- Continued.

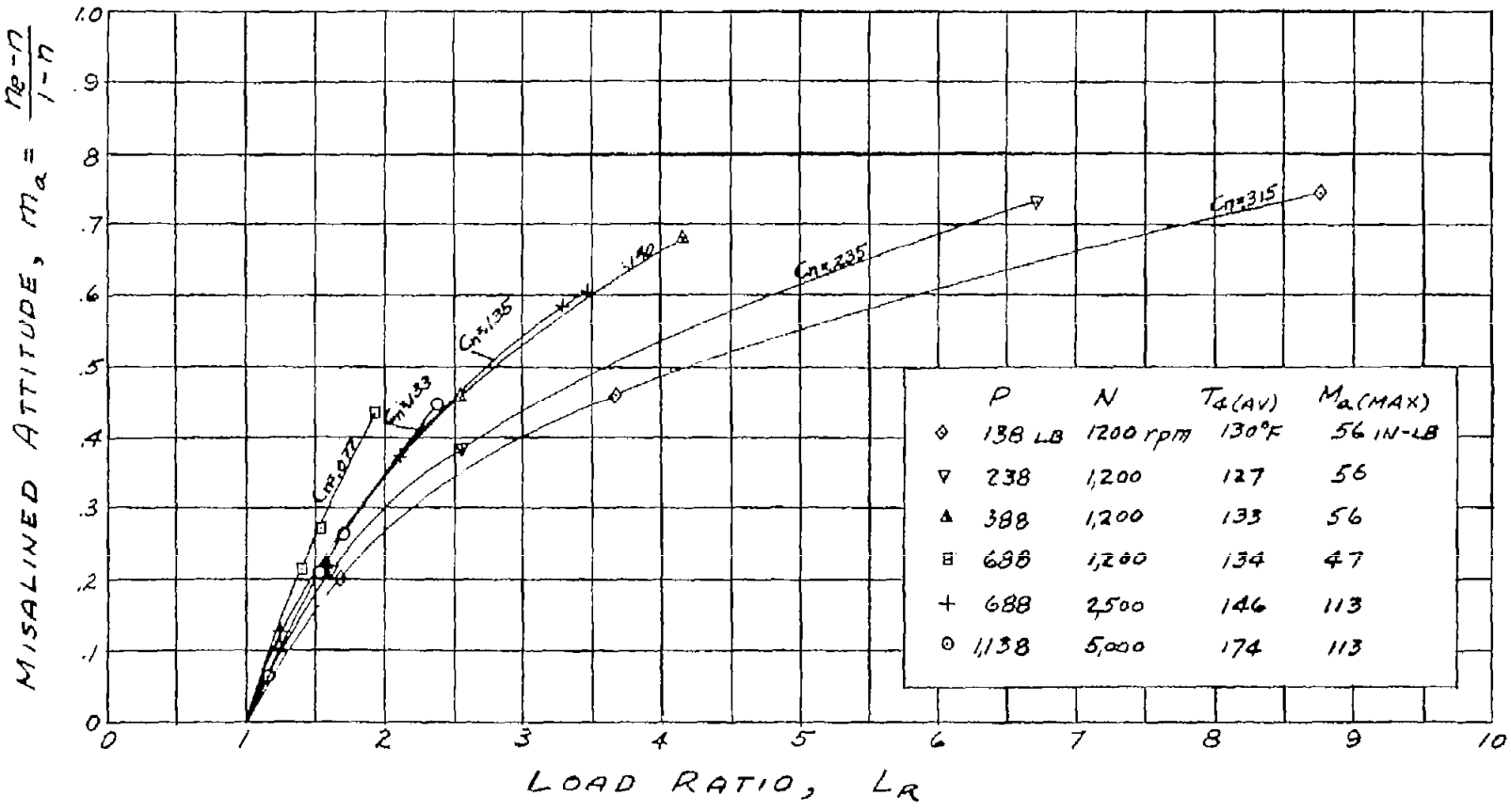

(e) Curves for capacity number; axial misalinement; shaft 6D; l/d = 1.0; $d = 1\frac{3}{8}$ inches; $l = 1\frac{3}{8}$ inches; c_d = 0.00183 inch at room temperature. Load ratio calculated from equation (5) and based on experimental curve of figure 4(c).

Figure 15.- Continued.

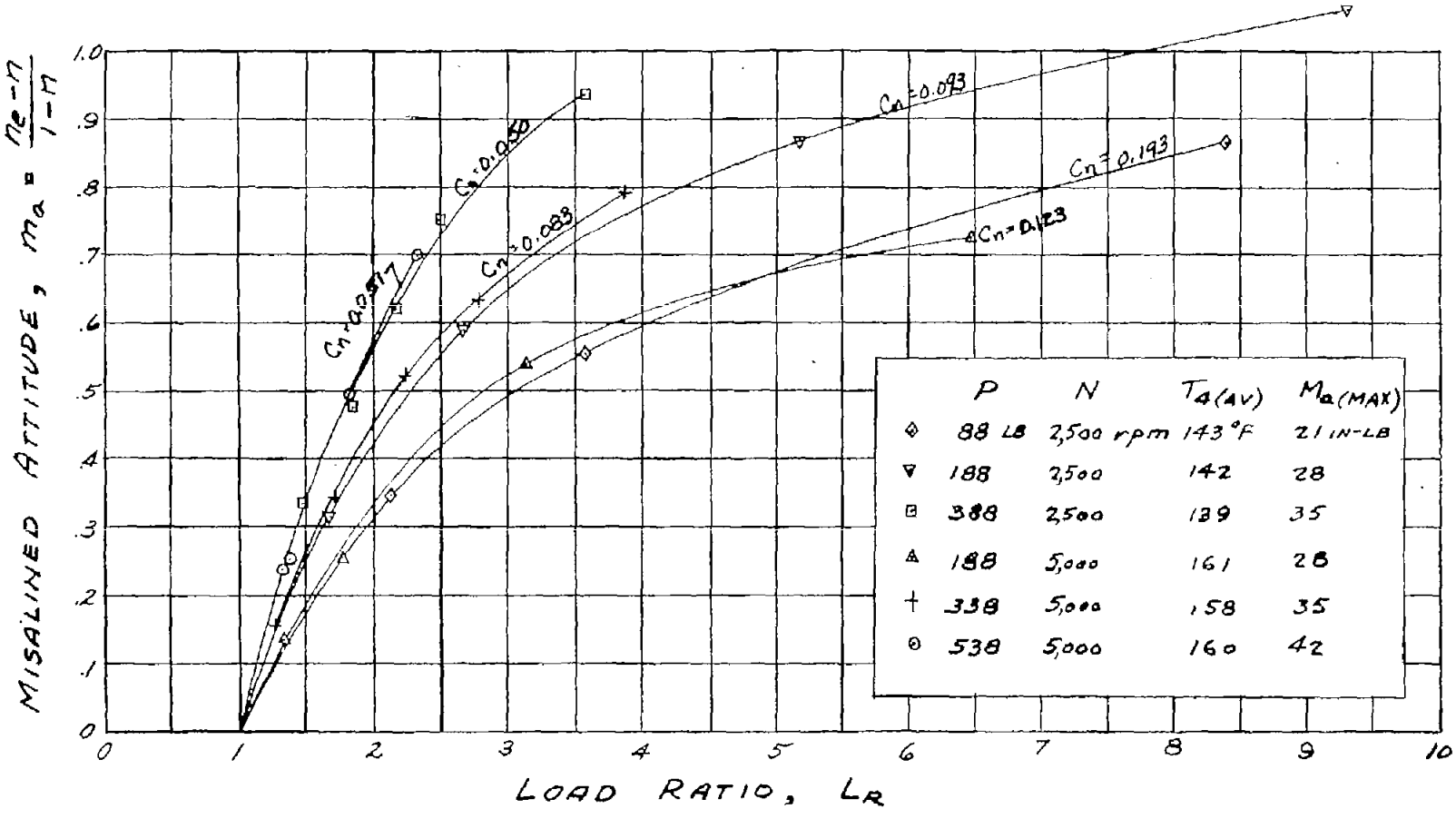

(f) Curves for capacity number; axial misalinement; shaft 6E; $l/d = 3/4$; $d = 1\frac{3}{8}$ inches; $l = 1\frac{1}{32}$ inches; $c_d = 0.00258$ inch at room temperature. Load ratio calculated from equation (5) and based on experimental curve of figure 4(c).

Figure 15.- Continued.

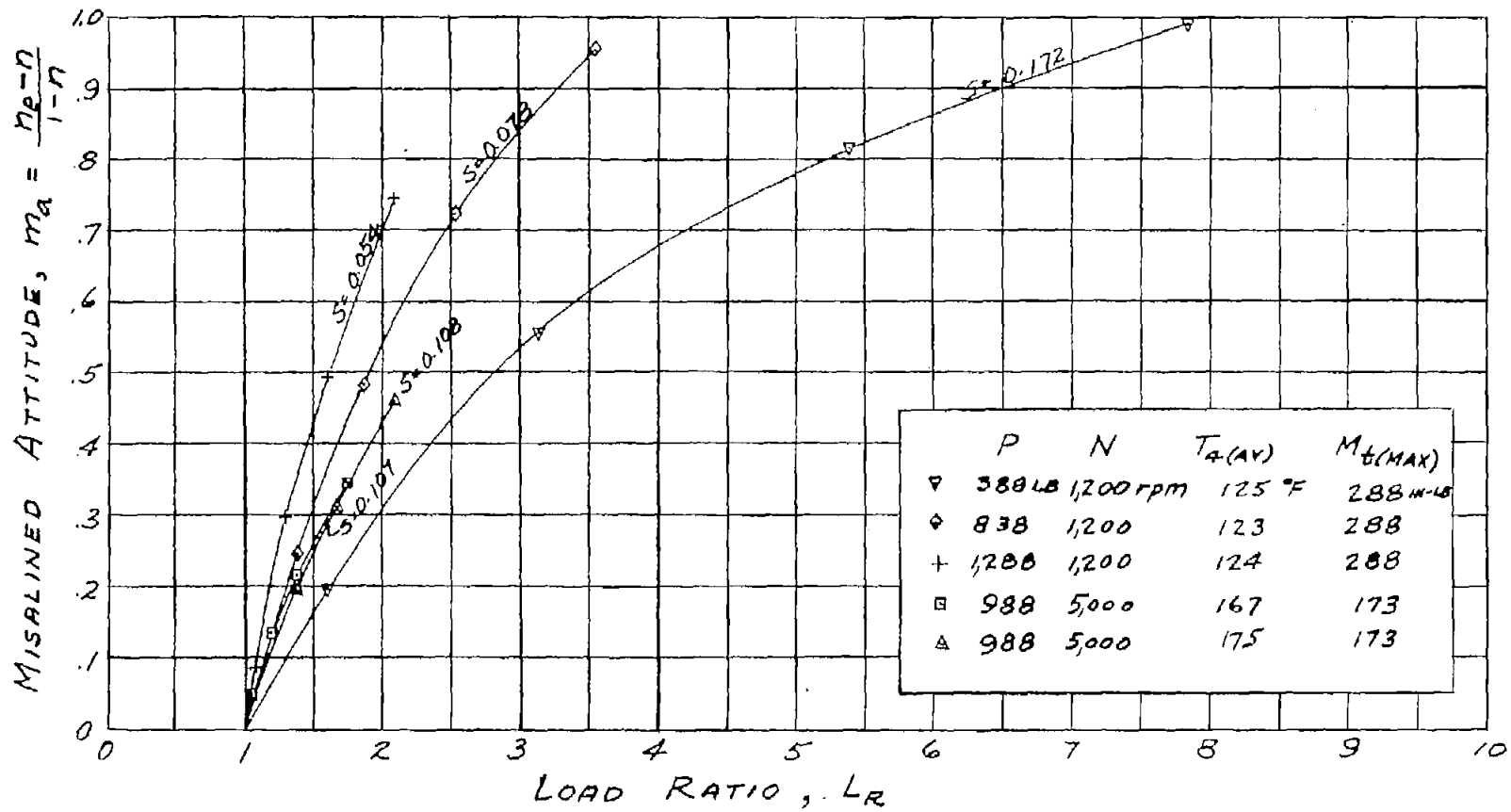

(g) Curves for Sommerfeld number; twisting misalinement; shaft 6A; $l/d = 2$; $d = 1\frac{3}{8}$ inches; $l = 2\frac{3}{4}$ inches; $c_d = 0.00252$ inch at room temperature. Load ratio calculated from equation (5) and based on experimental curve of figure 4(b).

Figure 15.- Continued.

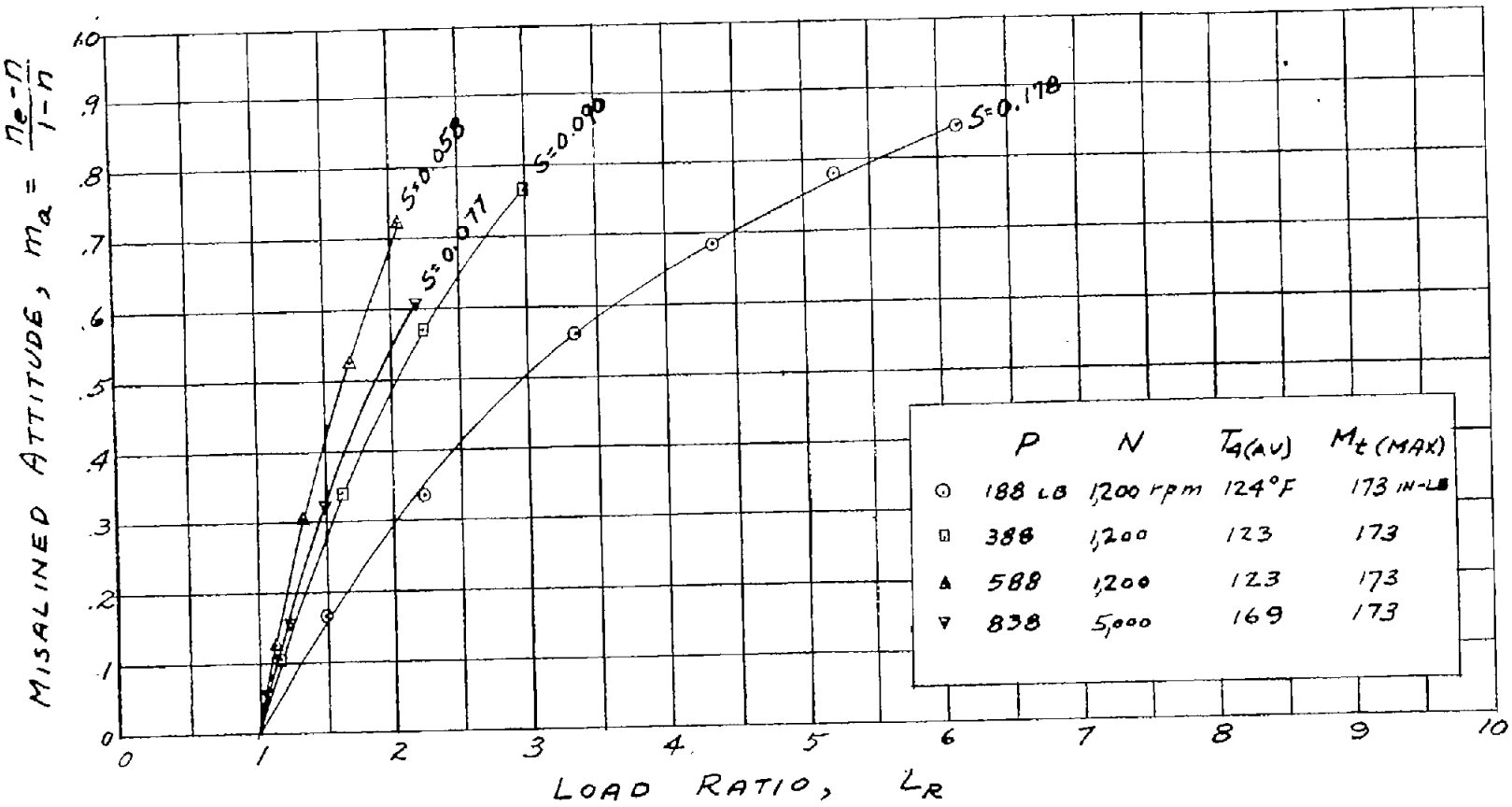

(h) Curves for Sommerfeld number; twisting misalinement; shaft 6B; $l/d = 2$; $d = 1\frac{3}{8}$ inches; $l = 2\frac{3}{4}$ inches; $c_d = 0.00376$ inch at room temperature. Load ratio calculated from equation (5) and based on experimental curve of figure 4(b).

Figure 15.- Continued.

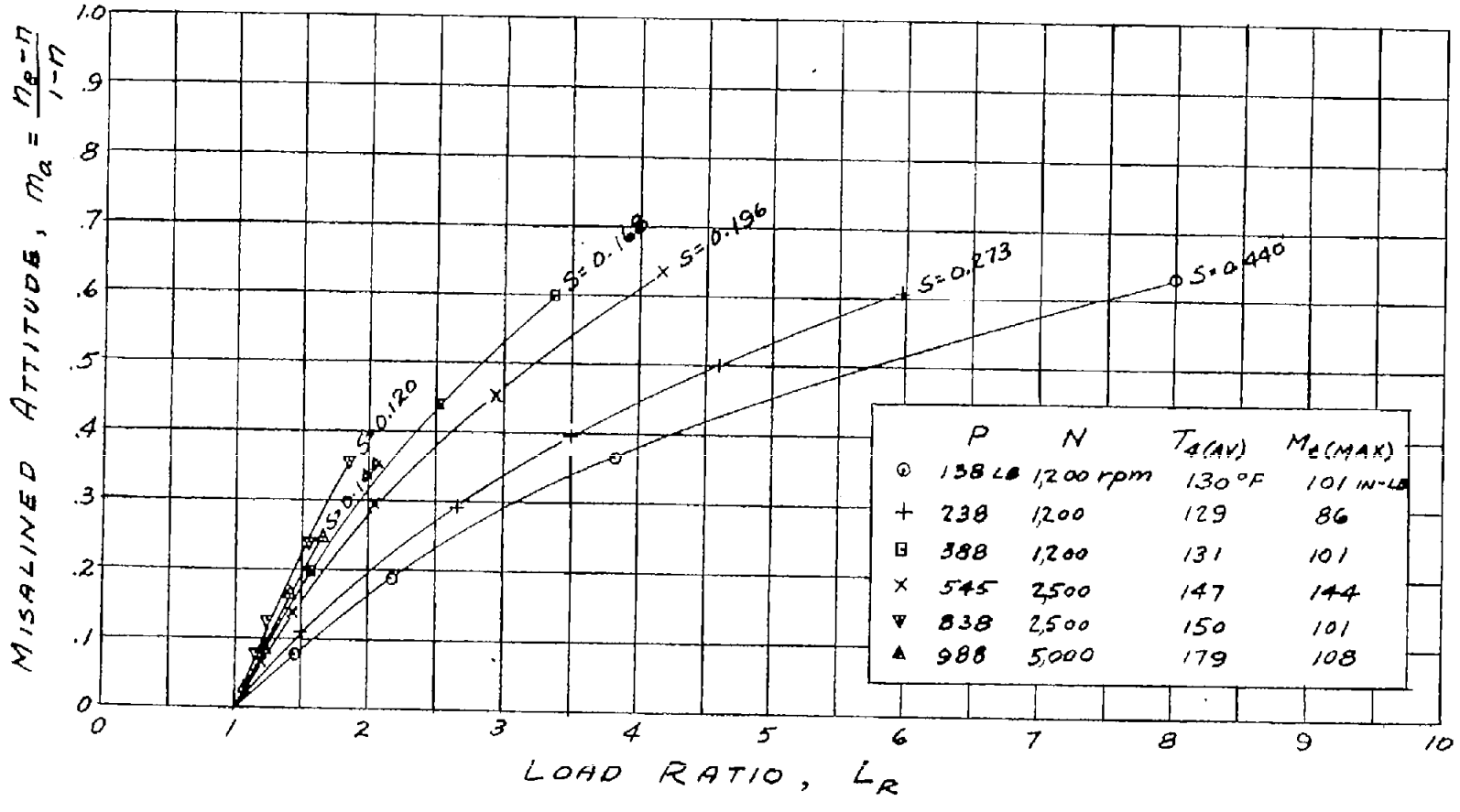

(i) Curves for Sommerfeld number; twisting misalinement; shaft 6C; $l/d = 1.5$; $d = 1\frac{3}{8}$ inches; $l = 2\frac{1}{16}$ inches; $c_d = 0.00196$ inch at room temperature. Load ratio calculated from equation (5) and based on experimental curve of figure 4(b).

Figure 15.- Continued.

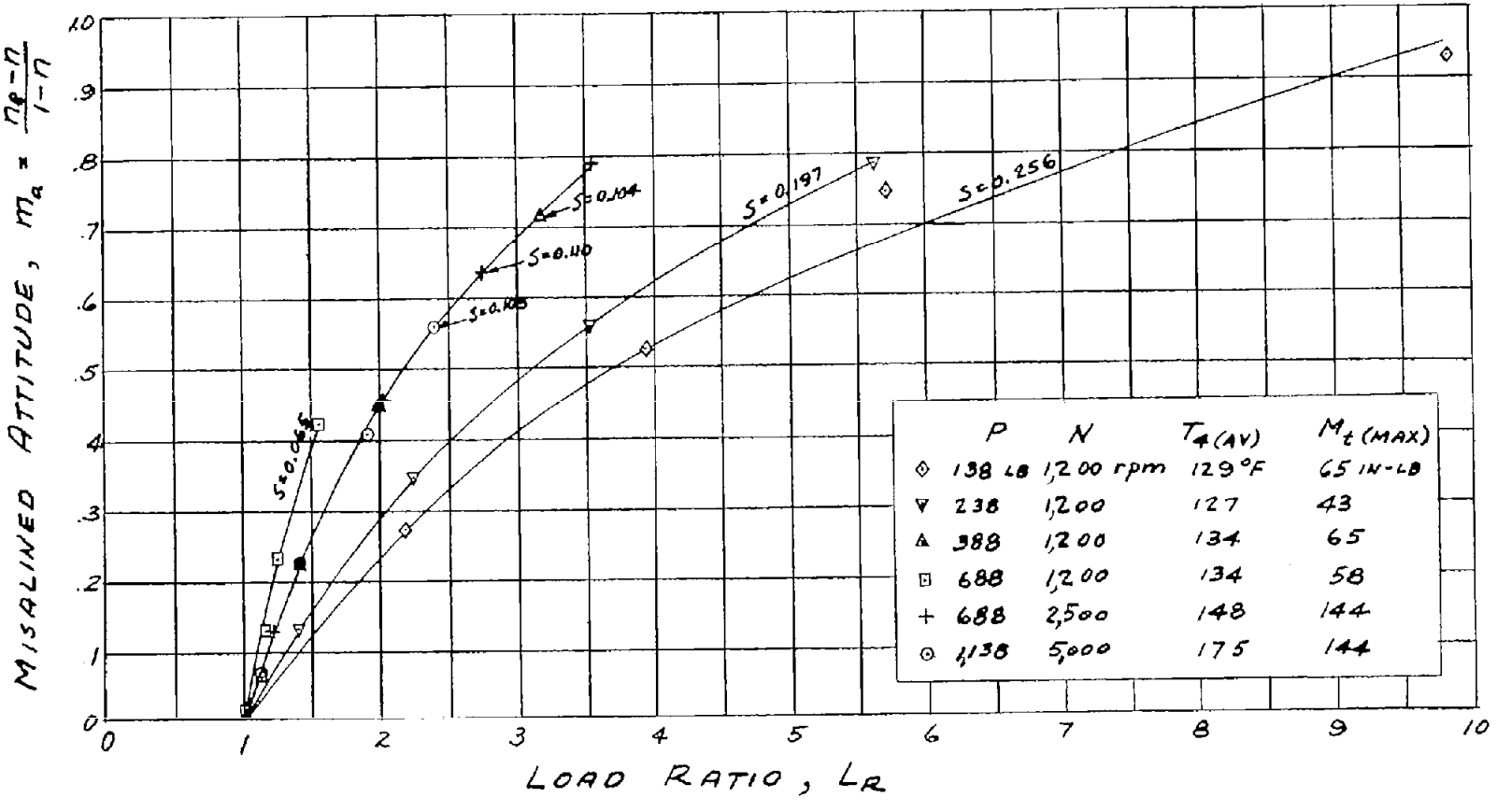

(j) Curves for Sommerfeld number; twisting misalinement; shaft 6D; $l/d = 1$; $d = 1\frac{3}{8}$ inches; $l = 1\frac{3}{8}$ inches; $c_d = 0.00183$ inch at room temperature. Load ratio calculated from equation (5) and based on experimental curve of figure 4(b).

Figure 15.- Continued.

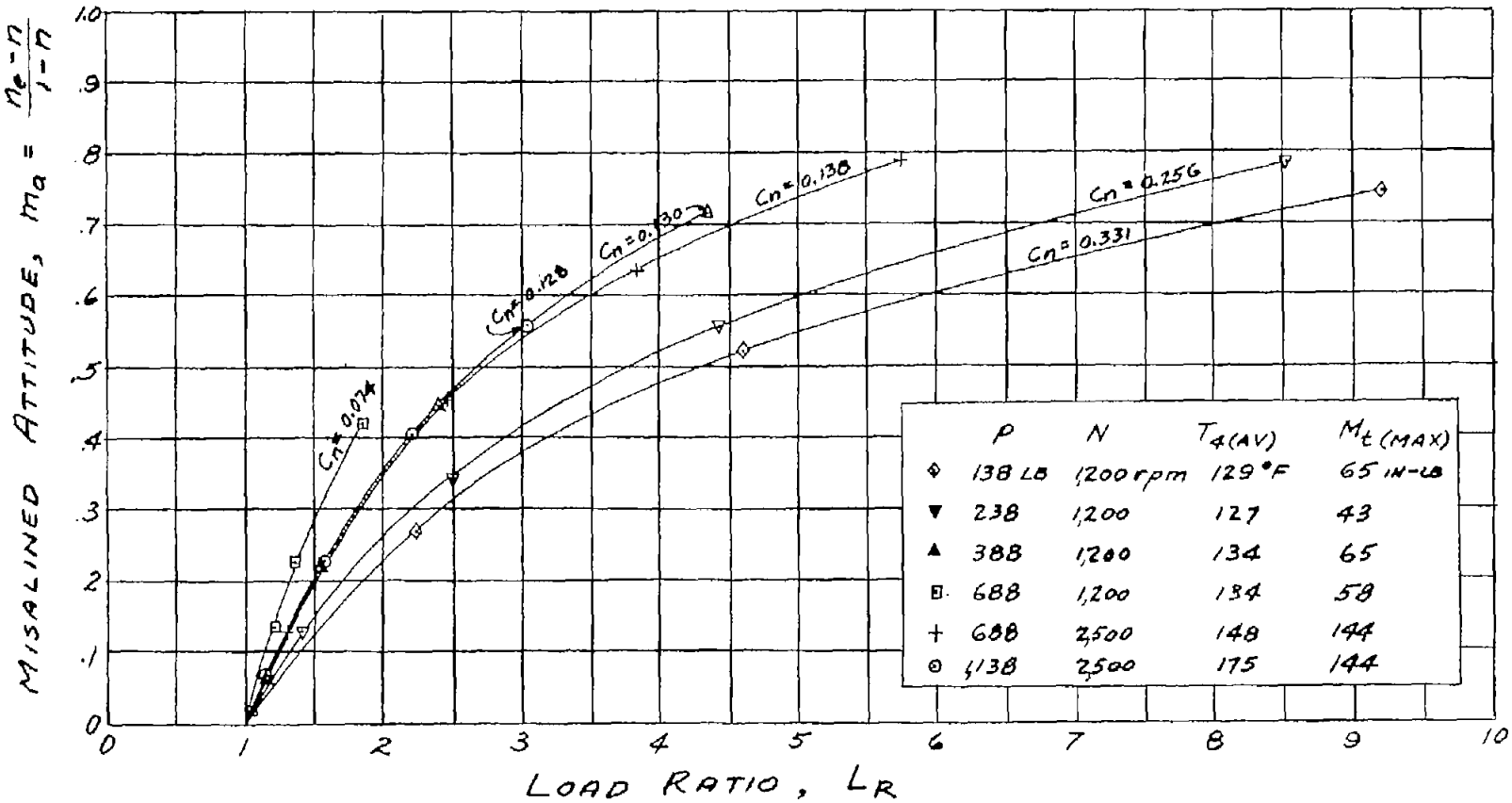

(k) Curves for capacity number; twisting misalinement; shaft 6D; $l/d = 1.0$; $d = 1\frac{3}{8}$ inches; $l = 1\frac{3}{8}$ inches; $c_d = 0.00183$ inch at room temperature.

Load ratio calculated from equation (5) and based on experimental curve of figure 4(c).

Figure 15.- Continued.

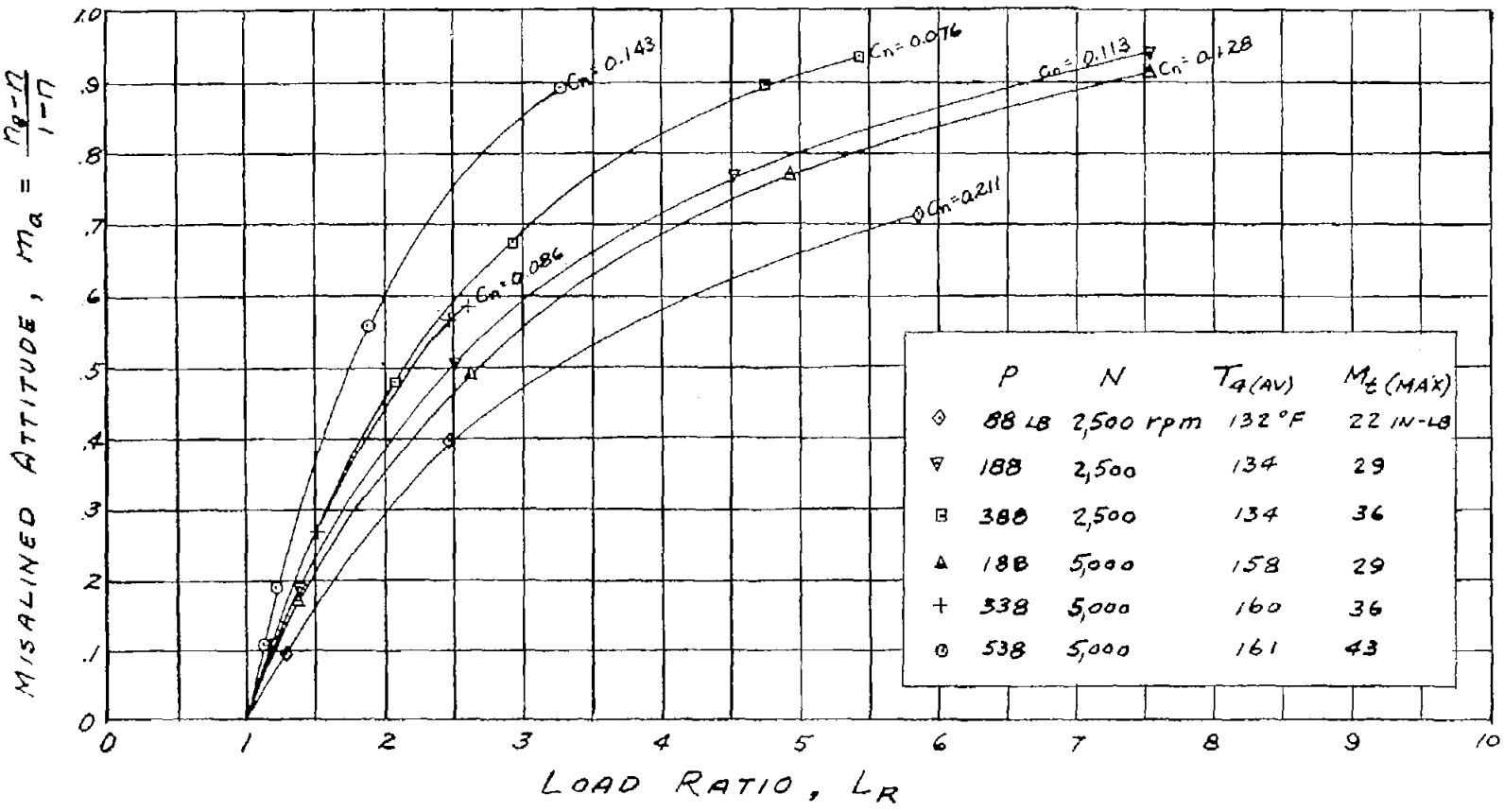

(l) Curves for capacity number; twisting misalinement; shaft 6E; $l/d = 3/4$; $d = 1\frac{3}{8}$ inches; $l = 1\frac{1}{32}$ inches; $c_d = 0.00258$ inch at room temperature. Load ratio calculated from equation (5) and based on experimental curve of figure 4(c).

Figure 15.- Concluded.

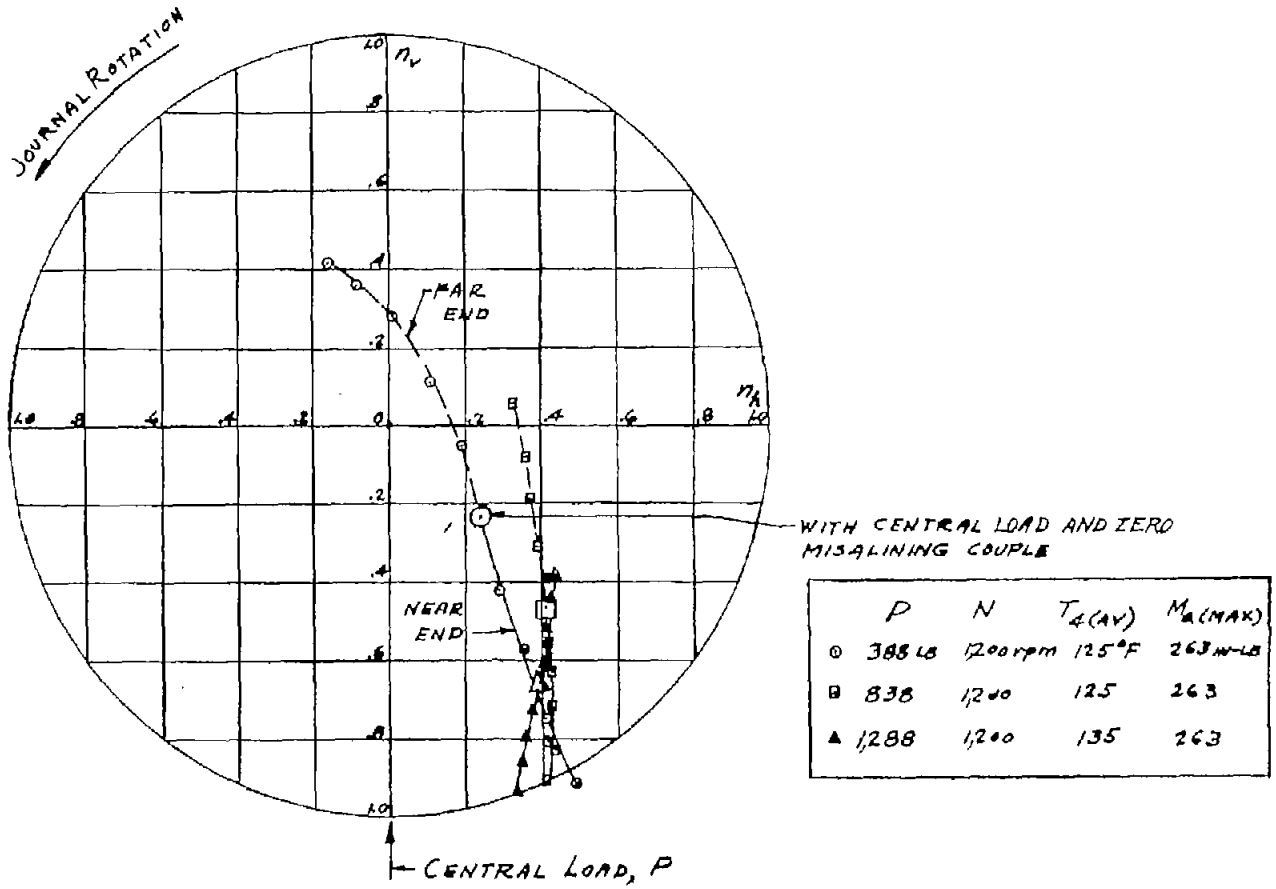

(a) Axial misalinement; shaft 6A; $l/d = 2$; $d = 1\frac{3}{8}$ inches; $l = 2\frac{3}{4}$ inches; $c_d = 0.00252$ inch at room temperature.

Figure 16.- End eccentricity ratios. SAE 10 oil; 140° F at heater; p_o = 80 pounds per square inch; 1/8-inch-diameter oil hole opposite central load.

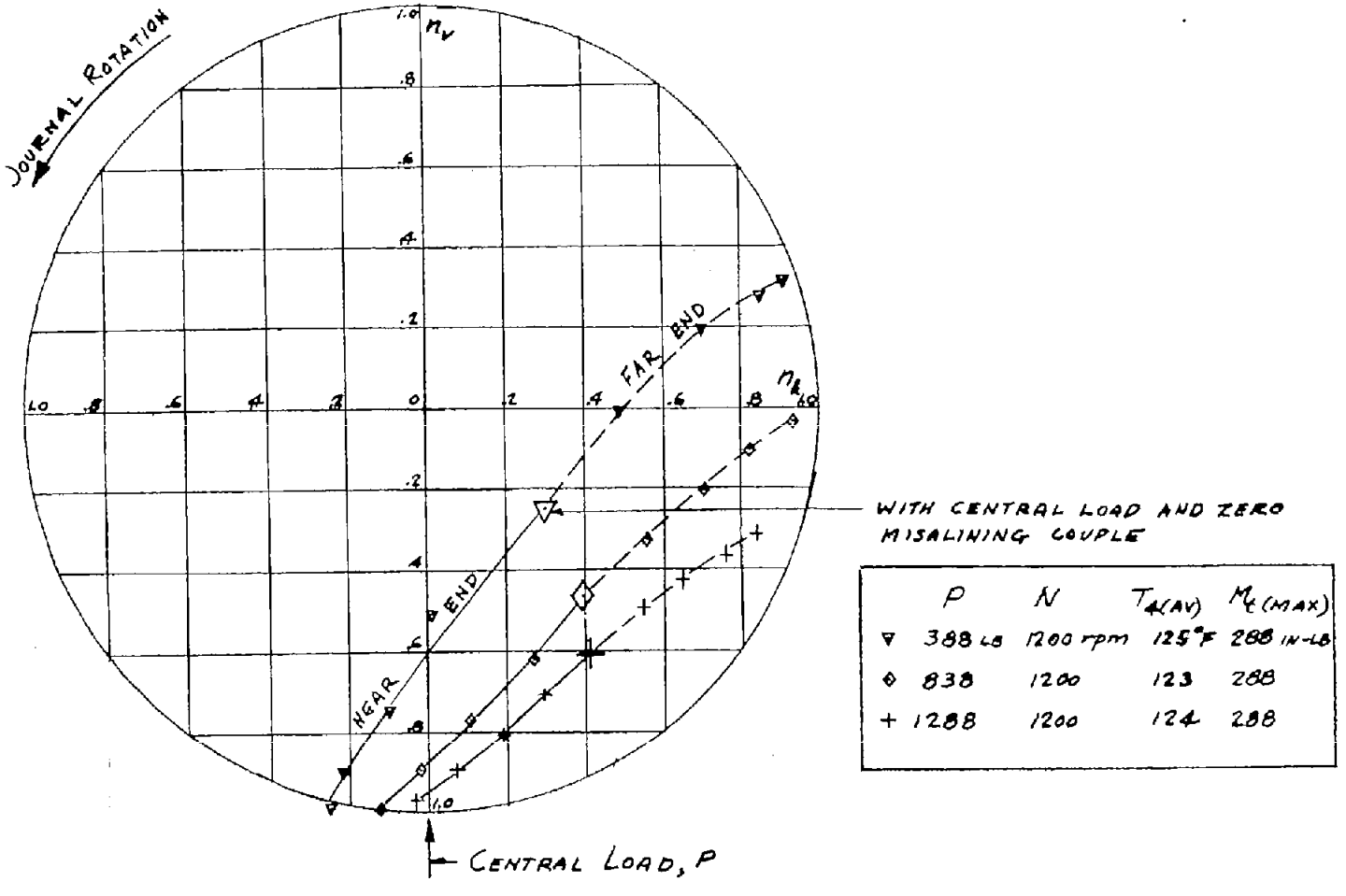

(b) Twisting misalinement; shaft 6A; $l/d = 2$; $d = 1\frac{3}{8}$ inches; $l = 2\frac{3}{4}$ inches; $c_d = 0.00252$ inch at room temperature.

Figure 16.- Continued.

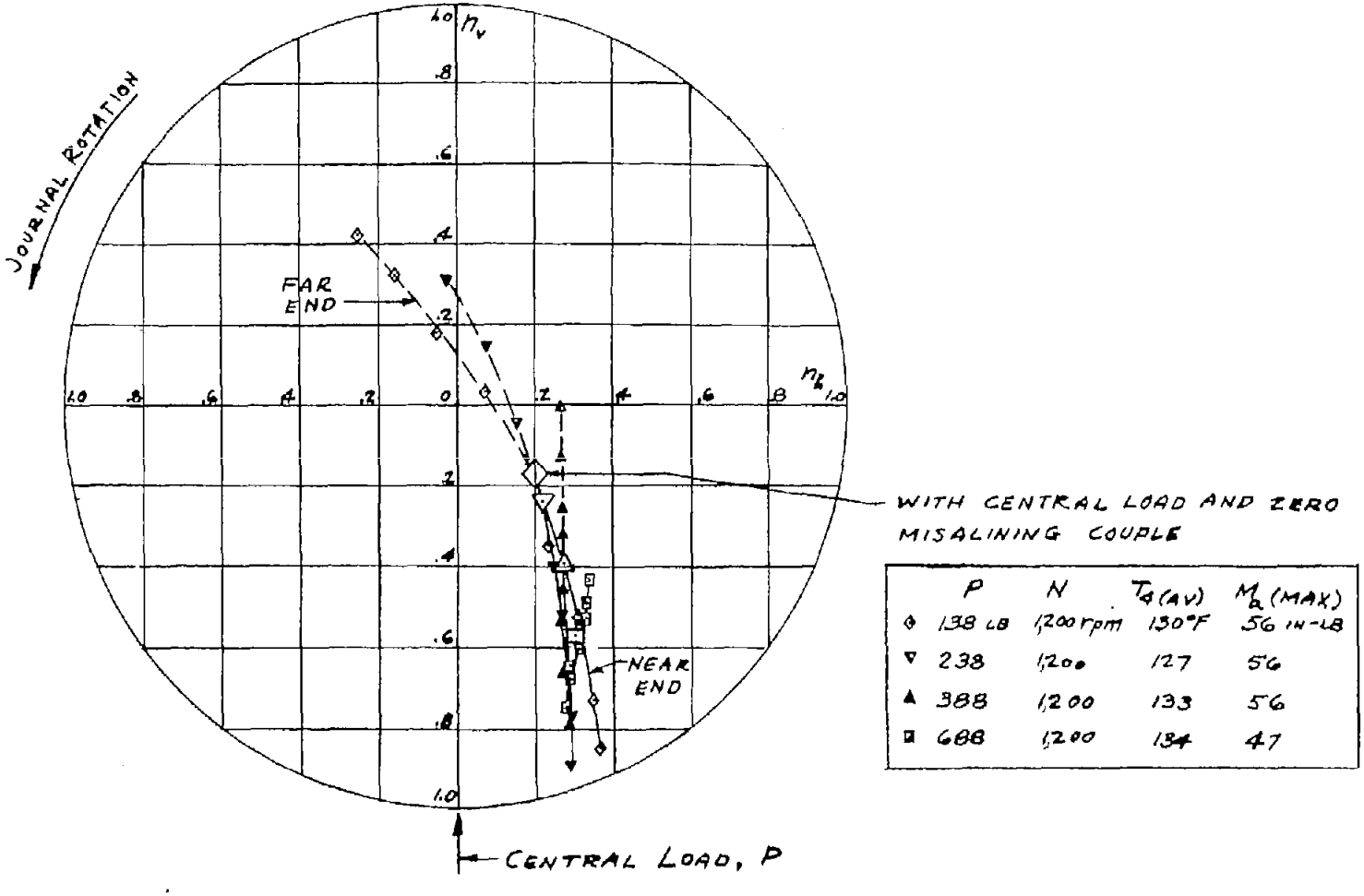

(c) Axial misalinement; shaft 6D; $l/d = 1$; $d = 1\frac{3}{8}$ inches; $l = 1\frac{3}{8}$ inches; $c_d = 0.00183$ inch at room temperature.

Figure 16.- Continued.

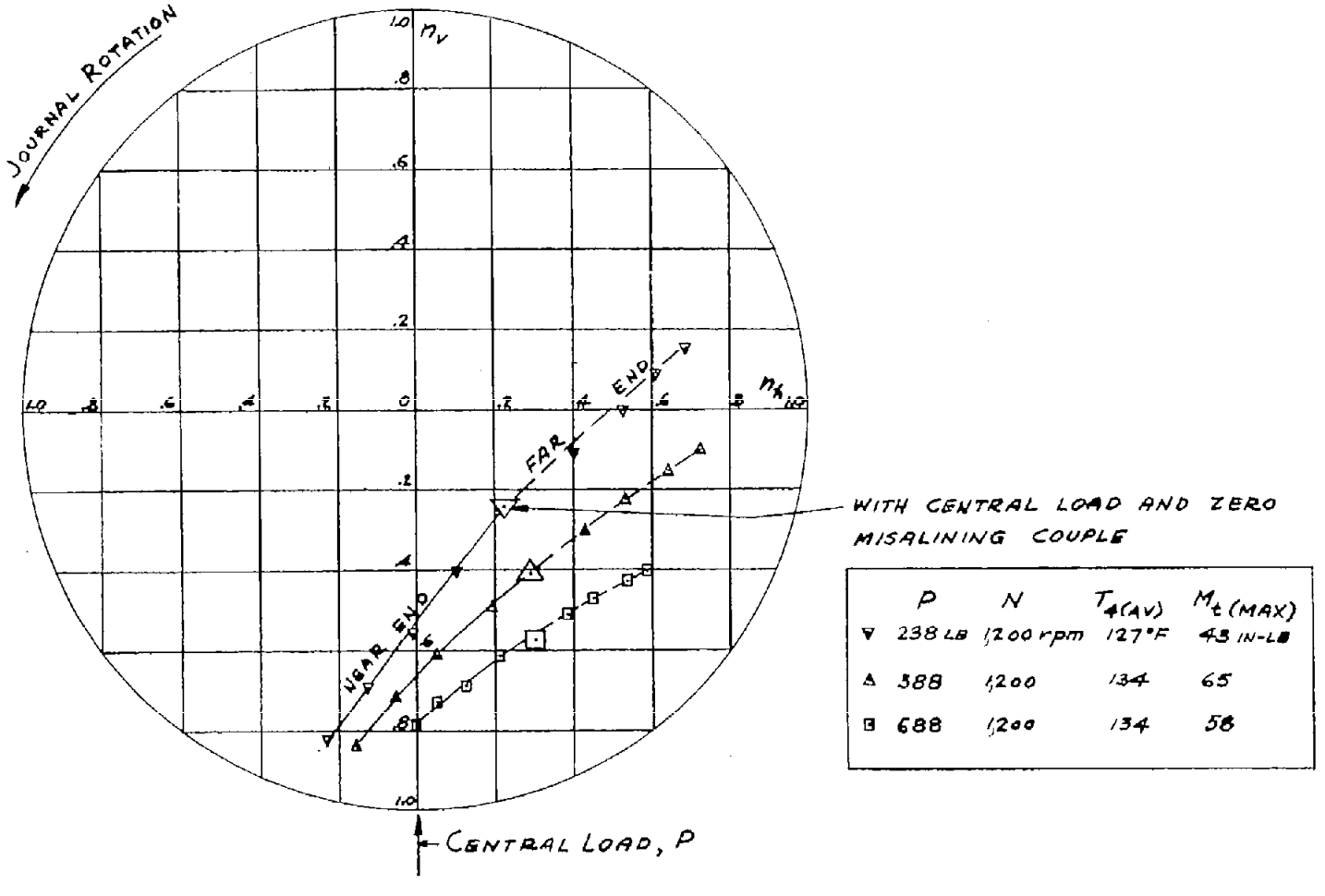

(d) Twisting misalinement; shaft 6D; $l/d = 1$; $d = 1\frac{3}{8}$ inches; $l = 1\frac{3}{8}$ inches; $c_d = 0.00183$ inch at room temperature.

Figure 16.- Concluded.

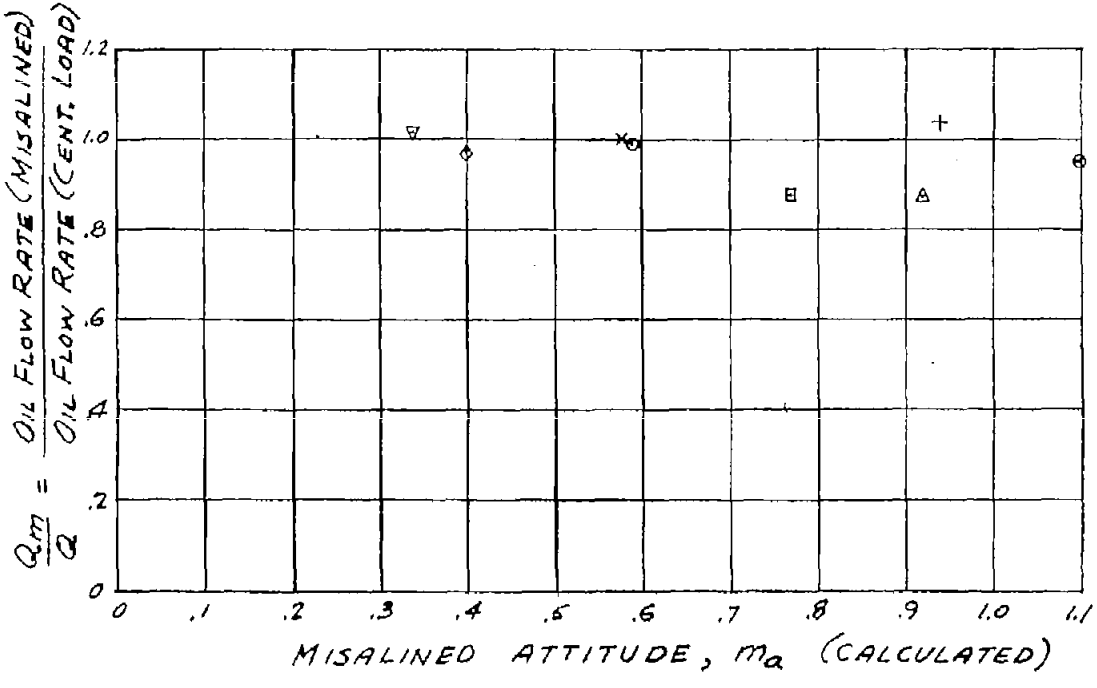

	SHAFT	P lb	N rpm	$T_{4(AV)}$ °F	$M_{a(MAX)}$ IN-LB
⊙	6A	838	1,200	135	225
+	6A	188	1,200	128	150
△	6A	388	1,200	132	150
◇	6C	838	5,000	178	113
▽	6C	1,288	5,000	180	113
⊟	6C	238	1,200	131	94
×	6C	738	1,200	133	94

(a) Axial misalinement. Shaft 6A: $l/d = 2$; $d = 1\frac{3}{8}$ inches; $l = 2\frac{3}{4}$ inches; $c_d = 0.00252$ inch. Shaft 6C: $l/d = 1.5$; $d = 1\frac{3}{8}$ inches; $l = 2\frac{1}{16}$ inches; $c_d = 0.00196$ inch.

Figure 17.- Effect of misalinement on oil flow rate. SAE 10 oil; 140° F at heater; p_o = 80 pounds per square inch; 1/8-inch-diameter oil hole opposite central load.

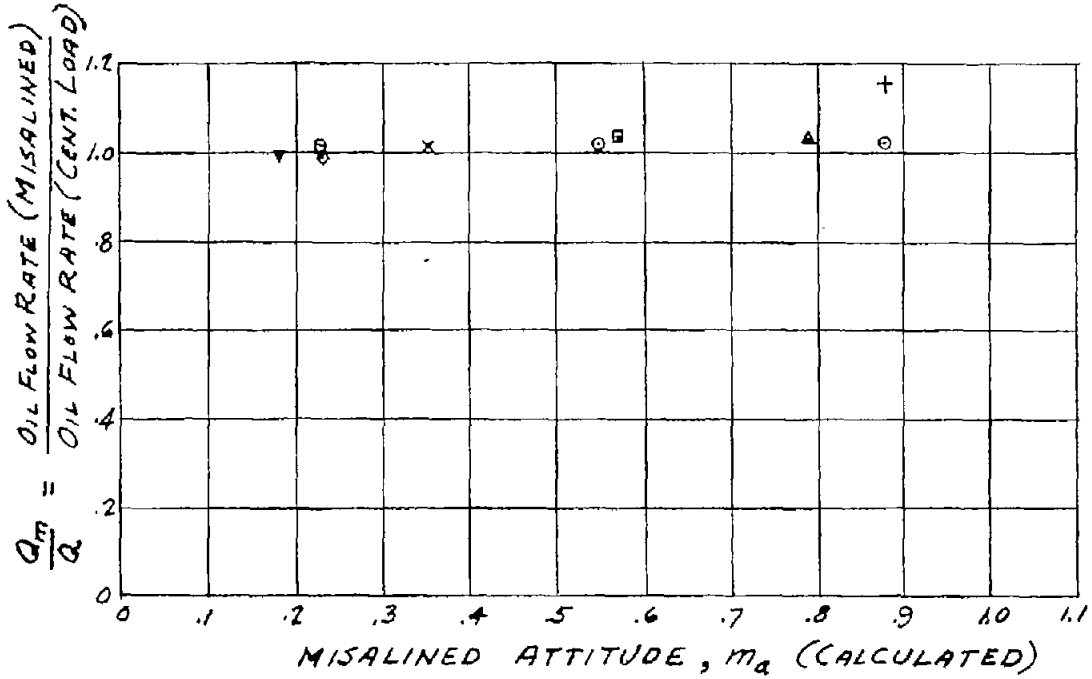

	Shaft	P, lb	N, rpm	$T_{f(av)}$, °F	$M_{f(max)}$, in-lb
⊖	6A	838	1,200	133	216
+	6A	188	1,200	128	173
▲	6A	388	1,200	132	173
◇	6C	838	5,000	178	101
▽	6C	1,288	5,000	180	101
⊡	6C	238	1,200	131	86
×	6C	738	1,200	133	86

(b) Twisting misalinement. Shaft 6A: $l/d = 2$; $d = 1\frac{3}{8}$ inches; $l = 2\frac{3}{4}$ inches; $c_d = 0.00252$ inch. Shaft 6C: $l/d = 1.5$; $d = 1\frac{3}{8}$ inches; $l = 2\frac{1}{16}$ inches; $c_d = 0.00196$ inch.

Figure 17.- Concluded.

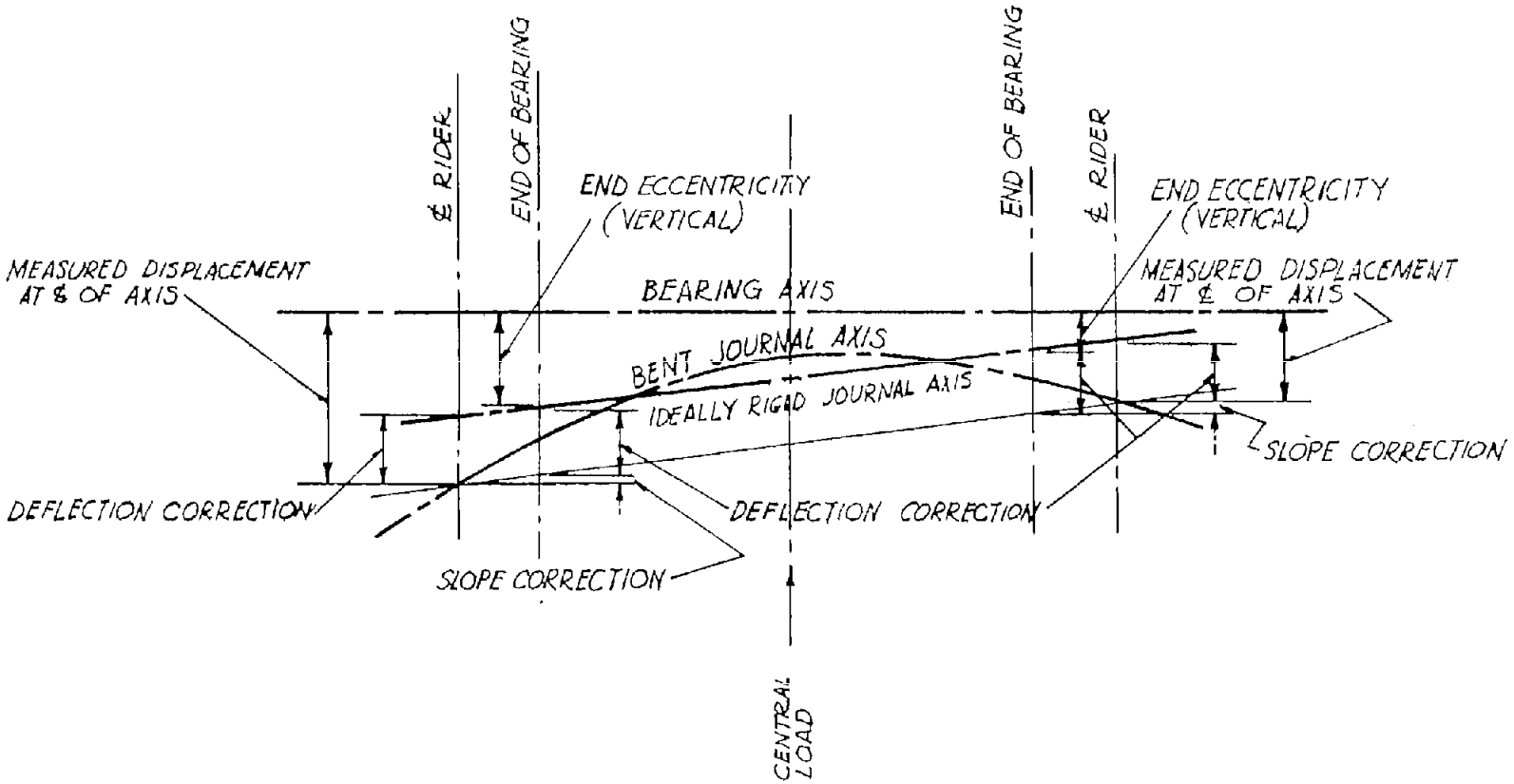

Figure 18.- Diagram showing corrections made to account for shaft inclination and shaft bending deflection in calculating eccentricities at ends of bearing from measured displacements at riders. Configuration shown applies to vertical eccentricities.

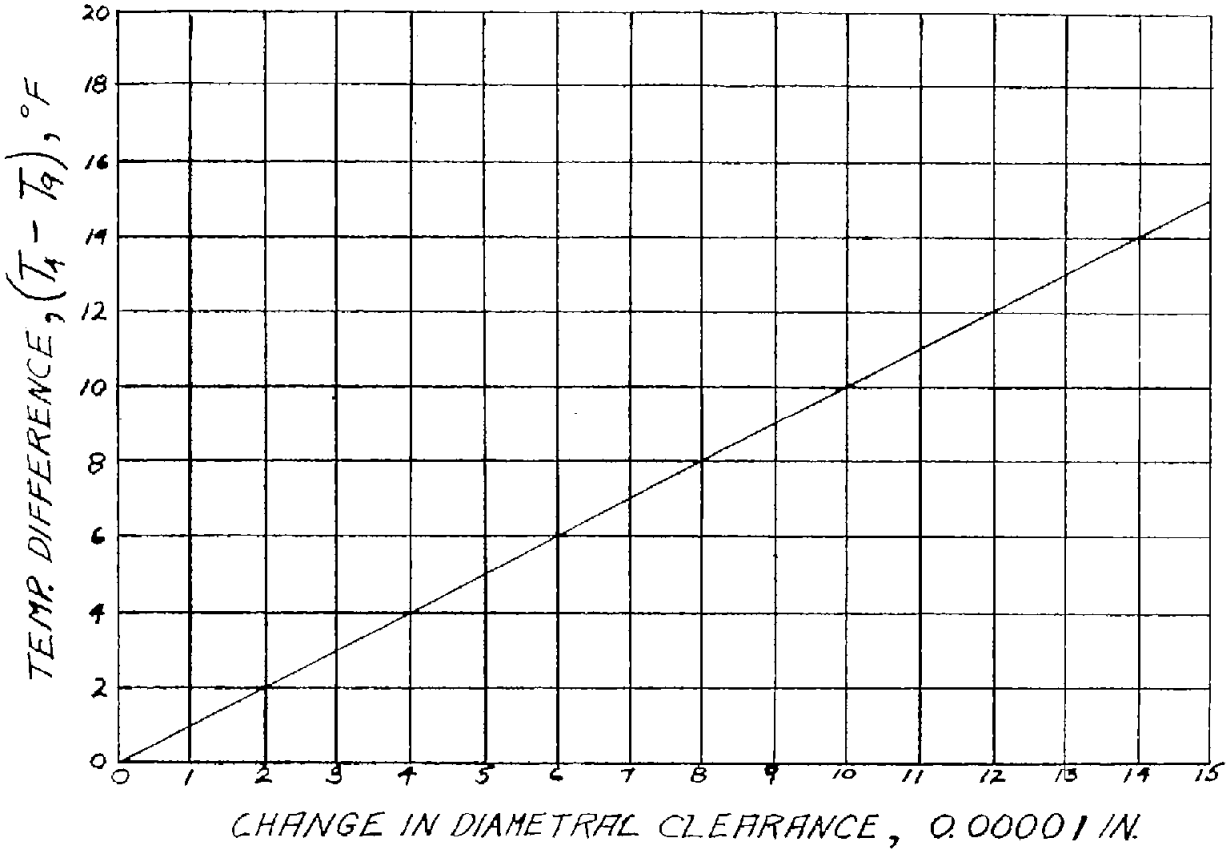

Figure 19.- Changes in diametral clearance as a function of temperature difference of two points in test-bearing wall. T_4 and T_9 are bearing temperatures at 1/16 inch and 2 inches, respectively, from bearing surface. Running clearances of test bearing are determined by subtracting change in clearance from room-temperature clearance.

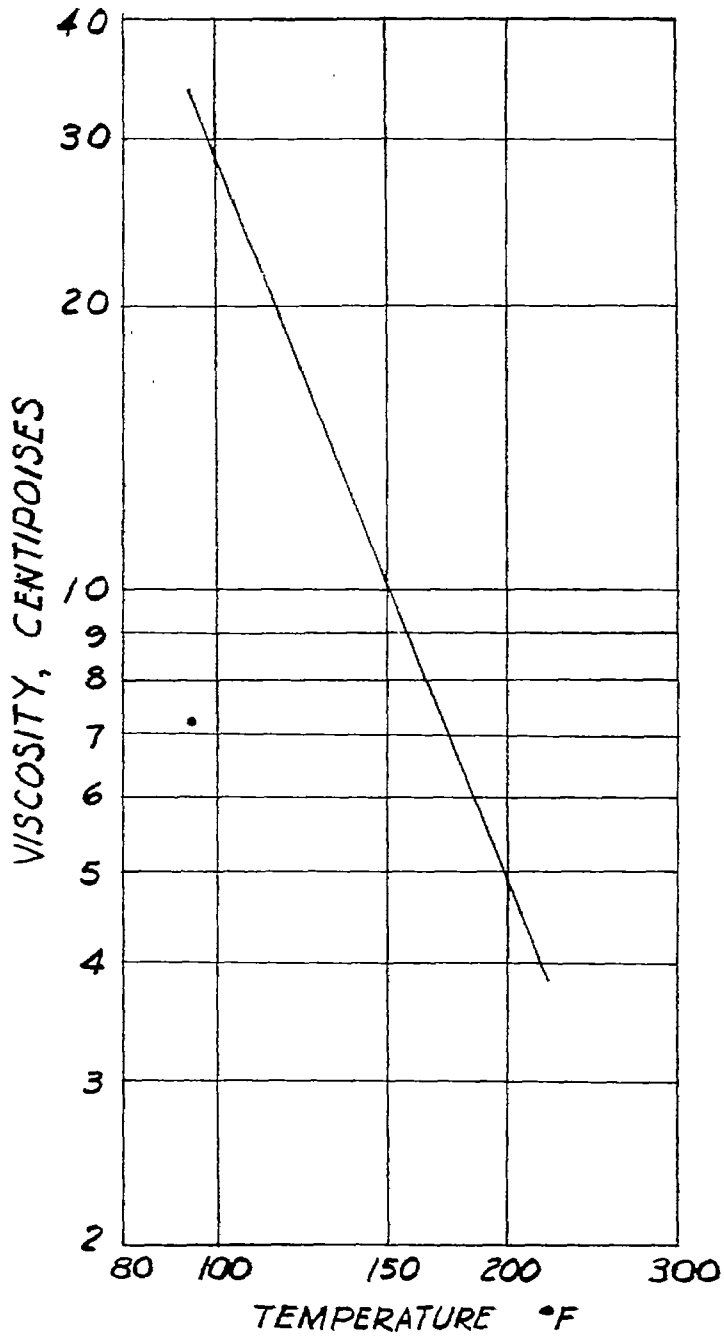

Figure 20.- Viscosity-temperature characteristics of SAE 10 oil used in experiments.

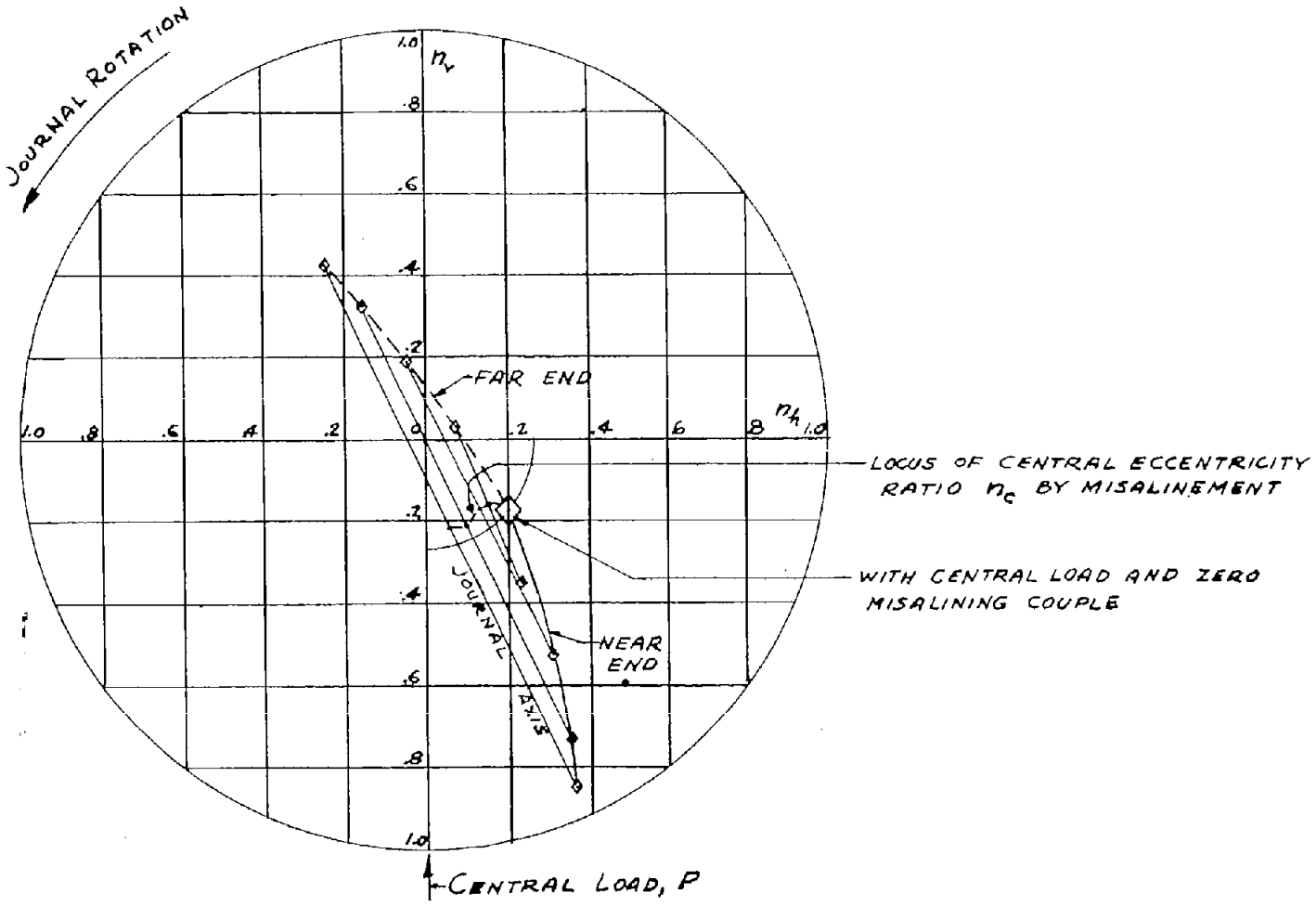

Figure 21.- Change of central eccentricity ratio n_c with axial misalinement. Shaft 6D; $l/d = 1$. Typical behavior with light central load. Heavier central loads show less change in n_c; see figure 16 for comparison.

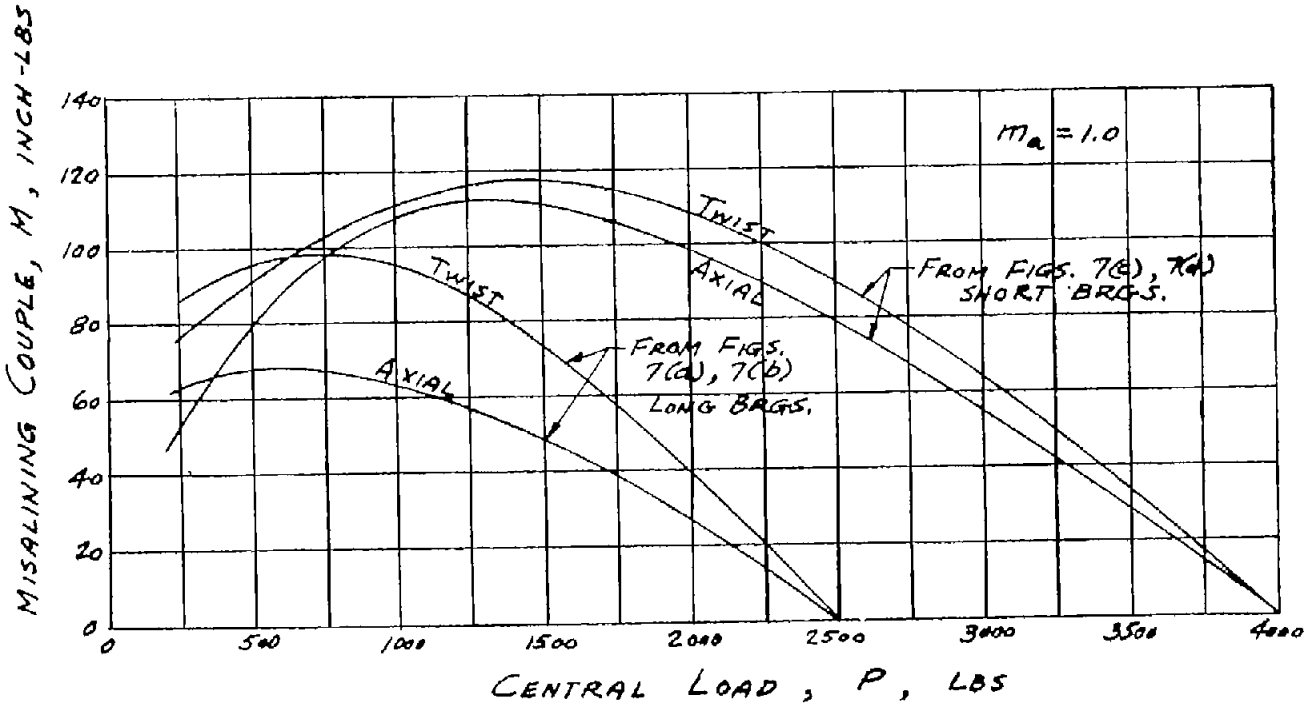

Example: $l = 1$ in. $d = 1$ in. $l/d = 1$ $c_d = 0.001$ in. $d/c_d = 1{,}000$

$\mu = 2.5 \times 10^{-6}$ reyn $N = 1{,}200$ rpm $N' = 20$ rps

$$P = \frac{\mu N' l d}{S}\left(\frac{d}{c_d}\right)^2 = \frac{50}{S}$$

$$M = \frac{C_m P l}{\left(d/c_d\right)^{1/2}\left(l/d\right)^{1/2}} = 1.58\,\frac{C_m}{S}$$

Figure 22.- Misalining couple for metallic contact ($m_a = 1.0$) as a function of central load.